Active Vibration Control and Optimal Location of Piezoelectric Patches on Flexible Plate by using Modal Analysis

Dissertaion-1I

Submitted in partial fulfilment of the requirement for the award of degree

Of

Master of Technology

IN

MECHANICAL ENGINEERING

By

B. THARUN KUMAR

(11500826)

Under the guidance of

Dr. Ashok Kumar

(20269)

DEPARTMENT OF MECHANICAL ENGINEERING
LOVELY PROFESSIONAL UNIVERSITY
PUNJAB

CERTIFICATE

I hereby certify that the work being presented in the dissertation entitled **"Active Vibration Control and Optimal Location of Piezoelectric Patches on Flexible Plate by using Modal Analysis"** in partial fulfilment of the requirement of the award of the Degree of master of technology and submitted to the Department of Mechanical Engineering of Lovely Professional University, Phagwara, is an authentic record of my own work carried out under the supervision of (Dr. Ashok Kumar, Assistant Professor) Department of Mechanical Engineering, Lovely Professional University. The matter embodied in this dissertation has not been submitted in part or full to any other University or Institute for the award of any degree**.**

(Date)

(B. THARUN KUMAR)

Regd no: 11500826.

This is to certify that the above statement made by the candidate is correct to the best of my knowledge.

(Date) (Dr. Ashok Kumar)

(U.ID:20269)

COD

The external viva-voce examination of the student was held on successfully

---

Signature of Examiner

TOPIC APPROVAL PERFORMA

School of Mechanical Engineering

Program : P178::M.Tech. (Mechanical Engineering) [Full Time]

COURSE CODE : MEC601 **REGULAR/BACKLOG :** Regular **GROUP NUMBER :** MERGD0192

Supervisor Name : Dr. Ashok Kumar **UID :** 20269 **Designation :** Assistant Professor

Qualification : _____ **Research Experience :** _____

SR.NO.	NAME OF STUDENT	REGISTRATION NO	BATCH	SECTION	CONTACT NUMBER
1	B Tharun Kumar	11500826	2015	M1571	09440032182

SPECIALIZATION AREA : Design **Supervisor Signature:** _____

PROPOSED TOPIC : Active vibration control and optimal location of piezoelectric patches on flexible plate by using modal analysis.

Qualitative Assessment of Proposed Topic by PAC		
Sr.No.	**Parameter**	**Rating (out of 10)**
1	Project Novelty: Potential of the project to create new knowledge	7.67
2	Project Feasibility: Project can be timely carried out in-house with low-cost and available resources in the University by the students.	7.00
3	Project Academic Inputs: Project topic is relevant and makes extensive use of academic inputs in UG program and serves as a culminating effort for core study area of the degree program.	7.33
4	Project Supervision: Project supervisor's is technically competent to guide students, resolve any issues, and impart necessary skills.	7.33
5	Social Applicability: Project work intends to solve a practical problem.	7.00
6	Future Scope: Project has potential to become basis of future research work, publication or patent.	7.33

PAC Committee Members		
PAC Member 1 Name: Jaiinder Preet Singh	UID: 14740	Recommended (Y/N): Yes
PAC Member 2 Name: Piyush Gulati	UID: 14775	Recommended (Y/N): Yes
PAC Member 3 Name: Dr. Manpreet Singh	UID: 20360	Recommended (Y/N): NA
DRD Nominee Name: Dr. Amit Bansal	UID: 18697	Recommended (Y/N): NA
DAA Nominee Name: Kamal Hassan	UID: 17469	Recommended (Y/N): Yes

Final Topic Approved by PAC: **Active vibration control and optimal location of piezoelectric patches on flexible plate by using modal analysis.**

Overall Remarks: Approved

PAC CHAIRPERSON Name: 12174::Gurpreet Singh Phull **Approval Date:** 03 Oct 2016

INDEX

Acknowledgement…….(i)

List of Contents…….…….....(ii)

List of Figures…….....(iv)

List of Tables……..……..……....(vi)

Abstract….……..…….....(viii)

ACKNOWLEDGEMENT

I feel immense pleasure in expressing my profound sense of gratitude to my thesis supervisor **Dr. Ashok Kumar (Assistant professor)**, School of Mechanical Engineering under whose supervision and inspiring guidance, I have the privilege to carry out my research work. I am indebted to them for their constant and ungrudging encouragement, valuable suggestions and ingenious ideas.

I would like to extend my thanks to **Mr.Gurpreet singh phull (H.O.S)** School of Mechanical Engineering for their support and all those who have directly and indirectly helped through my thesis.

Next, I extend my gratitude to my parents for their support throughout this work. Without their motivation it might not have been possible for me to complete this study. Blessings of my beloved parents helped me reach this end.

Finally, thanks are due to my friends for their advices and continued support.

(B. Tharun Kumar)

(11500826)

LIST OF CONTENTS

CHAPTER 1 INTRODUCTION ……..…….……..1

CHAPTER 2 TERMINOLOGY ……..…….…….……....5

CHAPTER 3 REVIEW OF LITERATURE…….…….……...…..... 7

CHAPTER 4 SCOPE OF STUDY …….…….……...18

CHAPTER 5 OBJECTIVES OF THE STUDY…….…….……..……..… 19

CHAPTER 6 MATERIALS AND RESEARCH METHODOLOGY …….…….…..…..20

6.1 Finite Element Modelling of steel plate…….……..….21

6.2 Viewing the Mode shapes of Neat plate…….……...……...21

6.3 Optimal Location of Piezoelectric Patch …….…….....…….....21

6.4 Finite Element Modelling of Plate-piezo electric patch…….……..….22

6.5Application of Viewing method ……..……22

6.6 Validation through Frequency Response Function ……..……..…..…..22

6.7 Active Vibration Control of a plate……..……22

6.7.1 Finite element formulation of plate…….……..……22

6.7.2 Finite element formulation of Piezoelectric patches …..…….……26

6.7.3 Development of state space representation for plate and

piezoelectric patch …….……..……..31

6.7.3 Design of Direct Output Feedback …….……...33

CHAPTER 7 RESULTS AND DISCUSSIONS …….……...……..……34

7.1 Mode shapes of a plate with different boundary conditions……..……34

7.1.1 Clamped boundary condition…….……..…….35

7.1.2 Cantilever boundary condition…….……..…….36

7.1.3 Free- Free boundary condition…….……..38

7.1.4 Simply supported boundary condition…….……...39

7.2 Validation through Frequency Response Function…….……..……40

7.3 Active Vibration Control of a plate …….……...42

CHAPTER 8 CONCLUSIONS AND FUTURE SCOPE …….……..56

REFERENCES…….…….……...58

APPENDIX

MATLAB CODE OF A PLATE…….……64

LIST OF PUBLICATIONS …….……79

LIST OF FIGURES

FIGURE 6.1: Coordinate system of a plate with integrated Piezo-electric patches.....23

FIGURE 7.1: FRF graph for optimum location of piezoelectric patch on a plate with clamped at all edges boundary condition…...……..……...40

FIGURE 7.2: FRF graph for optimum location of piezoelectric patch on a plate with cantilever boundary condition……...……..41

FIGURE 7.3: FRF graph for optimum location of piezoelectric patch on a plate with Free-free boundary condition……...……41

FIGURE 7.4: FRF graph for optimum location of piezo electric patch on a plate with simply supported boundary condition. ……42

FIGURE 7.5: Pole zero map at G_v=0 and G_d=0. ……..……43

FIGURE 7.6: Nodal displacement response at G_v=0 and G_d=0……...43

FIGURE 7.7: Pole zero map at $G_v = 0$ and $G_d \neq 0$ ……...45

FIGURE 7.8: Nodal displacement response at $G_v = 0$ and $G_d \neq 0$……45

FIGURE 7.9: Pole zero map at G_d=0 and $G_v = 0.08$……47

FIGURE 7.10: Nodal displacement response at G_d=0 and $G_v = 0.08$……...48

FIGURE 7.11: Pole zero map at G_d=0.08 and $G_v = 0.08$……..50

FIGURE 7.12: Nodal displacement response at G_d=0 and $G_v = 0.08$……...50

FIGURE 7.13: Finite element Mesh of plate with piezoelectric patch of different cases with respect to node number……51

FIGURE 7.14: Displacement response at node number f=103; r=72……...51

FIGURE 7.15: Displacement response at node number f=103; r=74……...52

FIGURE 7.16: Displacement response at node number f=103; r=116……52

FIGURE 7.17: Displacement response at node number f=103; r=14……...53

FIGURE 7.18: Displacement response at node number f=103; r=32……...53

FIGURE 7.19: Displacement response at node number f=103: r=103……....54

FIGURE 7.20: Displacement response at node number f=107; r=107..…… ……..54

FIGURE 7.21: Displacement response at node number f=103; r=119..…… ……..55

LIST OF TABLES

TABLE 7.1: Mode shapes of bare plate with clamped at all edges boundary condition……34

TABLE 7.2: Mode shapes of bare plate with cantilever boundary condition…….34

TABLE 7.3: Mode shapes of bare plate with free-free boundary condition……..……...35

TABLE 7.4: Mode shapes of bare plate with simply supported boundary condition……..……35

TABLE 7.5: Optimum location of piezoelectric patch on bare plate for clamped at all edges boundary condition……..…….36

TABLE 7.6: Optimum location of piezoelectric patch on a plate for cantilever boundary condition……...37

TABLE 7.7: Optimum location of piezoelectric patch on bare plate for free-free boundary condition……..……...39

TABLE 7.8: Optimum location of piezoelectric patch on bare plate for Simply supported boundary condition……..40

TABLE 7.9: Changes in Design Parameters with respect to $G_v = 0$ and $G_d \neq 0$…….……44

TABLE 7.10: Changes in Design Parameters with respect to $G_v = 0$ and $G_d \neq 0$…….…..…44

TABLE 7.11: Changes in Design Parameters with respect to $G_d = 0$ and $G_v \neq 0$ …….……..……46

TABLE 7.12: Changes in Design Parameters with respect to

$G_d = 0$ and $G_v \neq 0$ ……...…46

TABLE 7.13: Changes in Design Parameters with respect to

$G_d = 0$ and $G_v \neq 0$ ……..……..…47

TABLE 7.14: Changes in Design Parameters with respect to

$G_d=0$ and $G_v = 0.08$……48

TABLE 7.15: Changes in Design Parameters with respect to

$G_d=0$ and $G_v = 0.08$……49

TABLE 7.16: Changes in Design Parameters with respect to

$G_d=0$ and $G_v = 0.08$……49

ABSTRACT

In this thesis, the most favourable location of collocated piezoelectric patches on a bare plate by considering different boundary conditions as free-free, simply supported, cantilever, clamped at all edges for vibration control is found out by viewing the mode shapes of steel plate. The steel plate is modelled in ABAQUS CAE software. Then the modal analysis of the flexible steel plate is obtained. A method was proposed for most appropriate location of piezoelectric patches by viewing the modal shapes of the plate. Through viewing method, it can be observed that the patches cannot be on the nodal line where displacement is zero as it doesn't provide an effect and vibration control cannot be done.

Passive methods are not so effective in controlling low frequency noise. So, this leads to the efforts for developing active vibration control strategy. A direct output feedback method was proposed for active vibration control. A pole placement technique was used to find out the optimal value of direct output feedback gain (G_v). This is carried out by two steps. Initially, through pole placement graph, the dynamic properties of the structure are predicted. Then in later step, the velocity gain (G_v) value is varied in order to get the optimal controller gain value for desired changes in the properties of the structure. Then choosing the node number for applying hammer excitation force at which the control of vibrations will be reduced to minimum which are produced by the structure. This results are extracted by doing codding in MATLAB software

CHAPTER-1

INTRODUCTION

The control of vibration by using a piezoelectric actuator and sensor had been the topic of interest of many researchers as it was the major problem in structures like automobile wings, tennis rackets, knocking sensors, sports, aircrafts, railway compartments, ultrasonic structures, and few more cavities in order to control the vibrations or disturbances produced by a system. Even though there are lots of techniques for vibration control such as damping system, remodelling of structure, extra mass adding, adding vibration isolation, high stiffness materials which are having good damping proportion, vibration absorber, increasing the width or thickness of plate are not so appropriate to control the vibrations produced i.e. low natural frequencies.

These techniques are failing due to lower frequencies; the wavelength will increase enormously which leads to the layer thickening of the noise absorbing systems and it will append the extra weight to the structure therefore it gets hard. As many advancements arrived in modern laptops had found an alternative at lower natural frequencies for this passive control systems in order to eradicate the unnecessary disturbance or sound. Based on the natural frequency range, the active and passive control methods are divided as disturbance below 1000Hz is active method and if disturbance above 1000Hz is passive method. But most of the times the active control method is preferred because it has a competency to operate at antithetical conditions.

As technology was growing rapidly, the active noise control also increasing. Loudspeakers use internal auditory origin to abandon the incoming decibel with error signal from acoustic sensors which will comes under active noise cancellation of first classification. Piezoelectric patches are used for error signal in the auditory field comes under second classification and Active structural acoustic control system engages with both actuators and sensors will comes under third classification. In this acoustic control system, the actuators like piezoelectric materials, magneto-rheological fluids, and optics will incorporate into the walls in order to reduce or control the vibrations or noise produced by the structures. The piezoelectric patches are placed on the both sides of structure and gives sufficient input to structure in order to control the response.

The disturbances or unwanted noise which was formed in aircraft and automotive vehicles because of surrounding systems. Mainly two techniques are used to control the internal disturbance control as one of them is feed forward control and other is feedback. In automobiles, during the IC engine operations and in jet engines for aircraft structures, an unwanted noise will arise can be controlled by feedforward method. But this method will not work properly when the disturbance was caused by hard surface of the road, wind turbulence effect in case of aircrafts and during landing case also.

The Piezoelectricity means to generate electric charge. This electricity is formed due to pressure that which propagates on materials such as ceramics, solid crystals. The effect produced by piezo will acts as relation between electrical and mechanical systems. This effect was reversible when mechanical force is applied results in generation of electrical field. Similarly, it will act as irreversible when electrical forces are applied results in generation of mechanical field.

From the literary survey, it was found that if absence of piezoelectric patch may lead to deflection and buckling of material due to load. Then in presence of piezoelectric, deflection and buckling was avoided. Piezoelectric patch was used for vibration control purpose which was produced in systems because of reliability, easiness and regarding mass added to structures will not make heavy. But while fixing piezo patch, on top surface sensor is located and at bottom surface actuator is located. From sensor, the actual control loop signal will generate and then this signal is transferred to actuator. From there actual effect will be acting on the system to control the vibrations.

Some of the piezoelectric devices are transducers, generators, actuators, sensors and combination of them. A transducer is a device which will transforms the quantities like light, pressure, sound into electrical signal or vice-versa. The direct piezoelectric material is mainly used in microphones, gas lighters etc., and voltage generated is used as sensors whereas indirect piezoelectric effect was used in dynamic control of variables and static control of variables such as medical applications, aircraft applications, automobile industry etc.,

Equipment's like ultrasound, transducer will transform electrical energy to mechanical vibrations with in a fraction of seconds, but the sound produced by the ultrasound will be too high which a human being cannot sustain. These vibrations are used mainly in

medical services like scanning. From Microphone device, the sound waves which are generated will be transformed into electric signals with the help of piezoelectric material by adding on the surface. Similarly, in gramophone an electric signal will generate which is converted to sound signals by piezoelectric. Indirect piezoelectric effect was used in watches as generation of electrical energy due to battery will make it to oscillate thousand times more in a second. These electrical signals are converted to mechanical energy with the help of small mortar which a piezoelectric is attached.

For optimization, vibration control, detection of any damages in structures or systems and better improvement of dynamic characteristics a modal analysis had been a prominent technology. This modal analysis not only limited to mechanical, automobiles but also applicable for aircraft structures, buildings, bio-medicals etc., when no external load is acting on a system, then free vibrations will occur due to oscillations produced by an initial deflection. Then system possess some amount of natural frequencies due to stiffness distribution and mass distribution and degrees of freedom. If it is a continuous system, it will result in infinite no of degrees of freedom and infinite no of frequencies.

The vibrations which are produced by external structure is controlled by considering the application of active vibration control. Active vibration control is a strategy which will impose equal and opposite forces produced by structure. Now-a-days, active vibration control method was applied to aerospace applications which is providing most gratification and very low weigth as compared to passive strategies. Active vibration control will develop an internal force in order to oppose the vibrations produced by structure. This strategy, external controller may absorb or supply the energy by using a vibration control algorithm. If the vibrations produced by structure are in periodic form then by considering this strategy it will provide cancellation of vibrations by simply providing the opposite acceleration.

An open loop pole gain can be obtained with out using any feedback in the controller. Open loop sytem will be completely acting on the input and output without the effect on control action. But closed loop system will alter the output according to the control action.

The state space representation was used in order to solve the high complexity which will be produced by the system of multiple inputs and outputs. The sample state space representation of a physical system was given as

$$\dot{w}(t) = Aw(t) + Bv(t) \tag{1}$$

$$p(t) = Cw(t) + Dv(t) \tag{2}$$

Wher w is called the state vector and it is a function of time, A is called the state matrix, B is the input matrix, C is the output matrix, D is the direct transistion matrix, v is the input matrix and is the function of time, p is the output matrix which is the function of time. The representation of the system is not unique as it varies for different physical structures.

In this thesis, it was discussed in order to control the vibrations produced by disturbances is done by placing a piezoelectric patch on the bare plate at most appropriate location where no nodal lines will pass through patch. This location was found out by viewing method. In this method, the mode shapes are viewed by conducting modal analysis for the plate in Abaqus software. Different boundary conditions like free-free, simply supported, cantilever, clamped at all edges of the plate is considered. From mode shapes, it is observed that piezoelectric patch cannot be placed on nodal lines where displacement is zero. The obtained result was validated by conducting Frequncy Response Function (FRF) analysis. Through analysis, it can be found that if piezo is not placed at an optimum location, the detection of all modes is not possible.

Then active vibration control strategy was applied in order to oppose the disturbances which is produced by external elements. Pole placement methodology was proposed in order to find an optimal value of the velocity gain (G_v) controller. Then choosing the node number for applying hammer excitation force at which the control of vibrations produced by structure. State space representation is used for plotting the open loop and closed loop pole zero maps.

CHAPTER-2

TERMINOLOGY

Finite Element Method: This method is a technique or strategy used for unlocking the complications produced in mathematical engineering. Some Huge elements will be divided into smaller but the properties will remain same is a finite method.

Shape Function: As the structure is divided into distinct elements like meshing. Shape functions are used in order to append the solution between the distinct elements for appropriate solution.

Piezoelectric patch: The Piezoelectricity means to generate electric charge. This electricity is formed due to pressure that which propagates on materials such as ceramics, solid crystals. The effect produced by piezo will acts as relation between electrical and mechanical systems. This effect was reversible when mechanical force is applied results in generation of electrical field. Similarly, it will act as irreversible when electrical forces are applied results in generation of mechanical field.

Nodal lines: when the structure is in vibration state, the vibrating structure remains stagnant at these lines and while remaining portion of structure will be in the mode of vibration.

Viewing Method: In this method, the optimal location is found out by observing the modal shapes of plate, piezo cannot be placed on the nodal line where displacement is zero and strain is also zero it doesn't provide a vibration control.

Mode shapes: A mode shapes is a distinct pattern of vibrations which are carried out by a mechanical system at a particular frequency.

Pole zero map: A map in which open loop and closed loop pole maps are used for designing the direct output feedback strategy for the optimal velocity gain value.

Some of the nomenclatre is represented below as:

d = displacement field vector

d_i = nodal displacement field

w = displacement field in z direction [m]

D = electric displacement vector [C/m^2]

E = Young's modulus [N/m^2]

V = volume [m^3]

K= stiffness matrix

M = mass matrix

T = kinetic energy [J]

u = displacement field in x direction [m]

U = potential energy [J]

v = displacement field in y direction [m]

W = work [J]

N = shape function

Greek Symbols

ε = strain field

σ = stress [N/m]

ν = Poisson ratio

ξ = dielectric tensor

ζ = nodal displacement vector

Φ = electric potential [Volts]

ω = frequency [rad/s]

ρ = material density [kg/m]

Subscripts

a = refers to the actuator

b = relative to the body

p = relative to the plate structure

s = relative to the sensor

sa =relative to the sensed voltage in the actuator

x = relative to x direction

y= relative to y direction

qq = relative to the stiffness

qΦ = relative to the piezoelectric stiffness

ΦΦ = relative to the dielectric stiffness

Superscripts

e = relative to the element

S = relative to constant strain

T = matrix transpose

CHAPTER-3

REVIEW OF LITERATURE

K. B. Lim 1992[1]**:** In this paper, most prominent location of piezoelectric actuator and sensor was found out by a method which is based on the orthogonal projection of structural modes. From these modes, the observability and controllability grammians are used to weight the projections in which the three-dimensional design space was created. From this design, optimal location was found. A set of closed loop performance was a main objective for an efficient location

J.H Han and I Lee 1999[2]: In this paper, efficient location of two piezoelectric sensor and actuator was found out by using genetic algorithm. The objective function was determined by considering the spill over prevention, observability and controllability and observed that the reduction occurs in first three modes of vibration.

A M Sadri et al. 1999[3]**:** This paper summarises about the two controllability criteria such as Modal controllability and controllability Grammian were used for optimal location of two piezoelectric actuators on isotropic plates. The fitness function used in the controllability of system was taken from genetic algorithm. The analysis used for finding the optimal location is also used as to find the size of actuators in order to obtain maximum controllability of systems.

M. Strassberger et al. 2000[4]**:** This paper deals with the noise, disturbance caused by mechanical equipment's which are controlled by placing some noise controllers such as piezo patch at a most appropriate location. General methods or equipment's are not sufficient to control the vibrations in space applications. It is concluded that the amplitudes which was caused by piezo patch which was measured by electrical devices to reduce the vibrations.

L. Bin et al. 2000[5]**:** In this paper, optimal location of piezoelectric actuators on flexible plate was found out by Maximal Modal Force rule which was taken from modal control theory. The emulation which was done by computer for control of vibration from plate is showed that the rule is correct and so effective.

H Zhang et al. 2000[6]: Optimal location of piezoelectric actuator and sensor for smart collocated cantilever beam was found out by float-encoded genetic algorithm technique by solving integrated optimisation problem. The result shows that the technique is so effective for generic optimisation tool.

K. Hiramoto et al. 2000[7]: In this paper, Optimal location of two pairs of actuator and sensor on flexible structures is found out by using the modified H_∞ based on simple addition and multiplication matrices in order to reduce the computational time then compared to standard norm.

O.J. Aldraihem et al. 2000[8]: Optimum placement of piezoelectric actuators and sensors was found out by the modal controllability, observability methods. It was found that using two pairs of actuators/ sensors will be more effective for vibration control then compared to single pair.

D. Sun et al. 2001[9]: In this paper, a novel approach was used to find the optimal location of piezoelectric sensors and actuators on a plate with a simply supported boundary condition. It was found that the location which was found by using this approach was most effective for vibration control. The optimum actuator location was found out by minimising the control spill over and energy and for sensor element is found out by minimising the observation error caused by sensor.

P. Liu and V. S. Rao 2002[10]: In this paper, optimal placement of actuator and sensor for cantilever plate was found out by considering the both open loop system and closed loop optimal criteria. In open loop system, the controlled modes are calculated on the basis of observability and controllability. In closed loop criteria, the location having high index values was determined by techniques like preferable pole location, H_2 and H_∞ norms. With the help of this technique, optimal location is very easy with high control performance and reduction of burden in computation.

Y J Yan and L H Yam 2002[11]: Optimum location of actuator is found out by using redundant binary-valued genetic algorithm codding in structures for vibration control. Then the location found by this method is more effective for achieving better vibration control.

D. Halim and S.O.R. Moheimani 2003[12]: In this paper, optimal location of collocated piezoelectric actuator and sensor on a thin plate with simply supported boundary conditions is found out by the notions of modal controllability and by adding an extra spatial controllability constraint in the optimization procedure. This optimum location is validated by conducting experimental analysis in which Analytical and finite element modelling was done by using STRAND7 software. But it is found out that optimisation methodology was applicable only up to limited modes.

G. Caruso et al. 2003[13]**:** This paper summarises about the vibration control of an elastic plate by using multiple piezoelectric sensors and actuators. To evaluate the performance obtained by different combinations of actuators and sensors was done by H2 control laws. The result obtained is compared with the simulation results. It was found out that if an excessive control voltage will damage the piezoelectric actuators and performance of a vibration control will be high if multiple sensors and actuators.

P.U. Sik et al. 2003[14]: This paper summarises about the optimal location of piezoelectric sensors and actuators by using measures modal controllability and observability which was defined in balanced coordinate. It was found that the method used was more accurate and practically more useful then the convection measures.

I.S. Sadek et al. 2003[15]**:** In this paper, the several laws which are applied on plates was examined by carrying a piezo patch. This piezo element results are transformed to way of integral form in order to rectify the problem caused by displacement which contains feedback control. Finally, the results obtained are converted to linear solution and then comparison was made between the two plates.

G. L. C. M. de Abreu et al. 2004[16]**:** This paper summarises about the how plate is modelled when it was attached with piezo patch material. In order to derive eq.s for patch material, plate was modelled according to Kirchhoff theorization. Then the results obtained are compared analytically with ANSYS workbench software and it was found approximately same in both cases. From this paper, it was understood how electro-mechanical coupling is done by placing piezo patch element.

J.M.S. Moita et al. 2006[17]**:** In this paper, optimal location of piezoelectric patch for structures was found out by structural optimisation methodology which was based on simulated annealing algorithm.

W. Seemann et al. 2006[18]**:** In this paper, the waves which are excited from elastic materials and nested by considering two piezo patches on both sides. It is concluded by doing comparison between these methods and observed that the method which was actuation will result in quick effect of materials and sizes

K. R Kumar et al. 2007[19]**:** This paper summarises about the optimal placement of collocated piezoelectric actuator–sensor pairs on a thin plate by using a GENETIC ALGORITHM based on linear quadratic regulator (LQR) controller performance. The region where high model strain energy is produced is the Optimum location of actuator-sensor pairs on plate. The classical control laws, like direct proportional feedback, constant-gain negative velocity feedback and optimal control law which is based on LQR theory was used to study the performance of active vibration control. It is concluded that LQR optimal control will be more effective in vibration control then compared to other laws.

W. Gawronski and K. B. Lim 2007[20]**:** In this paper, optimal location of piezoelectric patch on flexible structures was found out by evaluation of joint controllability and observability property by using the r.m.s law of Hankel singular values.

Z. c Qiu et al. 2007[21]**:** In this paper, optimal location of piezoelectric actuator and sensor is based on degree of observability and controllability indices for cantilever plate. The results which obtained through theoretical are compared by conducting experimental study and found out that the results are feasible.

M. Pietrzakowski 2008[22]**:** This paper deals with the control of vibrations produced by rectangle plates. For this reduction, piezo element is placed on both sides of plate which will perform the control of velocity. This model was carried out by Kirchhoff conjecture. It is concluded that if electrical bend and mechanical merging is made then plate stiffness and natural frequencies will increase and damping performance will be poor on thin laminated plates.

G. Zhao et al. 2008[23]: Optimum location of piezoelectric patches was found out by topological optimisation method and a continuous variable optimisation method. A new sensitivity analysis method which was based on Newmark time integration of structural transient dynamic responses was developed for topological optimisation

M. Guney and E. Eskinat 2008[24]: In this paper, a closed loop method is used in which unconstrained nonlinear optimization algorithm i.e. gradient based optimisation algorithm was developed in order to find the optimum location. It was found that the eq.s which are obtained in optimisation are simply reduced to quadratic eq.s. Time consumed for solving these eq.s is less then compared to solving AREs fully.

K.D. Dhuri, P. Seshu 2009[25]**:** In this paper, Multi-objective genetic algorithm was used in order to find the optimal location of piezoelectric actuator. Finite element technique has been used for the evaluation of the objective function in algorithm. The obtained result was compared with the exhaustive search method. It was found that result was same for multiple and short piezo.

Z. Qiu et al. 2009[26]**:** This paper discusses about the requirement of aerospace applications such as it should be light weight and high resistance strength. Due to external disturbances in space, lot of bending and rotational vibrations will affect the plane and leads to imbalance of plane, causes danger. In order to avoid this piezoelectric patch as actuator and sensor are placed at best preferred location. Gyroscopic sensor is also placed in order to control the vibrations. Finally, it is concluded by conducting experimental setup and made validation that piezo and gyro-sensor will lower the vibrations.

V. Gupta et al. 2010[27]: In this paper, A broad technical review was given about the optimization criteria for the optimal location of piezoelectric sensors and actuators on plate is presented.

I. Bruant et al. 2010[28]: In this paper, optimal placement of a piezoelectric actuator and sensor on a plate for simply supported boundary condition was found out by genetic algorithm and the result which is obtained was validated by finite element modelling results. It was found that the procedure can be applied to more complex structures for vibration control.

Levent 2010[29]**:** This paper reviews about the problems related to vibrations can be easily solved by one stage of finite technique through ANSYS work bench software then results obtained are validated through analytical technique. ANSYS software is considered by testing analytical results of locating the control of mechanical system which includes piezoelectric. It is concluded that control of vibrations produced by structures is analysed by finite element analysis with the help of Integration control.

M.R. Sajizadeh and I. Z. M. Darus 2010[30]: In this paper, optimum location of piezoelectric actuator on a square plate is found out by observability Grammian by using the Genetic Algorithm and Developed Optimisation Algorithm. It was observed that most vibration control was found in first and second mode of frequency.

L. Starek et al. 2010[31]: In this paper, optimal location of piezoelectric actuator and sensor was found out by a method which was based on grammians. The results which are obtained were compared with the matrix norms of H_∞ and observed that the result was same. The method which used grammians was applicable for the location of small actuator and sensor.

B. Behjat et al. 2011[32]**:** This paper is deals with the free vibrations and transient responses integrated with piezoelectric patch material are found out by shear deformation theory when electrical and mechanical loads are loaded is carried out by finite element modelling method. It is extracted that when power index is increased then the influence will be high in larger finite graded piezoelectric material parameter. If this clamped plate is having high volume index, then it has higher frequencies then compared to simply supported plate.

R. Dutta et al. 2011[33]: In this paper, optimal location of two collocated piezoelectric actuator and sensor was found out by two new swarm intelligence algorithms such as artificial bee colony and glow worm swarm optimisation algorithms. It was found out that the result which is obtained from this algorithm are so robust in practise and these algorithms can also be applied for optimal location of five piezoelectric actuator and sensor on plate.

A H Daraji and J M Hale 2012[34]: In this paper, optimal placement of piezoelectric actuator and sensor pair on isotropic plates was found by using finite element modelling and Hamilton's principle which was based on first order shear deformation by considering piezoelectric electro-mechanical coupling effects, mass and stiffness. For the location of eight

and ten piezoelectric actuators an MATLAB m-code genetic algorithm was built incorporating the new half and quarter chromosome technique. Due to this new technique, the reduction in calculations and search space of genetic algorithm was very high.

F. Bachmann et al. 2012[35]: In this paper, optimum location of piezoelectric patch was found by strain energy which was based on finite element approach. The obtained result was compared with the state of the art approach.

J. M Hale and A. H Daraji 2012[36]: In this paper, optimal placement of piezoelectric sensors and actuators on flexible structures was found out by genetic algorithm in which a new fitness function is taken based on modified H_{∞}. It is found out that new fitness function achieved a higher reduction in vibration control and cost of the computation is also low.

S. K. Parashar et al. 2013[37]**:** This paper deals with non-linear vibration behaviour such as amplitude and voltage of piezo-integrated structures when it is subjected to weak electric field for finite element modelling. The piezo-ceramic was considered because of high dielectric constant and top piezoelectric constant. In finite element modelling, the eq.s which are obtained are derived by introducing piezo-ceramics. These obtained eq.s are solved by modal reduction method.

A. Zolfagharian et al. 2013[38]**:** This paper summarises about how to control the unnecessary disturbance or vibration produced by automobile parts such as wipers. This is solved by considering passive control process in which multi body system testing in ABAQUS CAE software was used in order to find out the frequencies produced by them and validated through finite element analysis by prototyping. Finally, it is concluded that the disturbances or vibrations caused by wind, rain for wiper can be reduced by considering active controllers.

M. Ansari et al. 2013[39]**:** Vibration control in cantilever plate is done by attaching constrained layer damping patches on surface at optimum location. Optimum location of patch was found out by novel set method. This location was validated with the experimental results by proposed optimisation technique for 2D structures.

T. Nestorovic and M. Trajkov 2013[40]**:** In this paper, optimal location of piezoelectric actuator and sensor for large flexible structures is found out by balanced model reduction. This method is based on properties of the H_2 and H_∞ norms and approximations for their determining. This method was applied to cantilever beam, beam clamped on both sides and clamped plate to found out the optimal location of actuator and sensor It is concluded that the balanced model reduction method was an efficient modelling procedure with large no degrees of freedom.

K.A. M. Nor et al. 2013[41]**:** In this paper, optimal location of piezoelectric actuator and sensor for simply supported plate was found out by swarm intelligent algorithm called Ant Colony Optimization. The result obtained was verified by Genetic Algorithm.

N. Darivandi et al. 2013[42]**:** In this paper, it was proved that the optimisation algorithm is the faster and more accurate then compared to the genetic algorithm for finding the optimal location of piezoelectric actuator.

Z. Qiu et al. 2014[43]**:** This paper summarises how finite element modelling was used for a cantilever plate with the combination of piezo element. Then the frequencies obtained by finite method is verified by ANSYS APDL software. By placing sensor and actuator at most preferable location, then the vibrations which are produced by buckling can be reduced. First two frequencies which are obtained through them was having high modes.

M. Rahmoune 2014[44]**:** In this paper, optimal location of piezoelectric patch is found out by the application of topology optimisation combined with homogenization method. The result is valid only up to certain configurations and the calculation time is so conditional and very slow.

A. Kumar et al. 2014:[45] This paper summarises about the problems faced by the automobile passenger compartments and aerospace interior for control of low frequency interior noise. By active structural acoustic control approach issue related to the feedback control of interior sound was proposed. The feedback control strategy was used when signals are not derived in application. Kalman filter was designed to estimate the status of cavity structure subjected to deflection depending upon piezoelectric patch mounted on flat plate at

particular location. The optimal location for piezoelectric sensor and actuator was also proposed for effective detection of acoustic potential energy.

X. Huang et al. 2014[46]**:** This paper summarises about the optimal placement of piezoelectric sensors and actuators on thin cantilever plate by using modal-based linear quadratic independent modal space controller method. Linear quadratic regulations were taken as main objective for efficient location. In order to avoid the crossover and mutation probability, an adaptive genetic algorithm was considered. It was found that the technique is more effective and feasible.

Z. Qiu, et al. 2014[47]**:** In this paper, optimal location of piezoelectric patch on flexible plate at clamped boundary condition was found out by Genetic Algorithm which is modelled in ANSYS software. It was observed that filtered-X least mean square feedforward control algorithm showed more performance in vibration control then compared to proportionality Derivative control algorithm.

S.K. Vashist and D. Chhabra 2014[48]**:** In this paper, optimal location of piezoelectric actuators on thin cantilever plate was found out by integer codded genetic algorithm by taking controllability index as fitness function and Linear Quadratic Regulator optimal technique was applied in order to study the effectiveness of a vibration control. From results, location obtained through this technique was more effective for control of vibration.

S. Thenozhi et al. 2014[49]**:** In this paper, it was discussed about the control of vibration caused by environments can be done by algorithms such as proportional derivative. This derivative was applicable for both linear structures as well as non-linear structures also. Then algorithm was considered in order to get the permanence as if total vibrations produced by them are terminated. It is concluded from this paper even though selection of gains was not appropriate, these active variables will lower the vibrations.

Z. Shunqi et al. 2014[50]**:** This paper summarizes as appropriate vibration controller for thin-walled structures is finite element modelling which is based on first order shear deformation method. Vibrations may include free or forced depending upon structure. In order to control this PID is damped on both sides. Finally, comparison is made by using LQR method. This result is validated by piezoelectric layered smart plate for various excitations.

Conclusion is made from this as PID method gives most appropriate results then compared to LQR control whereas D control the free vibrations but has no effect on forced.

M. Kerboua et al. 2014[51]**:** This paper revises about the vibration controller by using smart materials such as piezoelectric by applying a shunt control method. Initially Finite element method is used for optimum location and design of a piezoelectric, then the results which is obtained was 42% in reduction of vibrations. This is validated by MATLAB software by calculating natural frequency results and location also.

N. Sehgal et al. 2014[52]: This paper reviews about the Meta-Heuristics Approaches for optimal location of piezoelectric actuator and sensor on a flexible cantilever plate such as swarm intelligence method, evolutionary approach, reactive tabu searching optimization technique and simulated annealing and comparison was made between them.

K. Khorshidi et al. 2014[53]**:** In this paper, vibrations produced by the circular plate was controlled by placing two piezo electric patches with different thickness on both sides as actuator and sensor was carried out by classical plate theory The transverse sound waves which are excited from circular plate are controlled by using Fuzzy Logic Controller (FLC) and Linear-Quadratic Regulator (LQR) techniques. It was concluded that the frequencies obtained through this theory was most efficient to reduce vibrations at very quickly.

M. K. Kwak et al. 2015[54]**:** This paper reviews about how the vibrations produced by plate are controlled. Piezo-electric actuator and sensor was bonded on two sides of plate in order to solve the problem. In experimental setup, the frequencies of a submerged plate are found out by introducing transfer function in this actuator and sensor. The frequency results which are obtained is validated by comparing with theoretical study of virtal mass model method. Finally, it was concluded that the natural frequency results which are obtained through this technique are most effective and also it was easy prediction for any changes in frequencies when it was partially submerged in a fluid.

M. J. Jweeg et al. 2015[55]**:** This paper reviews about the control of vibration on fluid pipes was done by piezoelectric patches and then carried out to experimentally and simulation was done in ANSYS workbench and APDL software. Finally, it was concluded that as fluid velocity increases which will reduces the natural frequency. If piezoelectric patch is placed at

optimum location, it will result in reduction of vibrations produced by pipe and reduces displacement.

W. Larbi et al. 2016[56]**:** In this paper, work is carried out by the sound which is transmitted through double laminated plate can be evaluated by piezoelectric shunt method. This gives to high cost, for low cost modal reduction method is used. In modal bases method, static correction was considered in order to take the higher modes effect. In spite of the size is reduced, this method was proved to be most efficient in case of simulation of laminated plates. In order to calculate the loss of sound transmission is done by Rayleigh integral method.

V. Jawali et al. 2016[57]**:** In this paper, most preferable location of piezoelectric sensor and actuator on a plate was found out by genetic algorithm by minimising the maximum non-detection probability as objective function and the result obtained was compared in MATLAB software by considering the continuous unit square plate with the help of fminimax solver. This technique was more effective for real structures.

A. Koszewnik and Z. Gosiewski 2016[58]**:** In this paper, best preferred location of piezoelectric actuator and sensor on flexible rectangular plate with simply supported boundary condition was found out by Mindlin plate theory and the finite element method. The obtained location was verified by conducting experimental analysis.

K. Kulinski et al. 2016[59]**:** This paper reviews about the beam of stability and disturbances produced when it is loaded at two ends and piezoelectric patch which is placed at optimal location. It is concluded that the piezo had affected the frequencies which are produced due to transverse vibrations. But the first two results obtained had more accuracy then compared to analytical model. If more piezo patches are placed, then the result will be more accuracy.

CHAPTER-4

SCOPE OF THE STUDY

- Vibrations produced in the systems such as automobiles, aerospace structures etc., are due to disturbances from surroundings.

- So, scope is to control the vibrations by attaching a piezoelectric element to the system.

- Patch cannot be placed at every location because where the displacement is zero, the strain will be zero.

- The exact location of piezoelectric element was found out by viewing method. This method was applied to the plate with different boundary conditions like free-free, simply supported, cantilever, clamped at all edges of the plate.

- Then pole placement methodology can be applied for the design of direct output feedback control. By plotting open and closed loop pole zero maps, there is scope of finding the optimal control gain value at optimum location of piezoelectric patch on plate.

CHAPTER-5

OBJECTIVES OF THE STUDY

There are three main objectives which represents the study are

- Intially, finding the optimum location of piezoelectric patch on plate.
- Later, finding out the optimal velocity gain value for the good control of vibrations
- Finally, finding the node number where to apply the hammer excitation force for maximum reduction of vibrations produced by structure.
- The above objectives can be resolved by these steps: A viewing method was used to find out the most preference location of piezo-electric patch on a plate.
- The direct output feedback control strategy was used for finding the optimal velocity gain value which was designed by used pole placement technique.
- In this technique, open loop poles map is plotted by taking the values of displacement gain (G_d) and velocity gain (G_v) has zero. Then closed loop poles map is plotted by considering the 3 different cases like [G_v=0; $G_d \neq 0$], [$G_v \neq 0$; $G_d \neq 0$] and [G_d=0; $G_v \neq 0$].
- Then nodal displacement response at different node number and different response number on plate for different cases of G_d and G_v are represented in order to check whether the displacement of a structure is damped out completely or not.

CHAPTER-6

MATERIALS AND RESEARCH METHODOLOGY

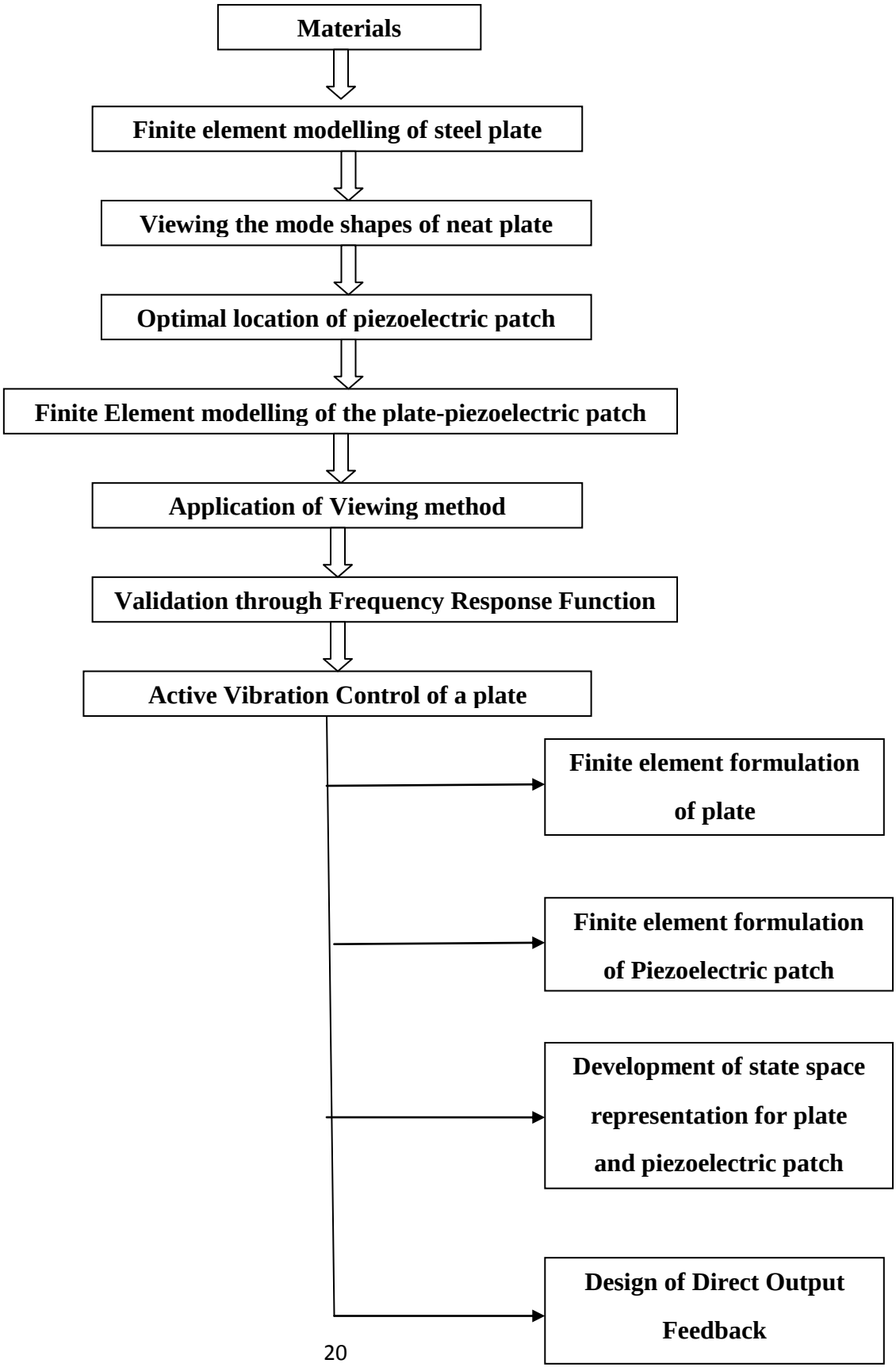

Consider a steel plate by considering as length of 0.261m, breadth of 0.3m, and thickness of 0.001m. Properties of steel are taken as Young's modulus of E=200 GPa, Density of ρ=7800Kg/m^3, Poisson ratio of ν = 0.3.

A piezo P-876 A12 Dura Act piezoelectric patch is considering by taking a length of 0.0522m, breadth of 0.05m and thickness of 0.0005m. Properties of piezoelectric patch is taken as Young's modulus of E=23.3 GPa, Density of ρ=7800Kg/m^3 Poisson ratio of ν = 0.34, Piezoelectric strain coefficient e31 = -8.9678 C/m^2, e32 = -8.9678 C/m^2, Dielectric constant ε33 = 6.6075e^{-9}[45].

Optimum location of piezo element patch on rectangular plate was found out by viewing method though the modal analysis from ABAQUS CAE software where inbuilt options like piezo element properties etc.,

6.1 Finite element modelling of steel plate: A Finite element model of the steel plate is created in ABAQUS software. Meshing is done by taking the size of 10×12. Then material steel properties are added to the plate. Then by selecting step manager, under that procedure like linear perturbation then frequency is selected. Then next selecting load, choosing the boundary condition as clamped at all edges i.e. displacement and rotation is zero. Finally, job was created and Modal shapes of plate are extracted out. Similarly, applying the cantilever boundary condition to the left side of the plate i.e., displacement and rotation at the left side of the plate are taken as zero and mode shapes are extracted. Similarly, free-free and simply supported boundary condition was applied to the plate.

6.2 Viewing the mode shapes of neat plate: In this method, the optimal location is found out by observing the modal shapes of plate, piezo cannot be placed on the nodal line where displacement is zero and strain is also zero it doesn't provide a vibration control.

6.3 Optimal location of piezoelectric patch: A patch cannot be placed at some locations on a plate because of vibrations produced by plate. In order to avoid these optimal location is found out. Optimum location is the place in which the piezoelectric patch was not placed on nodal line. If piezo is placed at a location other than optimum, then the control of vibrations produced by a plate will not be more effective Then Optimal location of piezoelectric patch on plate is found out by proposing a method as Viewing.

6.4 Finite Element modelling of the plate-piezoelectric patch: A Finite element model of piezo P-876 A12 Dura Act piezoelectric patch is created in ABAQUS software. Meshing is done by taking the size of 2×2. The patch is attached to the steel plate by using tie which is taken from constraint option in order to control the vibrations produced by the plate. Similarly, job was created and Modal shapes of plate-piezoelectric patch are extracted out.

6.5 Application of Viewing method: By using this method, the optimum location of the piezoelectric patch on the plate for different boundary conditions. Through this method, it is observed that if piezo is placed at a location where nodal lines are passing then the control of vibrations will not be so effective.

6.6 Validation through Frequency Response Function: Frequency response function is also called as a transfer function. It was used in modal analysis where the response of a vibration produced by structure was measured with respect to the applied force. The optimum location which was found for different boundary conditions like free-free, simply supported, cantilever, clamped at all edges was validated by conducting FRF analysis.

6.7 Active Vibration Control of a plate: In order to extract the results of mass and stiffness matrix of plate, the finite element formulation of plate was done. Then finite element formulation plate with piezoelectric patch was formulated for mass and stiffness matrix of a plate with piezoelectric patch.

6.7.1 Finite element formulation of plate: By using Kirchhoff assumptions as transverse normal stays as straight even after the deformation of plate and rotation of the plate will be always perpendicular to the mid surface of the plate, formulation of plate was modelled. Displacement fields like u, v and w with respect to x-axis, y-axis and z-axis are expressed by using Kirchhoff hypothesis.

Displacement of plates $$u = -z\frac{dw}{dx} \quad (3)$$

$$v = -z\frac{dw}{dy} \quad (4)$$

$$w = w(x, y) \quad (5)$$

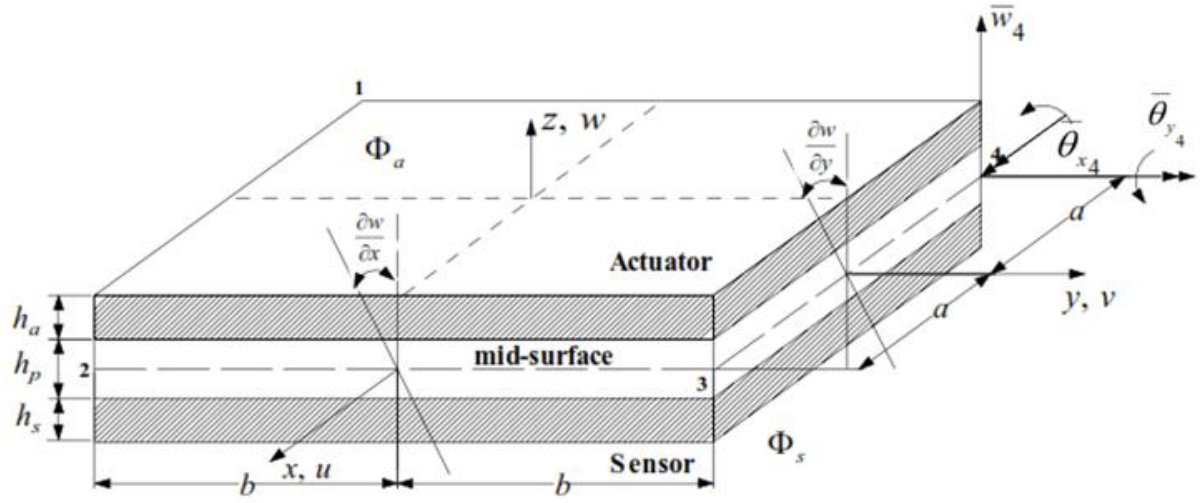

Fig (6.1): Coordinate system of a plate with integrated piezoelectric patches

Curvatures of plate $k_x = -\frac{\partial^2 w}{\partial x^2}$ (6)

$$k_y = -\frac{\partial^2 w}{\partial y^2} \quad (7)$$

$$k_{xy} = -2\frac{\partial^2 w}{\partial x \partial y} \quad (8)$$

As the deformation caused by transverse strain is neglected and strains expressed in the form of displacements are shown below as

Strains relation $\in_x = -z\frac{\partial^2 w}{\partial x^2}$ (9)

$$\in_y = -z\frac{\partial^2 w}{\partial y^2} \quad (10)$$

$$\gamma_{xy} = -2z\frac{\partial^2 w}{\partial x \partial y} \quad (11)$$

$$\in = \left\{\in_x \in_y \gamma_{xy}\right\}^T = -z\left\{\frac{\partial^2 w}{\partial x^2} \quad \frac{\partial^2 w}{\partial y^2} \quad 2\frac{\partial^2 w}{\partial x \partial y}\right\}^T \quad (12)$$

The nodal displacement matrix of a plate at node ‘i’ was represented as

$$\{d_i\} = \{w_i \quad \theta_{xi} \quad \theta_{yi}\}^T \quad (13)$$

The rotations are expressed in the form of transverse displacements as

$$\theta_x = \frac{\partial w}{\partial y} \tag{14}$$

$$\theta_y = -\frac{\partial w}{\partial x} \tag{15}$$

In order to produce a positive rotation with respect to y-axis, the '-'ve sign in θ_y relation as '-'ve displacement w is required.

Displacement function:

$$w(x_i, y_i) = a_1 + a_2 x_i + a_3 y_i + a_4 x_i^2 + a_5 x_i y_i + a_6 y_i^2 + a_7 x_i^3 + \\ + a_8 x_i^2 y_i + a_9 x_i y_i^2 + a_{10} y_i^3 + a_{11} x_i^3 y_i + a_{12} x_i y_i^3 \tag{16}$$

The transversal field 'w' was represented as

$$w = \{p\}^T \{a\} \tag{17}$$

$$\{p\}^T = \{1 \;\; x \;\; y \;\; x^2 \;\; xy \;\; y^2 \;\; x^3 \;\; x^2 y \;\; xy^2 \;\; y^3 \;\; x^3 y \;\; xy^3\} \tag{18}$$

The coefficient vector {a} was represented as

$$\{a\} = \{a_1 \;\; a_2 \;\; a_3 \;\; a_4 \;\; a_5 \;\; a_6 \;\; a_7 \;\; a_8 \;\; a_9 \;\; a_{10} \;\; a_{11} \;\; a_{12}\}^T \tag{19}$$

The nodal displacement field vector $\{d_i\}$ for rectangular plate was represented as

$$\{d_i\} = \{w_1 \;\; \theta_{x1} \;\; \theta_{y1} \;\; w_2 \;\; \theta_{x2} \;\; \theta_{y2} \;\; w_3 \;\; \theta_{x3} \;\; \theta_{y3} \;\; w_4 \;\; \theta_{x4} \;\; \theta_{y4}\}^T \tag{20}$$

$$\{d_i\} = [C]\{a\} \tag{21}$$

Where [C] is 12x12 matrix given by eq. (20)

$$[C]=\begin{bmatrix}
1 & x_1 & y_1 & x_1^2 & x_1y_1 & y_1^2 & x_1^3 & x_1^2y_1 & x_1y_1^2 & y_1^3 & x_1^3y_1 & x_1y_1^3 \\
0 & 0 & 1 & 0 & x_1 & 2y_1 & 0 & x_1^2 & 2x_1y & 3y_1^2 & x_1^3 & 3x_1y_1^2 \\
0 & -1 & 0 & -2x_1 & -y_1 & 0 & -3x_1^2 & 2x_1y & -y_1^2 & 0 & -3x_1^2y_1 & -y_1^3 \\
1 & x_2 & y_2 & x_2^2 & x_2y_2 & y_2^2 & x_2^3 & x_2^2y_2 & x_2y_2^2 & y_2^3 & x_2^3y_2 & x_2y_2^3 \\
0 & 0 & 1 & 0 & x_2 & 2y_2 & 0 & x_2^2 & 2x_2y & 3y_2^2 & x_2^3 & 3x_2y_2^2 \\
0 & -1 & 0 & -2x_2 & -y_2 & 0 & -3x_2^2 & 2x_2y & -y_2^2 & 0 & -3x_2^2y_2 & -y_2^3 \\
1 & x_3 & y_3 & x_3^2 & x_3y_3 & y_3^2 & x_3^3 & x_3^2y_3 & x_3y_3^2 & y_3^3 & x_3^3y_3 & x_3y_3^3 \\
0 & 0 & 1 & 0 & x_3 & 2y_3 & 0 & x_3^2 & 2x_3y & 3y_3^2 & x_3^3 & 3x_3y_3^2 \\
0 & -1 & 0 & -2x_3 & -y_3 & 0 & -3x_3^2 & 2x_3y & -y_3^2 & 0 & -3x_3^2y_3 & -y_3^3 \\
1 & x_4 & y_4 & x_4^2 & x_4y_4 & y_4^2 & x_4^3 & x_4^2y_4 & x_4y_4^2 & y_4^3 & x_4^3y_4 & x_4y_4^3 \\
0 & 0 & 1 & 0 & x_4 & 2y_4 & 0 & x_4^2 & 2x_4y & 3y_4^2 & x_4^3 & 3x_4y_4^2 \\
0 & -1 & 0 & -2x_4 & -y_4 & 0 & -3x_4^2 & 2x_4y & -y_4^2 & 0 & -3x_4^2y_4 & -y_4^3
\end{bmatrix} \quad (22)$$

$$\{a\}=[C]^{-1}\{d\} \quad (23)$$

Then substituting Eq. (21) in Eq. (15), the obtained expression is show in Eq. (22)

$$w=\{P\}^T[C]^{-1}\{d_i\} \quad (24)$$

$$w=[N]\{d_i\} \quad (25)$$

Where [N] is the shape function which was represented in eq. (26)

$$[N]=\{P\}^T[C]^{-1} \quad (26)$$

Curvature matrix was given as

$$\{k\}=\begin{Bmatrix}k_x\\k_y\\k_z\end{Bmatrix}=\begin{Bmatrix}-2a_4 & -6a_7x & -2a_8y & -6a_{11}xy\\ -2a_6 & -2a_9x & -6a_{10}y & -6a_{12}xy\\ -2a_5 & -4a_8x & -4a_9y & -6a_{11}x^2 & -6a_{12}y^2\end{Bmatrix} \quad (27)$$

$$\{k\}=[Q]\{a\} \quad (28)$$

[Q] is the coefficient of matrix, from relation {a]

$$\{k\}=[B]\{d\} \quad (29)$$

$$[B]=[Q][C]^{-1} \quad (30)$$

[D] is the consecutive matrix of isotropic materials

$$[D]=\frac{E_P}{1-\upsilon^2}\begin{bmatrix}1 & \upsilon & 0\\ \upsilon & 1 & 0\\ 0 & 0 & \dfrac{1-\upsilon}{2}\end{bmatrix} \tag{31}$$

Stiffness matrix of plate $[k]=\iint[B]^T[D][B]dxdy$ where

By substituting the results of [B], [D] in stiffness relation. It was found size of matrix is of order 12x12

Substitute Eq. (24) in Eq. (12) then

$$\{\in\}=-z\left\{\frac{\partial^2\{P\}^T}{\partial x^2}\quad\frac{\partial^2\{P\}^T}{\partial y^2}\quad 2\frac{\partial^2\{P\}^T}{\partial x\partial y}\right\}^T[C]^{-1}\{d_i\} \tag{32}$$

$$\{\in\}=-z[L_k][C]^{-1}\{d_i\} \tag{33}$$

$$[L_k]=\begin{bmatrix}\dfrac{\partial^2\{P\}^T}{\partial x^2} & \dfrac{\partial^2\{P\}^T}{\partial y^2} & 2\dfrac{\partial^2\{P\}^T}{\partial x\partial y}\end{bmatrix}^T \tag{34}$$

By differentiating the eq. (17) twice, the results are expressed in the eqns. (35), (36) and (37)

$$\frac{\partial^2\{P\}^T}{\partial x^2}=\begin{bmatrix}0 & 0 & 0 & 2 & 0 & 0 & 6x & 2y & 0 & 0 & 6xy & 0\end{bmatrix} \tag{35}$$

$$\frac{\partial^2\{P\}^T}{\partial y^2}=\begin{bmatrix}0 & 0 & 0 & 0 & 0 & 2 & 0 & 0 & 2x & 6y & 0 & 6xy\end{bmatrix} \tag{36}$$

$$\frac{\partial^2\{P\}^T}{\partial x\partial y}=\begin{bmatrix}0 & 0 & 0 & 0 & 1 & 0 & 0 & 2x & 2y & 0 & 3x^2 & 3y^2\end{bmatrix} \tag{37}$$

The obtained results are substituted in the eq. (34)

$$[L_k]=\begin{bmatrix}0 & 0 & 0 & 2 & 0 & 0 & 6x & 2y & 0 & 0 & 6xy & 0\\ 0 & 0 & 0 & 0 & 0 & 2 & 0 & 0 & 2x & 6y & 0 & 6xy\\ 0 & 0 & 0 & 0 & 2 & 0 & 0 & 4x & 4y & 0 & 6x^2 & 6y^2\end{bmatrix} \tag{38}$$

The displacement fields like w, u and v are represented in vector form {d} as shown in eq. (39)

$$\{d\}=\begin{Bmatrix}w & u & v\end{Bmatrix}^T \tag{39}$$

By substituting Eqns. (3), (4) and (5) in Eq. (39), gives the expression as shown in Eq. (40)

$$\{d\} = \begin{Bmatrix} w & -z\frac{dw}{dx} & -z\frac{dw}{dy} \end{Bmatrix}^T \tag{40}$$

Sub Eq. (21) in Eq. (40), the following expression obtained is shown in Eq. (41)

$$\{d\} = [L_M]^T [H][C]^{-1} \{d_i\} \tag{41}$$

Where $[L_M]^T$ and $[H]$ are shown in Eq. (42) and Eq. (43)

$$[L_M]^T = \begin{Bmatrix} \{P\}^T & \frac{\partial \{P\}^T}{\partial x} & \frac{\partial \{P\}^T}{\partial x} \end{Bmatrix}^T \tag{42}$$

$$[H] = \begin{bmatrix} 1 & 0 & 0 \\ 0 & -Z & 0 \\ 0 & 0 & -Z \end{bmatrix} \tag{43}$$

6.7.2 Finite element formulation of Piezoelectric patches: The stress tensor relation and electric displacement relations are taken from [16]

$$\{\sigma\} = [C^E]\{\in\} - [e]\{E\} \tag{44}$$

$$\{D\} = [e]^T \{\in\} + [\xi^S]\{E\} \tag{45}$$

where the superscript *S* means that the values are measured at constant strain and the superscript *E* means that the values are measured at constant electric field, {s} is the stress tensor, {*D*} is the electric displacement vector, {e} is the strain tensor, {*E*} is the electric field, $[C]^E$ is the elastic constants at constant electric field, [*e*] denotes the piezoelectric stress coefficients, and $[\xi^S]$ is the dielectric tensor at constant mechanical strain. Then relation between [*e*] and [*d*], the piezoelectric strain coefficient is represented in eq. (44)

$$[e] = [C^E][d] \tag{46}$$

Let's assuming the electric field (*E*) is constant through the actuator and sensor elements thickness, the gradient operators are:

$$E = \frac{-d\phi_z}{dz} = -B_z\phi = -\frac{\phi}{h} \tag{47}$$

Hamilton's principle was considered as for the finite element formulation of piezoelectric patch

$$\int_{y_1}^{y_2}\left[\delta\left(T-U+W_e-W_m\right)+\delta_W\right]dt=0 \tag{48}$$

T is the kinetic energy of a plate with piezoelectric patch which was expressed in eq. (49)

$$T=\frac{1}{2}\int_V \rho\{\dot{d}\}^T\{\dot{d}\}dv \tag{49}$$

Differentiating the eq. (41) with respect to y constant for the value of $\{\dot{d}\}$ then

U is the potential energy of a plate with piezoelectric patch which was expressed in eq. (50)

$$U=\frac{1}{2}\int_V \{\in\}^T\{\sigma\}\,dv \tag{50}$$

dv is defined as in the eq. (51)

$$dv=dv_p+dv_a+dv_s \tag{51}$$

From eq. (51) dv_p refers to the change in volume with respect to the plate and expressed in the eq. (52)

$$dv_p=\int_{-h_p/2}^{h_p/2}\int_{-a}^{a}\int_{-b}^{b}dxdydz \tag{52}$$

From eq. (51) dv_a refers to the change in volume with respect to actuator and expressed in the eq. (53)

$$dv_a=\int_{h_p/2}^{h_p/2+ha}\int_{-a}^{a}\int_{-b}^{b}dxdydz \tag{53}$$

From eq. (51) dv_s refers to the change in volume with respect to sensor and expressed in the eq. (54)

$$dv_s=\int_{h_p/2-h_s}^{h_p/2}\int_{-a}^{a}\int_{-b}^{b}dxdydz \tag{54}$$

From eq. (48) W_e represents the work done by the electrical forces which was given in eq. (55)

$$W_e=\frac{1}{2}\int_V \{E\}^T\{D\}dv \tag{55}$$

Here {D} is the electric displacement

From eq. (48) δW expression was given in eq. (56)

$$\delta W = \int_V \{\delta d\}^T \{f_b\} dv + \int_A \{\delta d\}^T \{f_S\} dA - \int_A \delta\phi\sigma_e dA \tag{56}$$

$\{f_b\}$, $\{f_S\}$ and σ_e represents the body force, surface force and electrical stress.

Then sub eq. (44) in eq. (50) and eq. (45) in eq. (55) then the modified expression of potential energy and work done by electrical force was given in eq. (57) and eq. (58)

$$U = \frac{1}{2}\int_V \{\in\}^T \left[C^E\right]\{\in\} - \frac{1}{2}\int_V \{\in\}^T [e]\{E\} dv \tag{57}$$

$$W_e = \frac{1}{2}\int_V \{E\}^T [e]^T \{\in\} + \frac{1}{2}\int_V \{E\}^T \left[\xi^S\right]\{E\} dv \tag{58}$$

Then sub eqns. (49), (56), (57), (58) in eq. (48), the modified expression was given in eq. (59)

$$\int_{y_1}^{y_2} \left[\begin{array}{l} \int_V \rho\{\delta d\}^T \{\ddot{d}\} dv - \int_V \{\delta \in\}^T \left[C^E\right]\{\in\} + \int_V \{\delta \in\}^T [e]\{E\} dv + \\ \int_V \{E\}^T [e]^T \{\in\} + \int_V \{E\}^T \left[\xi^S\right]\{E\} dv + \\ \int_V \{\delta d\}^T \{f_b\} dv + \int_A \{\delta d\}^T \{f_A\} dA - \int_A \delta\phi\sigma_q dA \end{array} \right] dt = 0 \tag{59}$$

Sub Eqns. (41), (25), (47) in eq. (59) then the modified expression was given in eq. (60)

$$\int_{y_1}^{y_2} \left[\begin{array}{l} \{\delta d\}^T \left[\left[M^e_{dd}\right]\{\ddot{d}_k\} + \left[K^e_{dd}\right]\{d_k\} + \left[K^e_{d\phi}\right]\{\phi\} - \{\bar{f}\} \right] + \\ + \{\delta\phi\} \left[\left[K^e_{\phi d}\right]\{d_k\} + \left[K^e_{\phi\phi}\right]\{\phi\} + \{Q_a\} \right] \end{array} \right] dt = 0 \tag{60}$$

Where $\left[M^e_{dd}\right]$, $\left[K^e_{dd}\right]$, $\left[K^e_{d\phi}\right]$ or $\left[K^e_{\phi d}\right]$, $\left[K^e_{\phi\phi}\right]$, $\{Q_a\}$ and $\{\bar{f}\}$ are expressed in the eqns. (61), (62), (63), (64), (65) and (66)

$$\left[M^e_{dd}\right] = \rho\int_V [C]^{-T} [L_M][H][L_M]^T [C]^{-1} dv \tag{61}$$

$$\left[K^e_{dd}\right] = [C]^{-T} \int_V z^2 [L_K][D][L_K]^T [C]^{-1} dv \tag{62}$$

$$\left[K^e_{d\phi}\right] = \left[K^e_{\phi d}\right]^T = -[C]^{-T} \int_V z [L_K]^T [e]^T B_Z dv \tag{63}$$

$$\left[K^e_{\phi\phi}\right] = -\int_V B_Z^T \left[\xi^T\right] B_Z dv \tag{64}$$

$$\{Q_a\} = \int_A \sigma_d \, dA \tag{65}$$

$$\{\bar{f}\} = \int_V \{f_b\} \, dv + \int_A \{f_A\} \, dv \tag{66}$$

By generalising coordinates in the eq. (60), then the obtained equilibrium equations are given by eqns. (67) and (68)

$$\left[M^e_{dd}\right]\{\ddot{d}_k\} + \left[K^e_{dd}\right]\{d_k\} + \left[K^e_{d\phi}\right]\{\phi\} - \{\bar{f}\} = 0 \tag{67}$$

$$\left[K^e_{\phi d}\right]\{d_k\} + \left[K^e_{\phi\phi}\right]\{\phi\} + \{Q_a\} = 0 \tag{68}$$

Where $\left[M^e_{dd}\right]$ and $\left[K^e\right]$ are the mass stiffness matrix and element stiffness matrix. Integrating the eq. (62) with respect to z-direction was given in eq. (69)

$$\left[K^e_{dd}\right] = \sum_{i=1}^{3} h_i \left[C\right]^{-T} \left[L_K\right]\left[D_i\right]\left[L_K\right]^T dA \left[C\right]^{-1} \tag{69}$$

Where h_1, h_2 and h_3 are represented in eqns. (70), (71) and (72)

$$h_1 = h_a \left[\frac{h_p}{2} + \frac{h_a}{2}\right]^2 + \frac{h_a^3}{2} \tag{70}$$

$$h_2 = \frac{h_p^3}{12} \tag{71}$$

$$h_3 = h_a \left[\frac{h_p}{2} + \frac{h_s}{2}\right]^2 + \frac{h_s^3}{12} \tag{72}$$

The values of $\left[D_i\right]$ for i=1, 2, 3 are calculated by considering the eq. (31) and the value of the dA was taken as $dxdy$.

Similarly, integrating the eq. (61) with respect to z-direction is given in eq. (73)

$$\left[M^e_{dd}\right] = \sum_{i=1}^{3} \rho_i \left[C\right]^{-T} \left[L_M\right]\left[H_i\right]\left[L_M\right]^T dA \left[C\right]^{-1} \tag{73}$$

Whereas ρ_i or ρ_a, ρ_p and ρ_s for i = 1, 2, 3 and similarly the values of $\left[H_i\right]$ are given by eqns. (72), (73) and (74)

$$[H_1]=[H_a]=\begin{bmatrix} h_a & 0 & 0 \\ 0 & h_1 & 0 \\ 0 & 0 & h_1 \end{bmatrix} \tag{74}$$

$$[H_2]=[H_p]=\begin{bmatrix} h_p & 0 & 0 \\ 0 & h_2 & 0 \\ 0 & 0 & h_2 \end{bmatrix} \tag{75}$$

$$[H_3]=[H_s]=\begin{bmatrix} h_s & 0 & 0 \\ 0 & h_3 & 0 \\ 0 & 0 & h_3 \end{bmatrix} \tag{76}$$

Similarly, electrical-mechanical coupling stiffness

$$\left[K_{d\phi}^{e}\right]_a=-\frac{1}{2}\left(h_p h_a+h_a^2\right)[C]^{-T}\int_A [L_K]^T [e]_a^T B_z dA \tag{77}$$

$$\left[K_{\phi\phi}^{e}\right]_s=-\frac{4ab\left[\xi_a^S\right]}{h_a} \tag{78}$$

$$\left[K_{d\phi}^{e}\right]_s=-\frac{1}{2}\left(h_p h_s+h_s^2\right)[C]^{-T}\int_A [L_K]^T [e]_s^T B_z dA \tag{79}$$

$$\left[K_{\phi\phi}^{e}\right]_s=-\frac{4ab\left[\xi_a^S\right]}{h_s} \tag{80}$$

6.7.3 Development of state space representation for plate and piezoelectric patch: A basic state space eq. for plate and piezoelectric patch was expressed in eq. (81). Which was employed from [60]

$$M_t \ddot{p}+C_S \dot{p}+K_t p=f_D \tag{81}$$

From above eq. (81), p is the structural displacement, M_t is the combination of plate and piezo-electric mass matrix, C_S is the structural damping, K_t is the combination of plate and piezo-electric stiffness matrix and f_D is the type of disturbances which makes the structure to

vibrate, $\dot{p}$ represents the displacement produced by structure and $\ddot{p}$ represents the acceleration of structure which was given by eq. (82)

$$\ddot{p} = M_t^{-1} f_D - M_t^{-1} C_S \dot{p} - M_t^{-1} K_t p \tag{82}$$

Then by choosing the structural displacement as ' p ' and structural velocity as ' $\dot{p}$ 'with state variables as p_1 and p_2 .

$$p_1(t) = p(t) \text{ and } p_2(t) = \dot{p}(t) \tag{83}$$

$$\dot{p}_1(t) = \dot{p}(t) = p_2(t) \tag{84}$$

$$\dot{p}_2(t) = \ddot{p}(t) = M_t^{-1} f_D - M_t^{-1} C_S p_2 - M_t^{-1} K_t p_1 \tag{85}$$

The state space representation of closed loop plate- piezoelectric system.

$$\begin{bmatrix} \dot{p}_1(t) \\ \dot{p}_2(t) \end{bmatrix} = \begin{bmatrix} 0 & I \\ -M_t^{-1} K_t & -M_t^{-1} C_S \end{bmatrix} \begin{Bmatrix} p_1(t) \\ p_2(t) \end{Bmatrix} + \begin{bmatrix} 0 \\ M_t^{-1} \end{bmatrix} f_D \tag{86}$$

The output eq. of a closed loop structural acceleration was represented in eq. (87)

$$\ddot{p}(t) = \begin{bmatrix} -M_t^{-1} K_t & -M_t^{-1} C_S \end{bmatrix} \begin{Bmatrix} p_1(t) \\ p_2(t) \end{Bmatrix} + M_t^{-1} f_D \tag{87}$$

By comparing eqns. (86) and (87) with the eqns. (1) and (2), the values of matrix A, B, C and D are represented in eqns. (88), (89), (90) and (91)

$$A^C = \begin{bmatrix} 0 & I \\ -M_t^{-1} K_t & -M_t^{-1} C_S \end{bmatrix} \tag{88}$$

$$B^C = \begin{bmatrix} 0 \\ M_t^{-1} \end{bmatrix} \tag{89}$$

$$C^C = \begin{bmatrix} -M_t^{-1}K_t & -M_t^{-1}C_S \end{bmatrix} \tag{90}$$

$$D^C = M_t^{-1} \tag{91}$$

6.7.3 Design of Direct Output Feedback: In order to design the direct output feedback gain for optimal value of controller gain (G_v), the pole placement method was used. Initially, in order to find the optimal gain value of velocity gain (G_v), the open loop pole zero maps were plotted by taking into consideration as displacement gain $G_d = 0$ and velocity gain $G_v = 0$. Then closed loop pole zero maps are plotted by varying G_d and G_v values in order to get the change in design parameters like percentage peak overshoot (PO) value is given in eq. (92) damping loss factor (ξ) and settling time (T_s) value is given in eq. (93). Then nodal displacement response for different values of G_d and G_v are represented in order to check whether the nodal displacement is damped out completely or not. Then hammer excitation force and response force is applied on the plate at the different nodes and from nodal displacement response it is possible to check that the vibrations produced by the plate is reduced completely or not.

$$PO(\%) = e^{\frac{-\xi_s^i \pi}{\sqrt{1-\xi_s^{i^2}}}} \tag{92}$$

$$T_s = \frac{4}{\xi_s^i \lambda_s^i} \tag{93}$$

CHAPTER-7

RESULTS AND DISCUSSIONS

7.1 Mode shapes of a plate with different boundary conditions:

Best preferable location of piezoelectric patch was found out in ABAQUS CAE software by viewing method. Mode shapes of bare plate for different boundary conditions like clamped at all edges, cantilever, free-free, simply supported conditions are found by conducting modal analysis in Abaqus software. Table 7.1 represents the mode shapes of a plate with clamped at all edges boundary condition. Table7. 2 represents the mode shapes of a plate with cantilever boundary condition. Table 7.3 represents the mode shapes of a plate with free-free boundary condition. Table 7.4 represents the mode shapes of a plate with simply supported boundary condition

Table 7.1: Mode shapes of bare plate with clamped at all edges boundary condition

Mode shapes	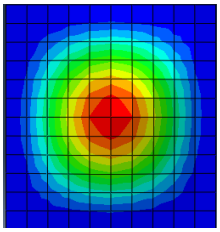 Mode 1	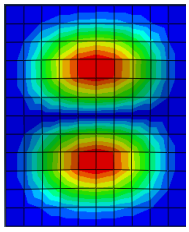 Mode 2	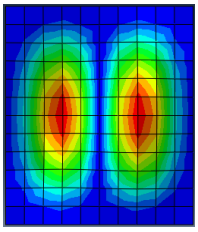 Mode 3	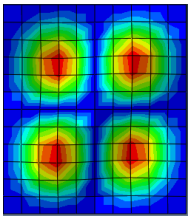 Mode 4	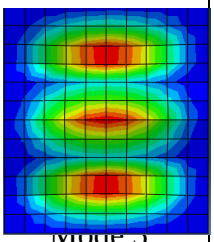 Mode 5
Frequency (Hz)	117	223	272	364	410.89

Table 7.2: Mode shapes of bare plate with cantilever boundary condition

Mode shapes	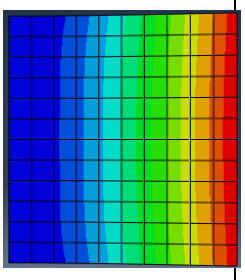 Mode 1	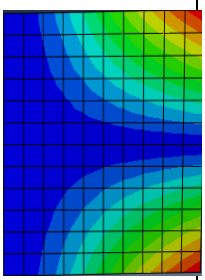 Mode 2	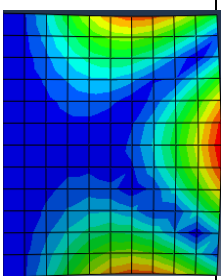 Mode 3	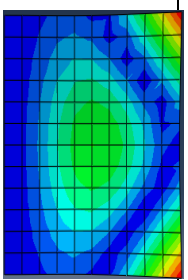 Mode 4	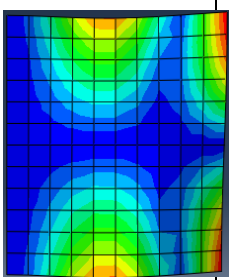 Mode 5
Frequency (Hz)	12.59	27.35	73.09	85	105.34

Table 7.3: Mode shapes of bare plate with free-free boundary condition

Modes shape	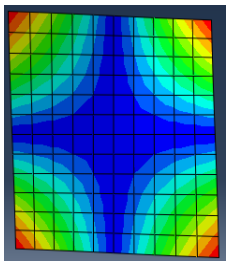 Mode 1	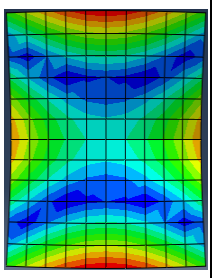 Mode 2	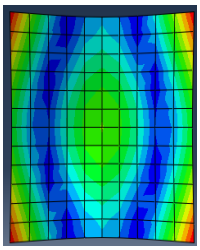 Mode 3	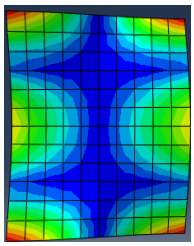 Mode 4	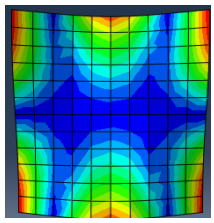 Mode 5
Frequency (Hz)	41.94	57.22	83.77	103.57	114.98

Table 7.4: Mode shapes of bare plate with simply supported boundary condition

Modes shape	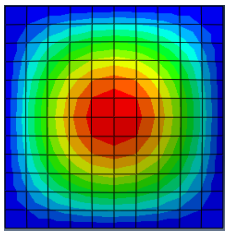 Mode 1	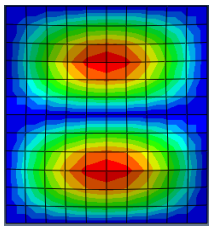 Mode 2	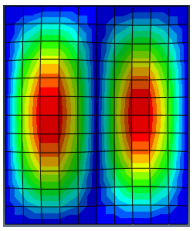 Mode 3	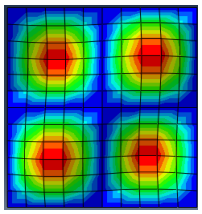 Mode 4	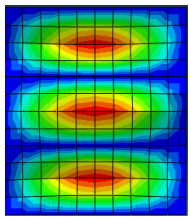 Mode 5
Frequency (Hz)	63.32 Hz	147.74 Hz	177.79 Hz	259.45Hz	298.40 Hz

7.1.1 Clamped boundary condition:

Initially, boundary condition like clamped at all edges is applied to the plate. In this case, the rotation and displacement of the plate in all directions was taken as zero. From 1st mode shape, it was observed that no nodal line was formed and piezo can be placed anywhere on the plate. From 2nd mode shape, it was observed that one horizontal nodal line was formed at the centre. From 3rd mode shape, it was observed that one vertical nodal line was formed at the centre. From 4th mode shape, it was observed that one horizontal and one vertical nodal line was formed. From 5th mode shape, it was observed that two horizontal lines are formed at above and below the centre. Piezo cannot be placed at a location where nodal lines are formed. The plate was divided into four quadrants as the boundary condition was clamped at all edges. Then by placing the piezo at one of the quadrants will be same as placing at all quadrants.

Initially, piezo is placed at centre location L1 (61, 62, 72, 73) and modal analysis had conducted for a plate with piezo. It was observed that only 1st and 5th mode shape is possible whereas 2nd, 3rd and 4th mode shape is not possible as nodal lines are passing through the piezo at centre. Then piezo is shifted to a horizontal location L2 (60, 61, 71, 72) away from the centre and observed that only 1st, 3rd and 5th mode shapes are possible whereas 2nd and 4th mode shape is not possible. Then piezo is moved to a vertical location L3 (59, 60, 70, 71) away from the centre and observed that only 1st, 2nd and 5th mode shapes are possible whereas 3rd and 4th mode shapes are not possible. Then piezo is shifted to different locations and observed that at location L4 (37, 38, 48, 49) all mode shapes are possible as no nodal line is passing through piezo. It was concluded that for simply supported boundary condition, the obtained location L 4 (37, 38, 48, 49) was an optimal location of the piezoelectric patch on the plate. Table 7.5 represents the mode shapes of the piezoelectric patch on the plate at an optimum location with frequency.

Table 7.5: Optimum location of piezoelectric patch on bare plate for clamped at all edges boundary condition

Location of Mode Shapes	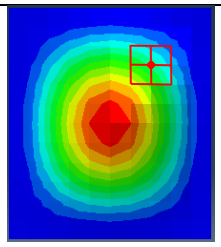 MODE 1	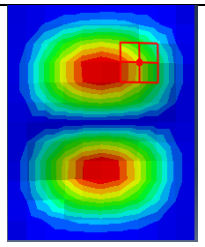 MODE 2	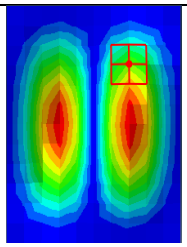 MODE 3	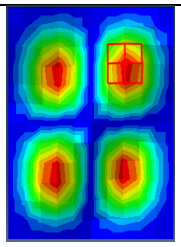 MODE 4	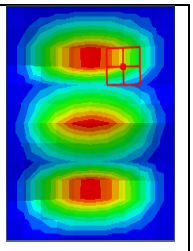 MODE 5
Frequency (Hz)	117	220	269	354	409
Sensing Modes	✓	✓	✓	✓	✓

7.1.2 Cantilever boundary condition:

Next cantilever boundary condition is applied to the left side of the plate. In this condition, displacement and rotation at the left side of the plate are taken as zero. By conducting modal analysis for the plate in Abaqus software, the mode shapes of a plate with cantilever boundary condition are extracted. From 1st mode shape, it was observed that vertical nodal line was formed at the complete left side of a plate. From 2nd mode shape, it was observed

that the combination of both vertical and horizontal nodal line was formed at the centre. From 3rd mode shape, it was observed that the combination of both vertical nodal line and from centre two cross 45^0 nodal lines was formed. From 4th mode shape, it was observed that the D-shaped nodal lines are formed on the plate. From 5th mode shape, it was observed that the one horizontal nodal line at centre and two vertical nodal lines are formed at the edges of the plate. the piezoelectric patch cannot be placed at a location where nodal lines are formed.

Now piezo is attached to the plate at centre location L1 (61,62,72,73) and modal analysis had conducted for a plate with piezo. It was observed that only 1st mode shape is possible as no nodal lines are passing through the piezo but 2nd,3rd, 4th mode shapes are not possible as nodal lines are passing through piezo. So, this is not taken as optimum location. Next piezo is shifted to a horizontal location L2 (60,61,71,72) from the centre and modal analysis had conducted. It was observed that only 1st, 4th mode shape is possible but 2nd, 3rd, 5th mode shapes are not possible. Then piezo is placed at vertical location L3 (59,60,70,71) above from centre and by conducting the modal analysis to plate with piezo it was observed that only 1st, 4th, 5th mode shapes are possible but 2nd and 3rd mode shapes are not possible. Then piezo is placed at different locations and observed that at location L (28,29,39,40) all mode shapes are possible. It was concluded that for cantilever boundary condition, the obtained location L (28,29,39,40) was an optimal location of the piezoelectric patch on the plate. Table 7.6 represents the mode shapes of the piezoelectric patch on the plate at an optimum location with frequency.

Table7.6: Optimum location of piezoelectric patch on a plate for cantilever boundary condition

Location of Mode Shapes	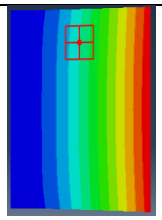 MODE 1	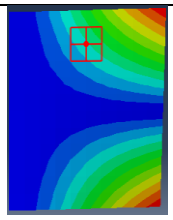 MODE 2	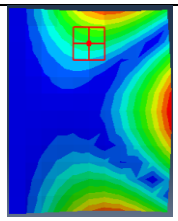 MODE 3	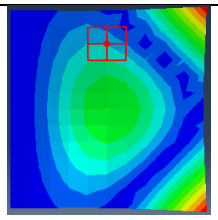 MODE 4	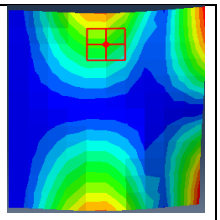 MODE 5
Frequency (Hz)	12.54	27.15	72.21	84.61	103.62
Sensing Modes	✓	✓	✓	✓	✓

7.1.3 Free- Free boundary condition:

Next free-free boundary condition was applied to the plate as displacement and rotation on all sides is not zero. By conducting modal analysis to the plate, it was observed that from 1st mode shape a horizontal and vertical nodal lines are formed. From 2nd mode shape, it was observed that two vertical semi-curve nodal lines are formed at above and below the centre. From 3rd mode shape, it was observed that two horizontal semi-curve nodal lines are formed at left and right side of the centre. From 4th mode shape, it was observed that one vertical at centre and two horizontal nodal lines are formed at above and below the centre. From 5th mode shape, it was observed that two vertical and one horizontal nodal lines are formed at the centre.

The piezoelectric patch is attached to the plate at centre location L1 (61,62,72,73). By conducting the modal analysis of a plate with piezo it was observed that only 2nd and 3rd mode shapes are possible whereas 1st, 4th, 5th mode shapes are not possible as a nodal line are passing through the piezo. Then piezo is shifted to a horizontal location L2 (60,61,71,72) away from the centre and observed that only 2nd, 3rd, 4th mode shapes are possible but 1st, 5th mode shapes are not possible as nodal lines are passing through the piezo. Then piezo is moved to a vertical location L3 (59,60,70,71) away from the centre and observed that only 3rd mode shape is possible whereas 1st, 2nd, 4th, 5th mode shapes are not possible as a nodal line are passing through the piezo. By placing the piezo at different locations of the quarter plate, it was observed that at location L (123,124,134,135) all mode shapes are a satisfying condition as no nodal lines are passing through piezo. It was concluded that the obtained location L (123,124,134,135) was an optimum location as no nodal lines are passing through piezo. Table 7.7 represents the mode shapes of the piezoelectric patch on the plate at an optimum location with frequency.

Table 7.7: Optimum location of piezoelectric patch on bare plate for free-free boundary condition

Location of Mode Shapes	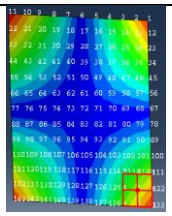 MODE 1	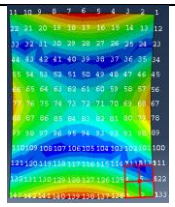 MODE 2	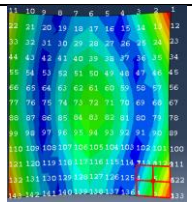 MODE 3	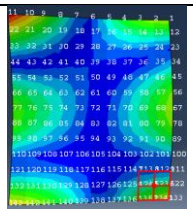 MODE 4	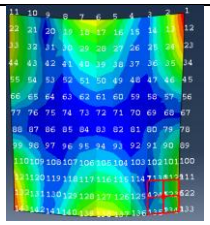 MODE 5
Frequency (Hz)	40.27	56.85	82.16	101.40	113.40
Sensing Modes	✓	✓	✓	✓	✓

7.1.4 Simply supported boundary condition:

The simply supported boundary condition was applied to the plate as displacement with respect to all directions and rotation with respect to the z-axis is taken as zero but a rotation with respect to x-axis and y-axis is not taken as zero. By conducting the modal analysis for the plate, it was observed that from 1st mode shape no nodal line was formed and piezo can be placed at any location. From 2nd mode shape, it was observed that one horizontal nodal line was formed at the centre. From 3rd mode shape, it was observed that one vertical nodal line was formed at the centre. From 4th mode shape, it was observed that both horizontal and vertical nodal line was formed at the centre. From 5th mode shape, it was observed that two horizontal nodal lines were formed at above and below the centre. The plate is divided into quadrants as simply supported boundary condition is applied. If piezo is placed at one of the quadrants, the result obtained will be same as remaining quadrants.

The piezoelectric patch is attached to the plate at centre location L1 (61, 62, 72, and 73). By conducting a modal analysis of a plate with piezo, it was observed that only 1st and 5th mode shape is possible whereas 2nd, 3rd and 4th mode shape are not possible as nodal lines are passing through the piezo at centre. Then piezo is shifted to a horizontal location L2 (60, 61, 71, 72) away from the centre and observed that only 1st, 3rd and 5th mode shapes are possible whereas 2nd and 4th mode shape is not possible. Then piezo is moved to a vertical location L3 (59, 60, 70, 71) away from the centre and observed that only 1st, 2nd and 5th mode shapes are possible whereas 3rd and 4th mode shapes are not possible. Then piezo is shifted to different locations and observed that at location L4 (37, 38, 48, 49) all mode shapes are possible as no nodal line is passing through piezo. It was concluded that for simply supported boundary

condition, the obtained location L4 (37, 38, 48, and 49) was an optimal location of the piezoelectric patch on the plate. Table 7.8 represents the mode shapes of the piezoelectric patch on the plate at an optimum location with frequency.

Table 7.8: Optimum location of piezoelectric patch on bare plate for simply supported boundary condition

Location of Mode Shapes	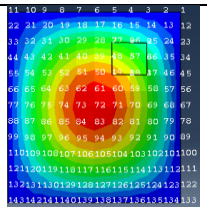 MODE 1	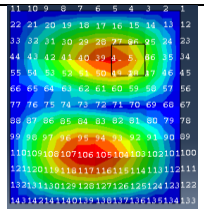 MODE 2	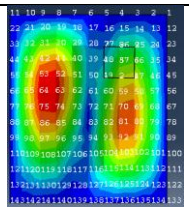 MODE 3	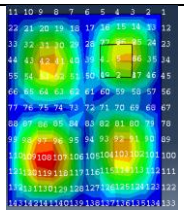 MODE 4	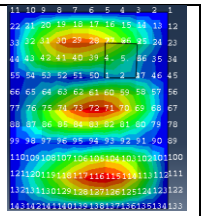 MODE 5
Frequency (Hz)	62.10	141.90	173.45	249.15	293.93
Sensing Modes	✓	✓	✓	✓	✓

7.2 Validation through Frequency Response Function:

Initially, clamped at all edges boundary condition was considered in order to plot FRF graph. If piezo is placed at a location where nodal lines are passing, the FRF graph cannot detect all mode shapes. From fig 7.1, it was observed that detection of all mode shapes was possible at optimal location. From frf output, it was found that the 1st mode shape is damping out very quickly then compared to other modes

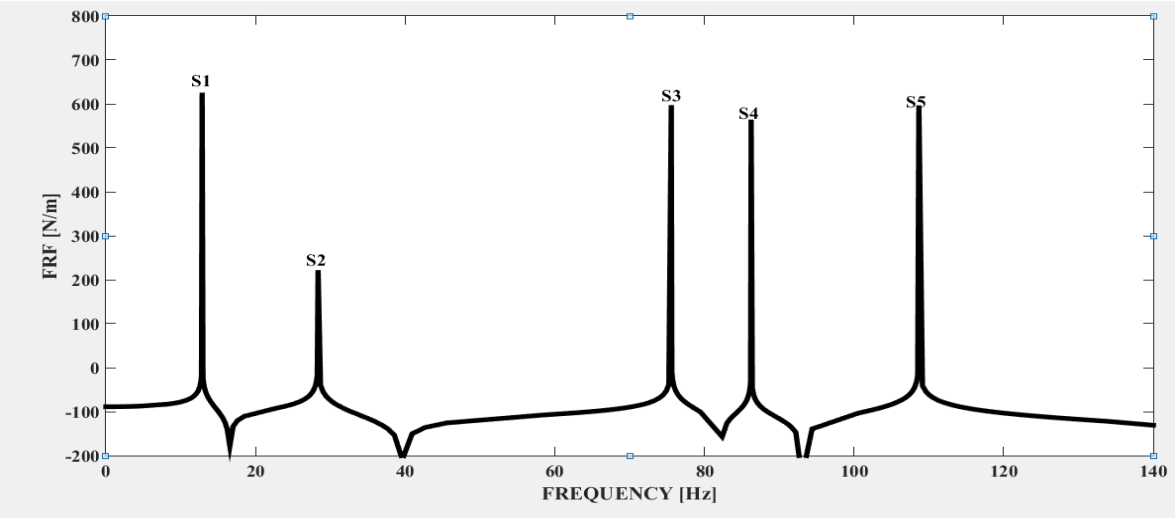

Fig 7.1: FRF graph for optimum location of piezo electric patch on a plate with clamped at all edges boundary condition

The FRF graph for cantilever boundary condition at the optimum location of the piezoelectric patch on the plate was plotted. From fig 7.2, it was observed that the detection of all mode shapes was possible at the optimum location. From frf output, it was found that the 1st, 2nd, and 3rd mode shape are damping out very quickly then compared to other modes

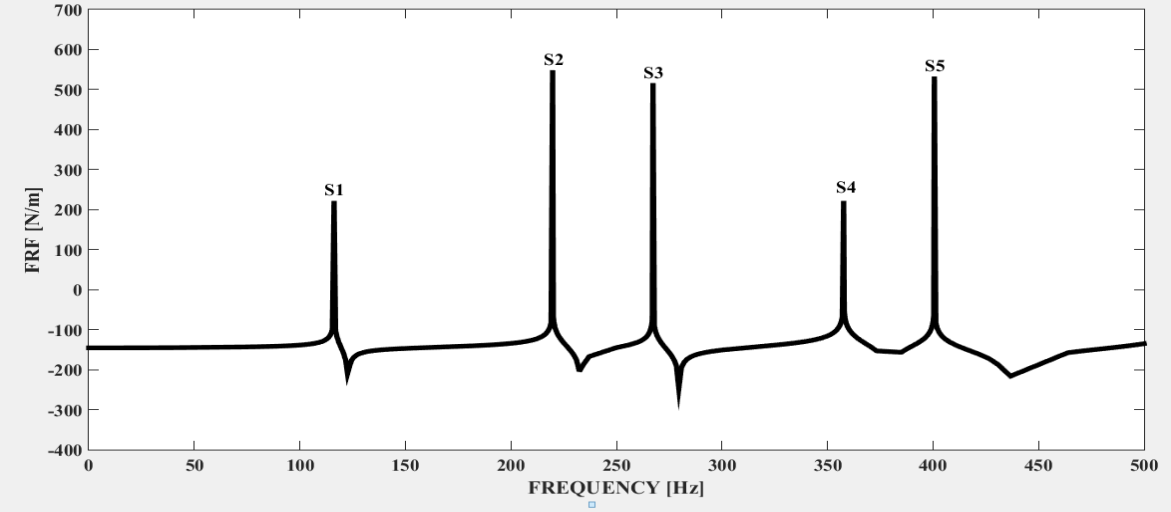

Fig 7.2: FRF graph for optimum location of piezo electric patch on a plate with cantilever boundary condition

The FRF graph for free-free boundary condition at the optimum location of the piezoelectric patch on the plate was plotted. From fig 7.3, it was observed that detection of all mode shapes was possible at the optimum location of the piezoelectric patch on the plate. From frf output, it was found that the 3rd and 5th mode shape is damping out very quickly then compared to other modes

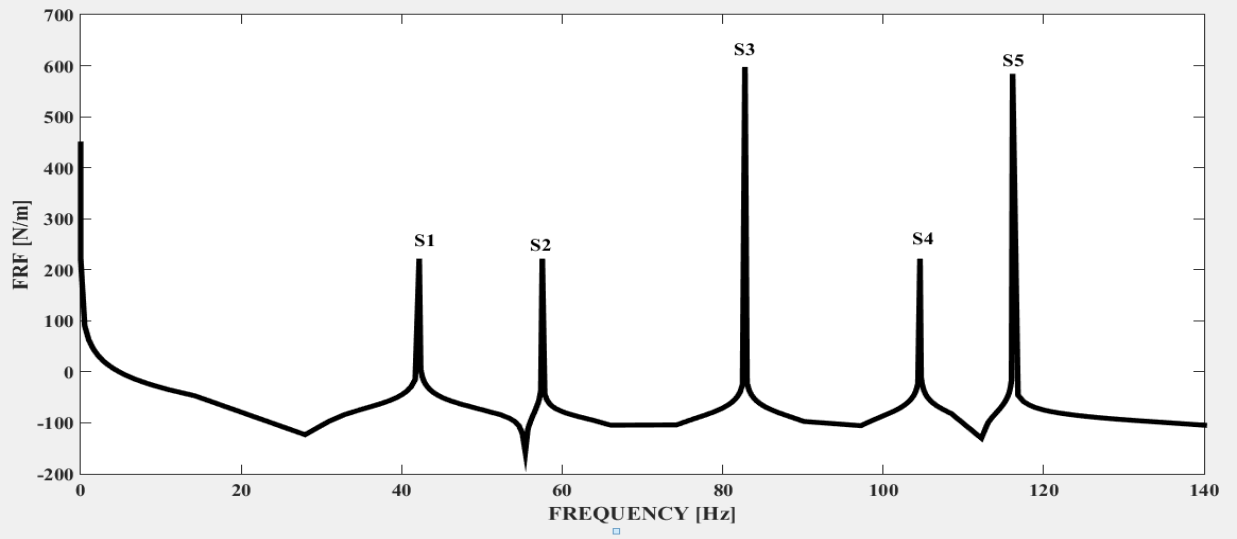

Fig 7.3: FRF graph for optimum location of piezoelectric patch on a plate with free-free boundary condition

The FRF graph for simply supported boundary condition at the optimum location of the piezoelectric patch on the plate was plotted. From fig 7.4, it was observed that the detection

of all mode shapes was possible at the optimum location of the piezoelectric patch on the plate. From frf output, it was found that almost all mode shapes are damping out very quickly.

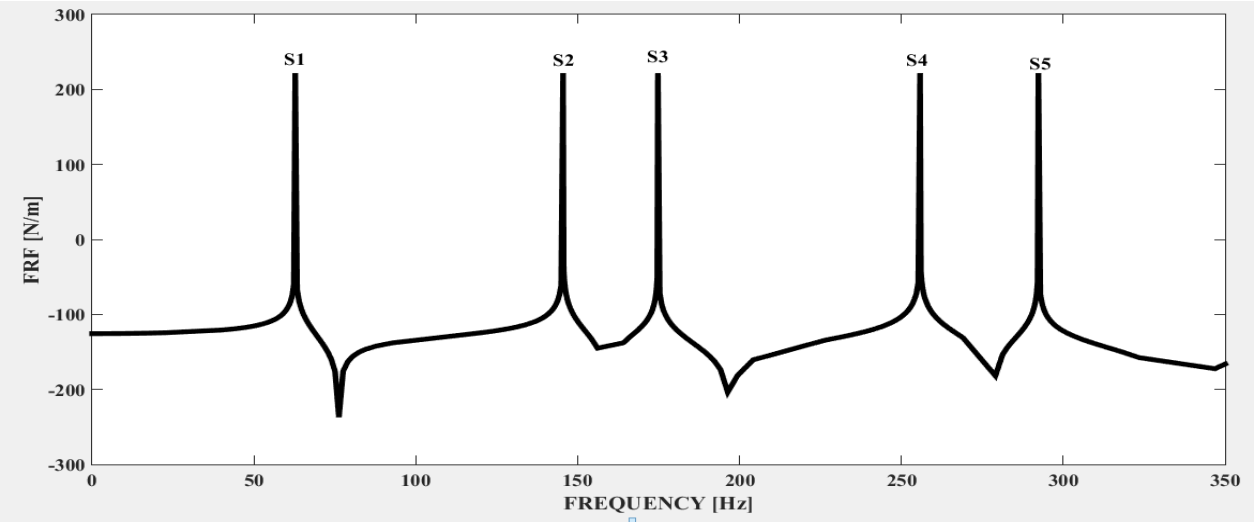

Fig 7.4: FRF graph for optimum location of piezoelectric patch on a plate with simply supported boundary condition.

7.3 Active Vibration Control of a plate:

Initially direct output feedback gain is designed for open loop pole zero maps at displacement aand velocity gain value equals to zero. Then closed loop pole zero maps are plotted by varying different displacement gain (G_d) and velocity gain (G_v) values which had considered in four different cases.

Case 1:

In this case, displacement gain and velocity gain values are taken as zero**.** From fig (7.5) and fig (7.6), it was observed that there is no control of vibrations which are produced by the structure.

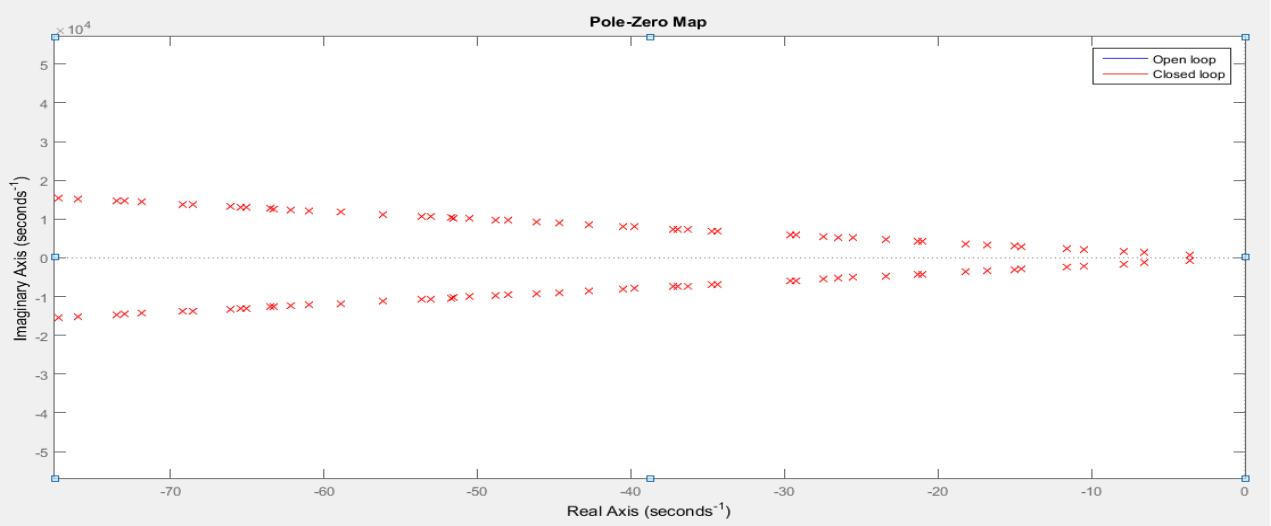

Fig 7.5: Pole zero map at $G_v = 0$ and $G_d = 0$

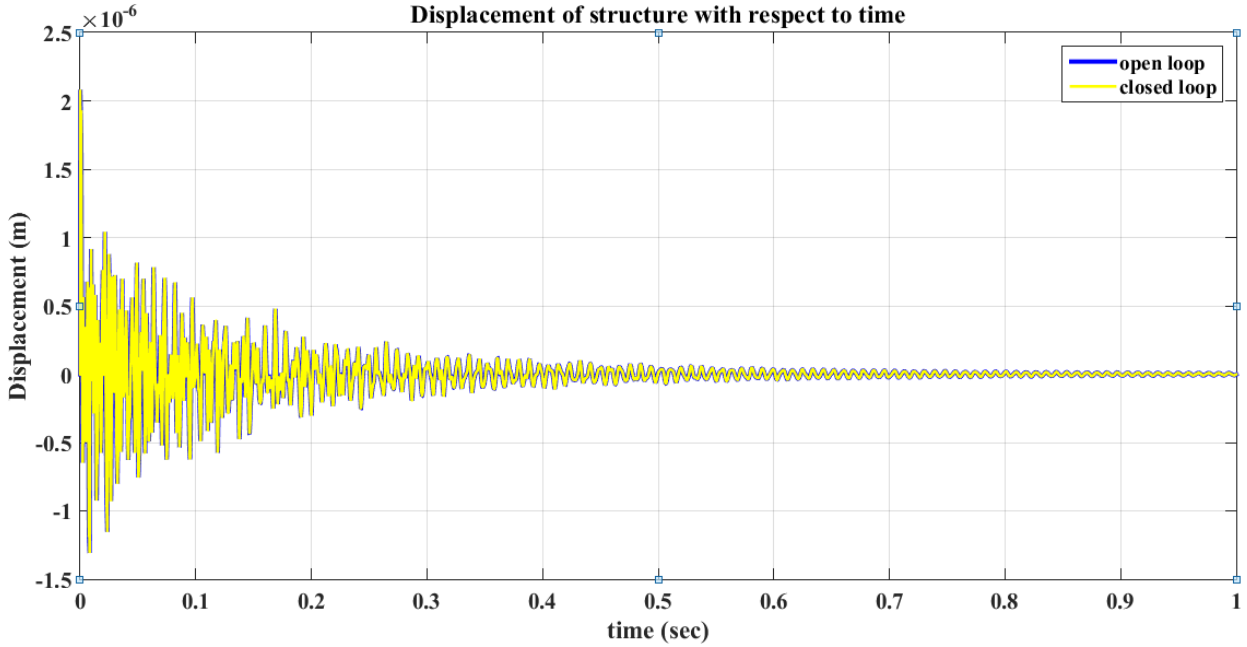

Fig 7.6: Nodal displacement response at $G_v = 0$ and $G_d = 0$

Case 2:

Initially taking the value velocity gain value as zero and the displacement gain values are taken from minimum of 0.01 to maximum of $1x10^5$. From tables (7.9) and (7.10), it was observed that there is no change in structural damping value. From figs. (7.7) and (7.8) it was observed that there is no effect in control of vibrations produced by structure.

Table (7.9): Changes in Design Parameters with respect to $G_v = 0$ and $G_d \neq 0$

Mode frequency [Hz]	**Design parameter**	**G_d 0.001**	**G_d 0.01**	**G_d 0.02**	**G_d 0.03**	**G_d 0.04**	**G_d 0.05**	**G_d 0.06**
114	ξ Ts (sec) PO (%)	0.005 1.117 98.4	0.005 1.117 98.4	0.005 1.117 98.4	0.005 1.117 98.4	0.005 1.117 98.4	0.005 1.117 98.4	0.005 1.117 98.4
208.4	ξ Ts (sec) PO (%)	0.005 0.610 98.4	0.005 0.610 98.4	0.005 0.610 98.4	0.005 0.610 98.4	0.005 0.610 98.4	0.005 0.610 98.4	0.005 0.610 98.4
250	ξ Ts (sec) PO (%)	0.005 0.50 98.4	0.005 0.50 98.4	0.005 0.50 98.4	0.005 0.50 98.4	0.005 0.50 98.4	0.005 0.50 98.4	0.005 0.50 98.4
332.6	ξ Ts (sec) PO (%)	0.005 0.382 98.4	0.005 0.382 98.4	0.005 0.382 98.4	0.005 0.382 98.4	0.005 0.382 98.4	0.005 0.382 98.4	0.005 0.382 98.4
369.2	ξ Ts (sec) PO (%)	0.005 0.3448 98.4	0.005 0.3448 98.4	0.005 0.3448 98.4	0.005 0.3448 98.4	0.005 0.3448 98.4	0.005 0.3448 98.4	0.005 0.3448 98.4

Table (7.10): Changes in Design Parameters with respect to $G_v = 0$ and $G_d \neq 0$

Mode frequency [Hz]	**Design parameter**	**G_d 0.07**	**G_d 0.08**	**G_d 0.09**	**G_d 0.1**	**G_d 1.0**	**G_d 1 e^3**	**G_d 1 e^5**
114	ξ Ts (sec) PO (%)	0.005 1.117 98.4	0.005 1.117 98.4	0.005 1.117 98.4	0.005 1.117 98.4	0.005 1.117 98.4	0.00499 1.117 98.4	0.00499 1.117 98.4
208.4	ξ Ts (sec) PO (%)	0.005 0.610 98.4	0.005 0.610 98.4	0.005 0.610 98.4	0.005 0.610 98.4	0.005 0.610 98.4	0.00496 0.610 98.4	0.00495 0.610 98.4
250	ξ Ts (sec) PO (%)	0.005 0.50 98.4	0.005 0.50 98.4	0.005 0.50 98.4	0.005 0.50 98.4	0.005 0.50 98.4	0.00495 0.50 98.4	0.00493 0.50 98.4
332.6	ξ Ts (sec) PO (%)	0.005 0.382 98.4	0.005 0.382 98.4	0.005 0.382 98.4	0.005 0.382 98.4	0.005 0.382 98.4	0.00493 0.382 98.4	0.00493 0.382 98.4
369.2	ξ Ts (sec) PO (%)	0.005 0.3448 98.4	0.005 0.3448 98.4	0.005 0.3448 98.4	0.005 0.3448 98.4	0.005 0.3448 98.4	0.00492 0.3448 98.4	0.00493 0.3448 98.4

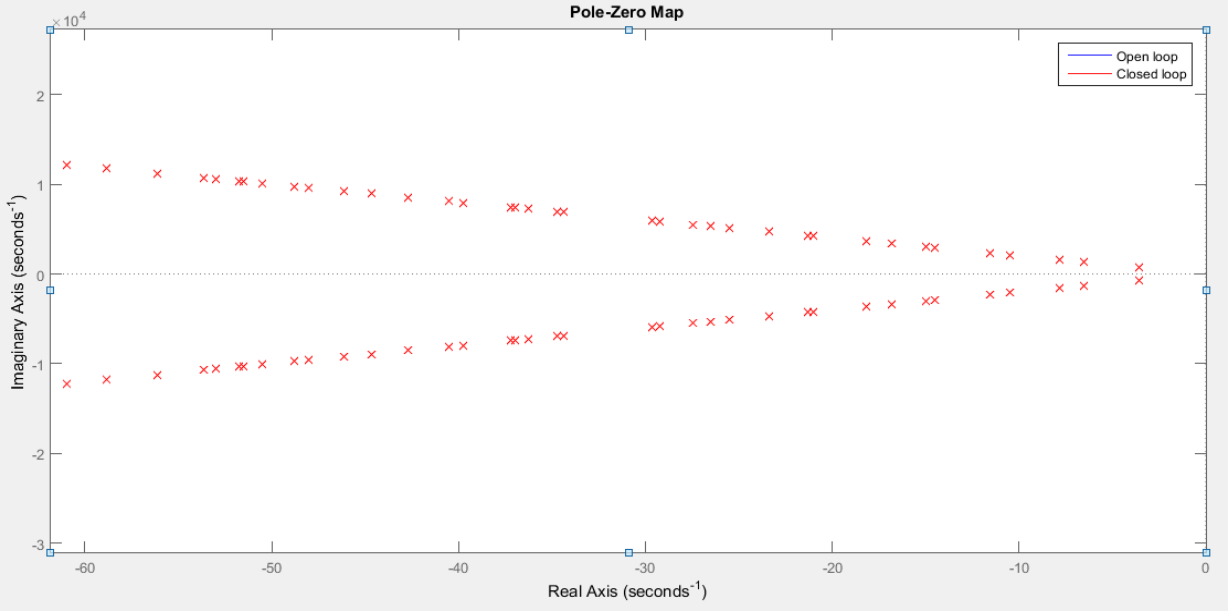

Fig 7.7: Pole zero map at $G_v = 0$ and $G_d \neq 0$

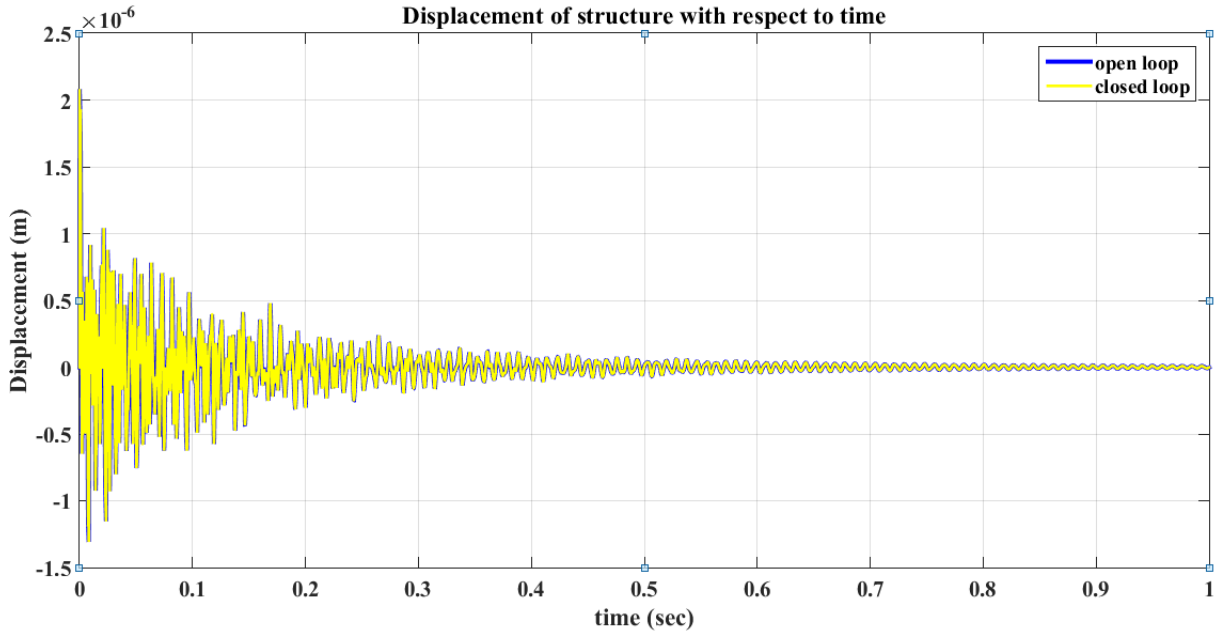

Fig (7.8): Nodal displacement response at $G_v = 0$ and $G_d \neq 0$

Case 3: In this case, the value of displacement gain is taken as zero and the velocity gain values are taken from minimum of 0.01 to maximum of $1x10^5$. From tables (7.11), (7.12) and (7.13), it was found that the gain values from 0.001 to 0.08 have adorable variation in design parameter and when the gain value is $1x10^5$, the design parameters are closer to the initial values. From fig (7.9), it was observed that when the gain value is 0.08, the most of the closed loop poles are shifted to the left side of the pole zero map. From fig (7.10), after applying the control it was found that the nodal displacement had damped out so quickly

compared to other gain values. So, the optimal direct output feedback value was taken as 0.08.

Table (7.11): Changes in Design Parameters with respect to $G_d = 0$ and $G_v \neq 0$

Mode frequency [Hz]	**Design parameter**	**G_V 0.001**	**G_V 0.01**	**G_V 0.02**	**G_V 0.03**	**G_V 0.04**
114	ξ Ts (sec) PO (%)	0.00504 1.10 98.4	0.00538 1.03 98.3	0.00573 0.94 98.2	0.00601 0.92 98.1	0.00621 0.89 98.1
208.5	ξ Ts (sec) PO (%)	0.00544 0.561 98.3	0.00917 0.332 97.2	0.012 0.254 96.3	0.0132 0.231 95.9	0.0133 0.229 95.9
250	ξ Ts (sec) PO (%)	0.00534 0.477 98.3	0.00813 0.313 97.5	0.0101 0.252 96.9	0.0108 0.235 96.7	0.0107 0.237 96.7
332.6	ξ Ts (sec) PO (%)	0.00627 0.305 98	0.016 0.12 95.1	0.0201 0.095 93.9	0.0191 0.100 94.2	0.0171 0.112 94.8
369.2	ξ Ts (sec) PO (%)	0.00567 0.304 98.2	0.0113 0.152 98.4	0.0152 0.113 95.3	0.0162 0.106 95	0.0156 0.110 95.2

Table (7.12): Changes in Design Parameters with respect to $G_d = 0$ and $G_v \neq 0$

Mode frequency [Hz]	**Design parameter**	**G_V 0.05**	**G_V 0.06**	**G_V 0.07**	**G_V 0.08**	**G_V 0.09**
114.11	ξ Ts (sec) PO (%)	0.00635 0.878 98	0.00642 0.87 98	0.00644 0.86 98	0.00644 0.86 98	0.00642 0.87 98
211.6	ξ Ts (sec) PO (%)	0.013 0.231 96	0.0124 0.45 96.2	0.0118 0.472 96.4	0.0112 0.49 96.5	0.0107 0.52 96.7
251.46	ξ Ts (sec) PO (%)	0.0103 0.245 96.8	0.00988 0.25 96.9	0.00945 0.27 97.1	0.00905 0.28 97.1	0.00871 0.29 97.3
342.18	ξ Ts (sec) PO (%)	0.0153 0.121 95.3	0.0138 0.134 95.8	0.0127 0.146 96.1	0.0118 0.157 96.4	0.0111 0.167 96.6
374	ξ Ts (sec) PO (%)	0.0146 0.116 95.5	0.0135 0.126 95.8	0.0126 0.135 96.1	0.0119 0.143 96.3	0.0112 0.151 96.5

Table (7.13): Changes in Design Parameters with respect to $G_d = 0$ and $G_v \neq 0$

Mode Frequency [Hz]	**Design parameter**	**G_V 0.1**	**G_V 1.0**	**G_V 1e+3**	**G_V 1e+5**
114.27	ξ Ts (sec) PO (%)	0.00638 0.873 98	0.0052 1.07 98.4	0.00499 1.116 98.4	0.00499 1.116 98.4
211.6	ξ Ts (sec) PO (%)	0.0103 0.291 96.8	0.00554 0.542 98.3	0.00495 0.607 98.5	0.00495 0.607 98.5
253	ξ Ts (sec) PO (%)	0.00841 0.30 97.4	0.00534 0.471 98.3	0.00496 0.507 98.5	0.00496 0.507 98.5
342.18	ξ Ts (sec) PO (%)	0.0105 0.177 96.8	0.0055 0.338 98.3	0.00493 0.377 98.5	0.00493 0.377 98.5
377.2	ξ Ts (sec) PO (%)	0.0107 0.157 96.7	0.00553 0.305 98.3	0.00492 0.343 98.5	0.00492 0.343 98.5

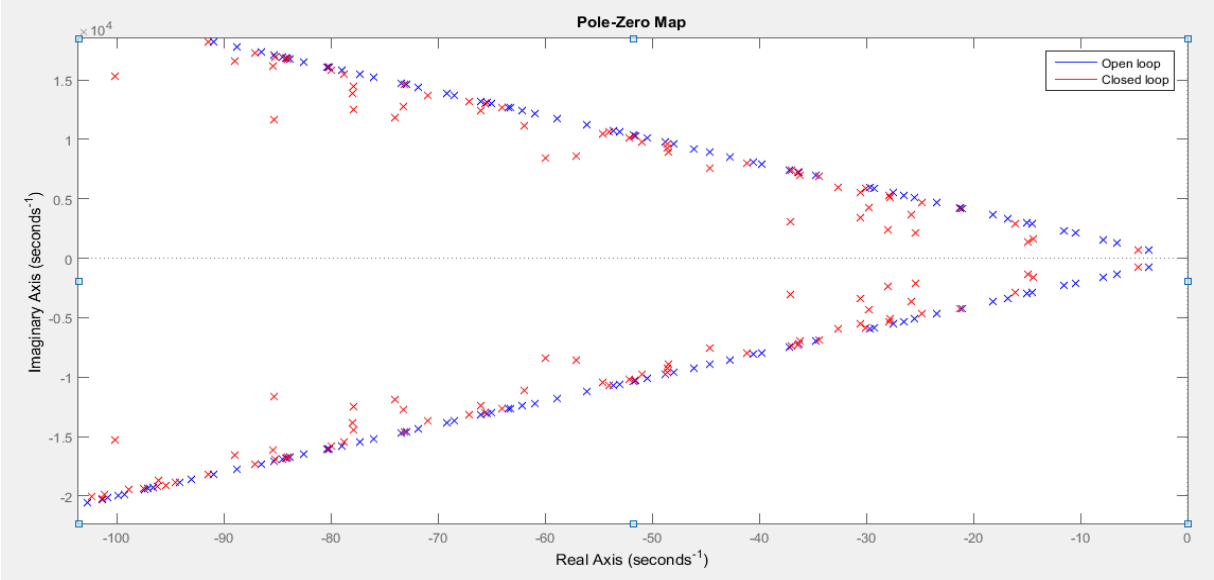

Fig (7.9): Pole zero map at $G_d = 0$ and $G_v = 0.08$

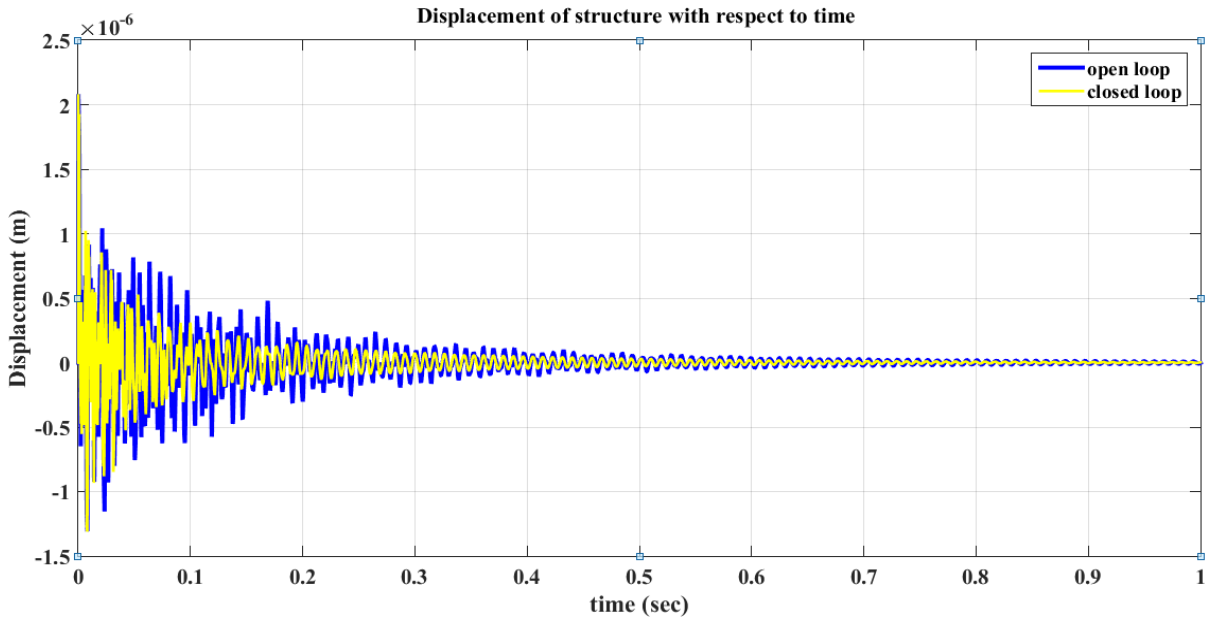

Fig (7.10): Nodal displacement response at $G_d = 0$ and $G_v = 0.08$

Case 4: In this case, the values of both displacement gain and velocity gain are varied from minimum of 0.01 to maximum of $1x10^5$. From tables (7.14), (7.15) and (7.16), it was found that the gain values from 0.001 to 0.08 have adorable variation in design parameter and when the gain value is $1x10^5$, the design parameters are closer to the initial values. From fig (7.11), it was observed that when the gain value is 0.08, the most of the closed loop poles are shifted to the left side of the pole zero map. From fig (7.12), after applying the control it was found that the nodal displacement had damped out so quickly compared to other gain values. So, the optimal direct output feedback value was taken as 0.08.

Table (7.14): Changes in Design Parameters with respect to $G_d \neq 0$ and $G_v \neq 0$

Mode Frequency[HZ]	**Design parameter**	**G_d=0.001 G_V=0.001**	**G_d=0.01 G_V=0.01**	**G_d=0.02 G_V=0.02**	**G_d=0.03 G_V=0.03**	**G_d=0.04 G_V=0.04**
114	ξ Ts (sec) PO (%)	0.00504 1.108 98.4	0.00538 0.974 98.3	0.00573 0.974 98.2	0.00601 0.929 98.1	0.00621 0.90 98.1
208.4	ξ Ts (sec) PO (%)	0.00544 0.561 98.3	0.00917 0.332 97.2	0.012 0.254 96.3	0.0132 0.231 95.9	0.0133 0.230 95.7
250	ξ Ts (sec) PO (%)	0.00534 0.477 98.3	0.00813 0.313 97.5	0.0101 0.252 96.9	0.0108 0.235 96.7	0.0107 0.238 96.7
342.18	ξ Ts (sec) PO (%)	0.00627 0.30 98	0.016 0.116 95.1	0.0201 0.092 93.9	0.0191 0.097 94.2	0.0171 0.108 94.8
369.2	ξ Ts (sec) PO (%)	0.00567 0.304 98.2	0.0113 0.152 96.5	0.0152 0.113 95.3	0.0162 0.106 95	0.0156 0.110 95.2

Table (7.15): Changes in Design Parameters with respect to $G_d \neq 0$ and $G_v \neq 0$

Mode frequency [Hz]	**Design parameter**	**G_d=0.05 G_V=0.05**	**G_d=0.06 G_V=0.06**	**G_d=0.07 G_V=0.07**	**G_d=0.08 G_V=0.08**	**G_d=0.09 G_V=0.09**
114	ξ Ts (sec) PO (%)	0.00634 0.881 98	0.00642 0.870 98	0.00644 0.867 98	0.00644 0.867 98	0.00641 0.871 98
208.4	ξ Ts (sec) PO (%)	0.0129 0.236 96	0.0124 0.246 96.2	0.0118 0.258 96.4	0.0113 0.270 96.5	0.0107 0.285 96.7
250	ξ Ts (sec) PO (%)	0.0103 0.247 96.8	0.00988 0.257 96.9	0.00944 0.27 97.1	0.00905 0.281 97.2	0.0087 0.292 97.3
342.18	ξ Ts (sec) PO (%)	0.0153 0.121 95.3	0.0138 0.134 95.8	0.0127 0.146 96.1	0.0118 0.157 96.4	0.0111 0.167 96.6
369.2	ξ Ts (sec) PO (%)	0.0146 0.118 95.5	0.0135 0.127 95.8	0.0126 0.136 96.1	0.0119 0.144 96.3	0.0112 0.153 96.5

Table (7.16): Changes in Design Parameters with respect to $G_d \neq 0$ and $G_v \neq 0$

Mode Frequency [Hz]	**Design parameter**	**G_d=0.1 G_V=0.1**	**G_d=1.0 G_V=1.0**	**G_d=1e^3 G_V=1e^3**	**G_d=1e^5 G_V=1e^5**
114.11	ξ Ts (sec) PO (%)	0.00638 0.874 98	0.0052 1.072 98.4	0.00499 1.117 98.4	0.00499 1.117 98.4
211.6	ξ Ts (sec) PO (%)	0.0103 0.30 96.8	0.00554 0.542 98.3	0.00495 0.607 98.5	0.00495 0.607 98.5
253	ξ Ts (sec) PO (%)	0.0084 0.29 97.4	0.00534 0.471 98.3	0.00496 0.507 98.5	0.00496 0.507 98.5
342.18	ξ Ts (sec) PO (%)	0.0105 0.177 96.8	0.0055 0.338 98.3	0.00493 0.377 98.5	0.00493 0.377 98.5
374	ξ Ts (sec) PO (%)	0.0107 0.157 96.7	0.00553 0.305 98.3	0.00492 0.343 98.5	0.00432 0.390 98.5

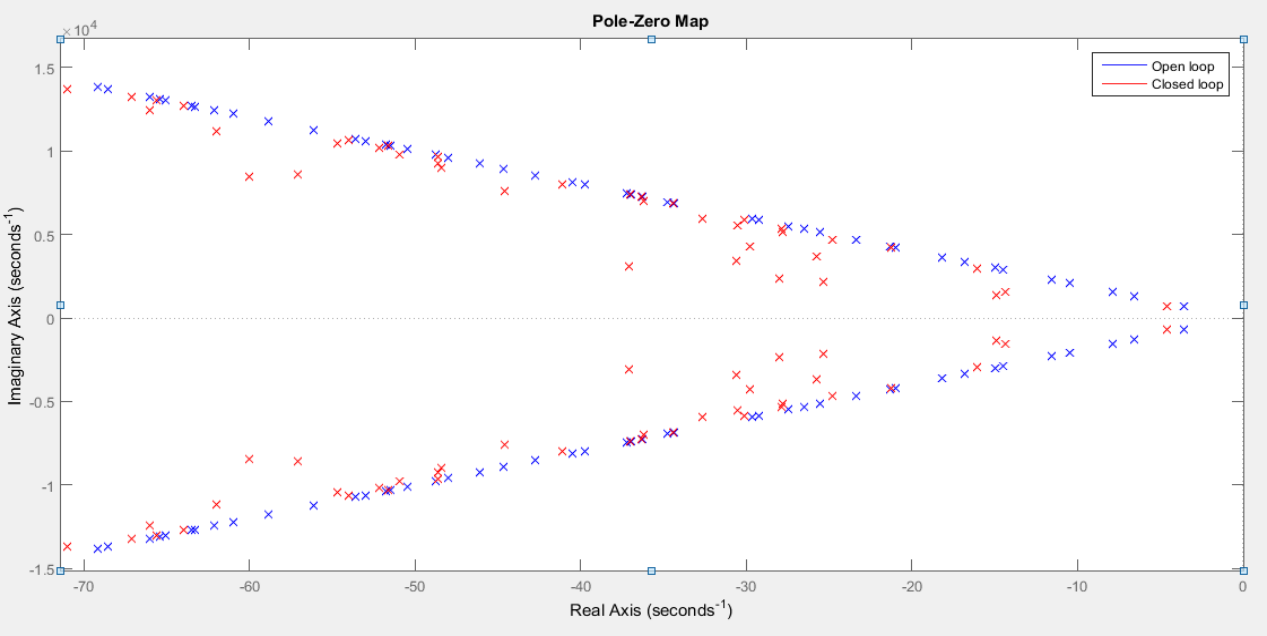

Fig (7.11): Pole zero map at $G_d = 0.08$ and $G_v = 0.08$

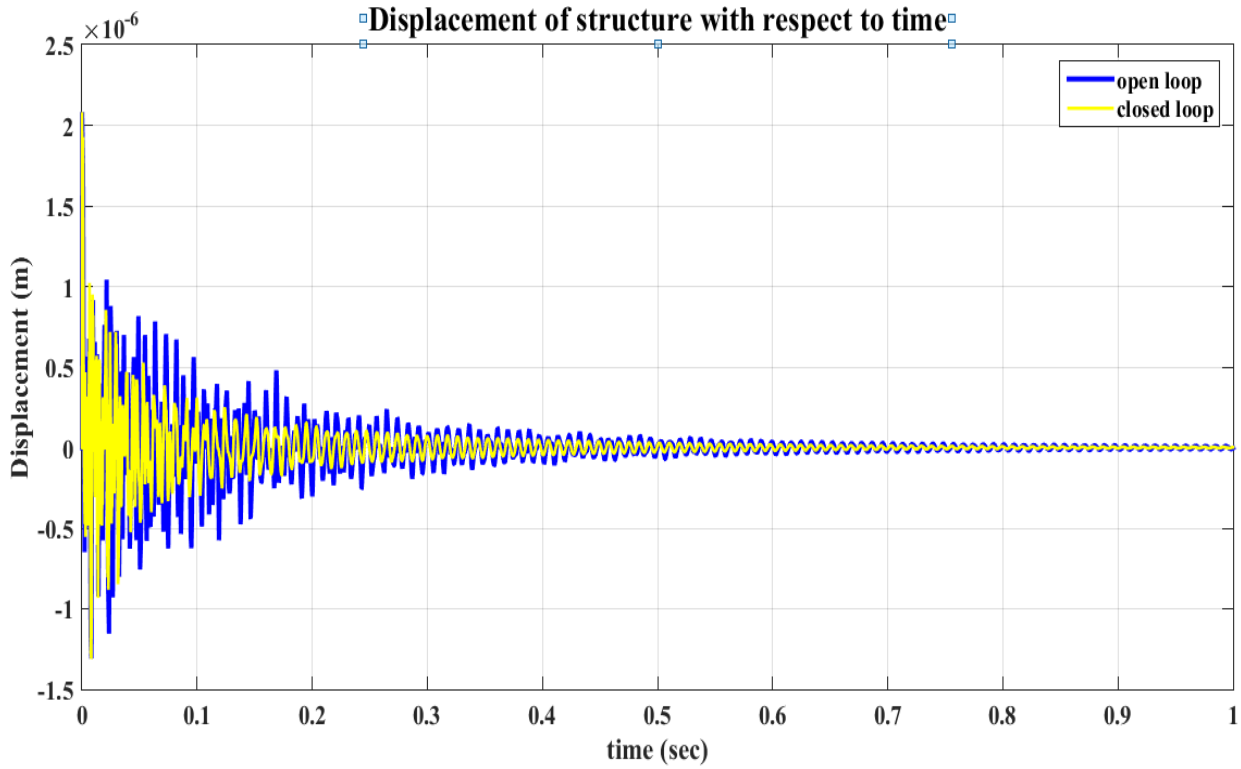

Fig (7.12): Nodal displacement response at $G_d = 0.08$ and $G_v = 0.08$

Next hammer excitation force and response force is applied on the plate of optimal velocity gain value (G_v) =0.08 at different nodes by taking the 8 different cases as represented in fig (7.13)

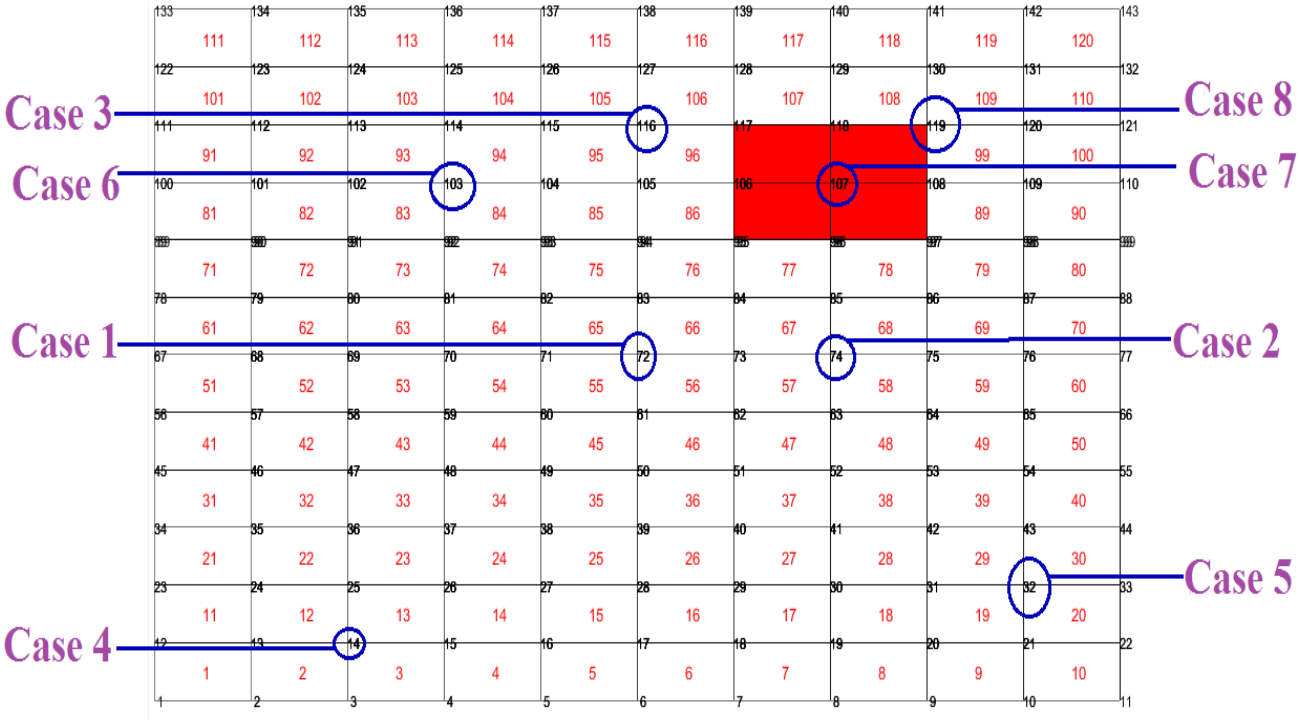

Fig (7.13): Finite element Mesh of plate with piezoelectric patch of different cases with respect to node number

Case 1: The hammer excitation force is applied at node 103 as no nodal lines are passing through that node number and response force is applied at the centre of plate i.e. node 72. The displacement respone of structure at node 72 was shown in fig (7.14). It was found that control of vibrations which are produced by structure was not so effective.

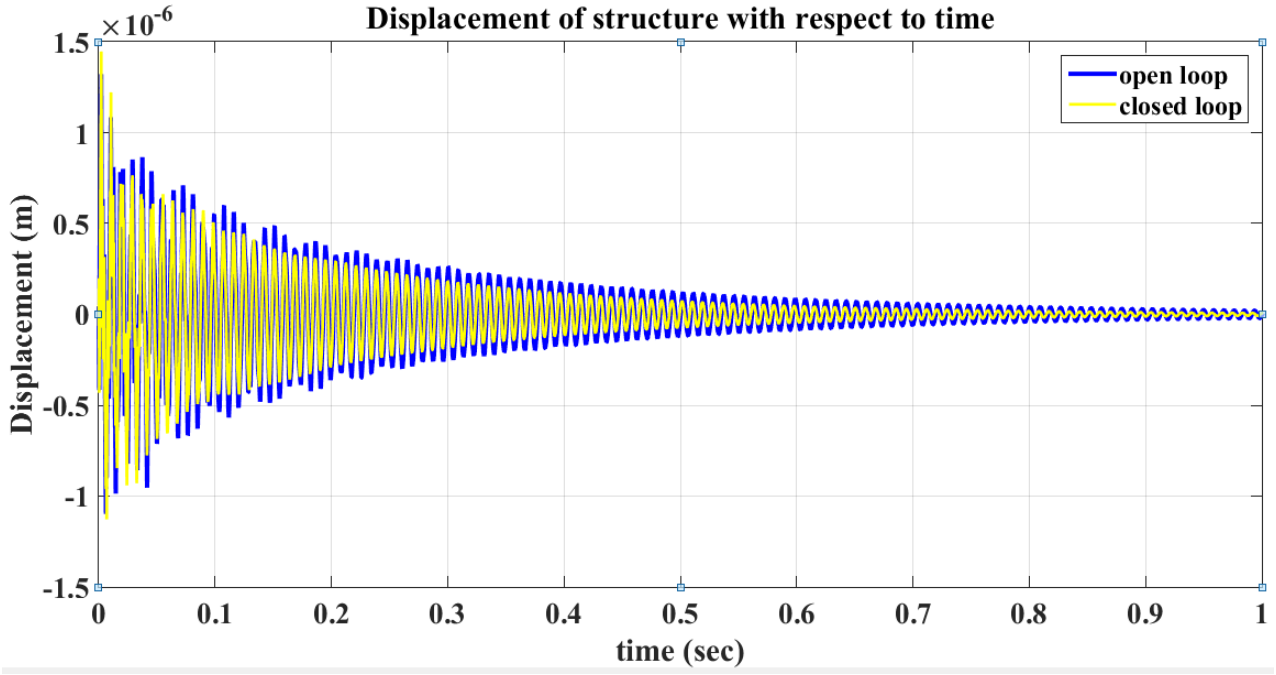

Fig (7.14): Displacement response at node number f=103; r=72

Case 2: Then response force is applied just away from the centre of plate in horizontal direction at node 74. The displacement respone of structure at node 74 was shown in fig (7.15). It was found that control of vibrations which are produced by structure was not so effective as nodal lines are passing.

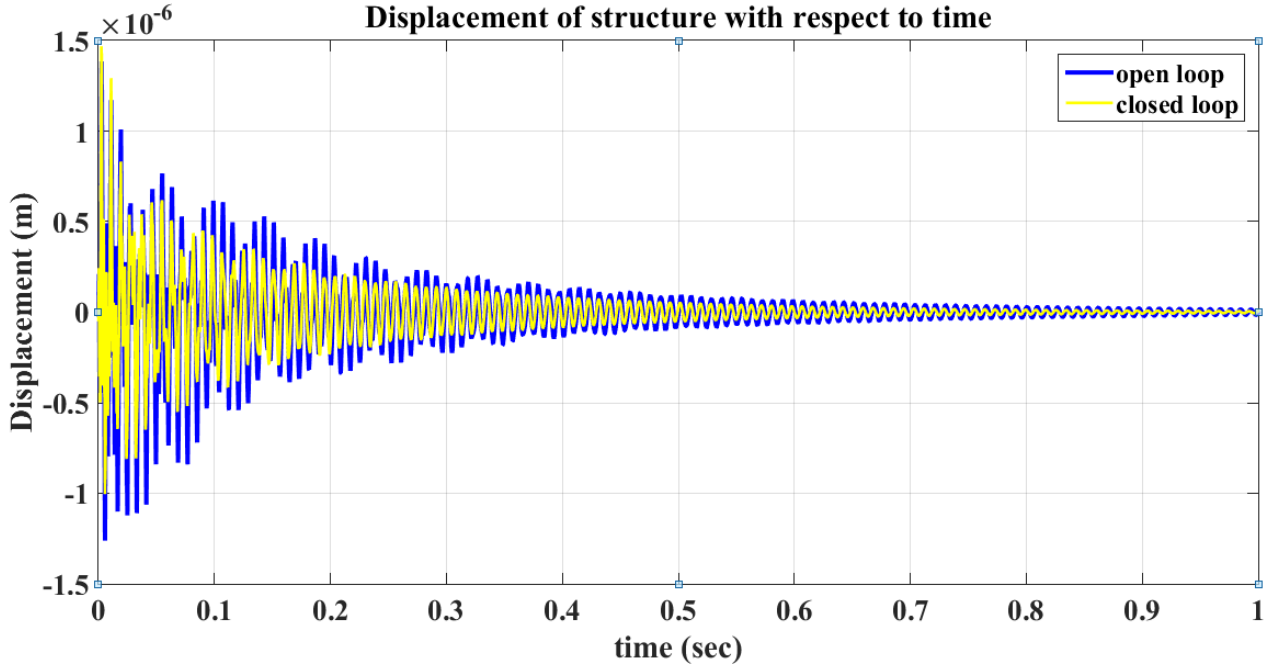

Fig (7.15): Displacement response at node number f=103; r=74

Case 3: Then response force is applied away from the centre of plate in vertical direction i.e. node 116. The displacement respone of structure at node 116 was shown in fig (7.16). It was found that control of vibrations which are produced by structure was not so effective as nodal lines are passing.

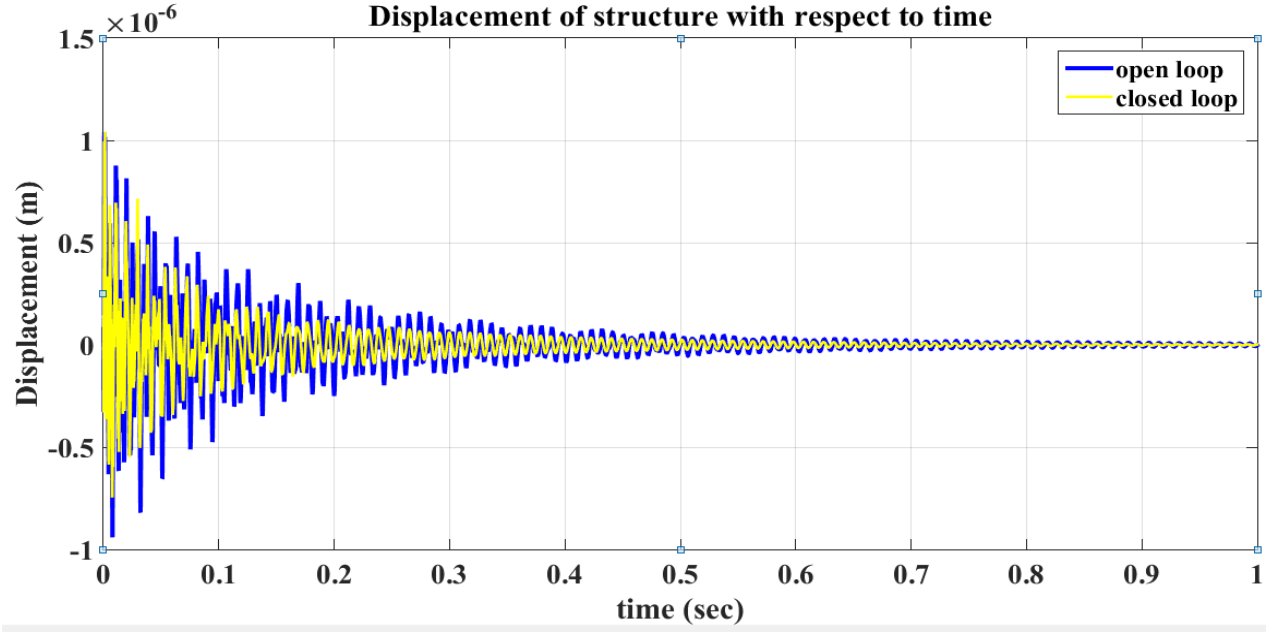

Fig (7.16): Displacement response at node number f=103; r=116

Case 4: In order to cover the complete plate, the response force is applied at the node 14. The displacement respone of structure at node 14 was shown in fig (7.17). It was found that control of vibrations which are produced by structure was not as effective as nodal lines are passing.

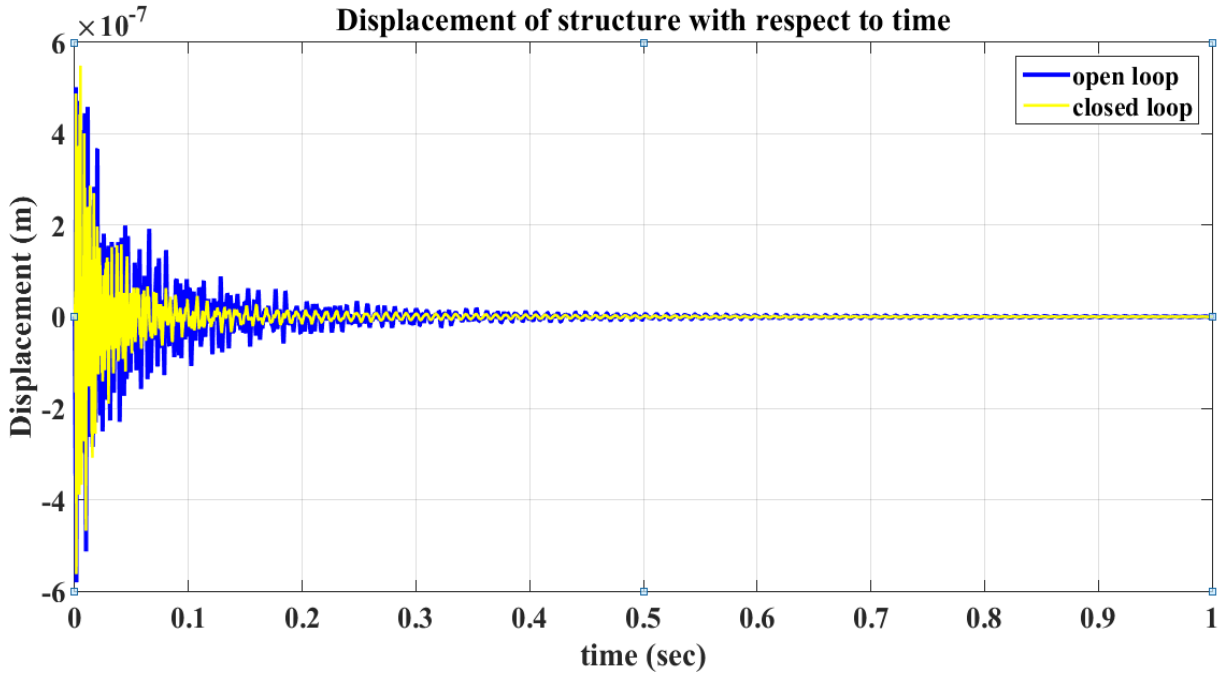

Fig (7.17): Displacement response at node number f=103; r=14

Case 5: Then response force is applied at the node 32. The displacement respone of structure at node 32 was shown in fig (7.18). It was found that control of vibrations which are produced by structure was not so effective as nodal lines are passing.

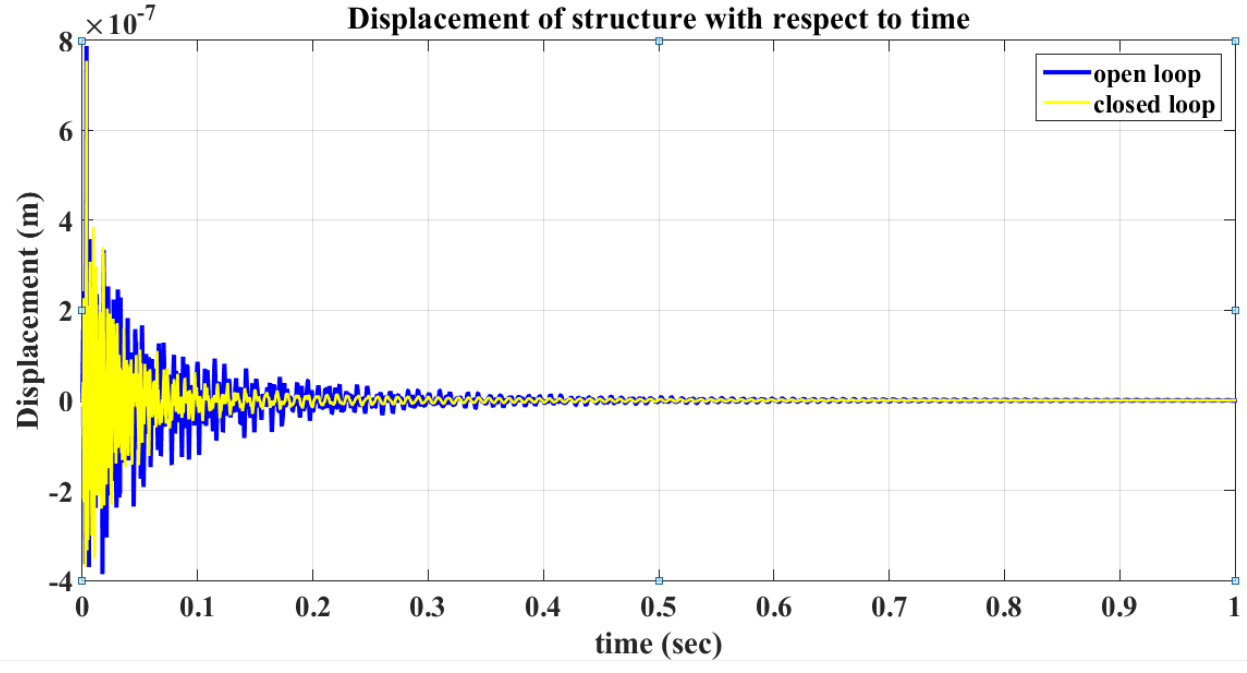

Fig (7.18): Displacement response at node number f=103; r=32

Case 6: Then response force is applied at the node 103. The displacement response of structure at node 103 was shown in fig (7.19). It was found that control of vibrations which are produced by structure was not so effective as nodal lines are passing.

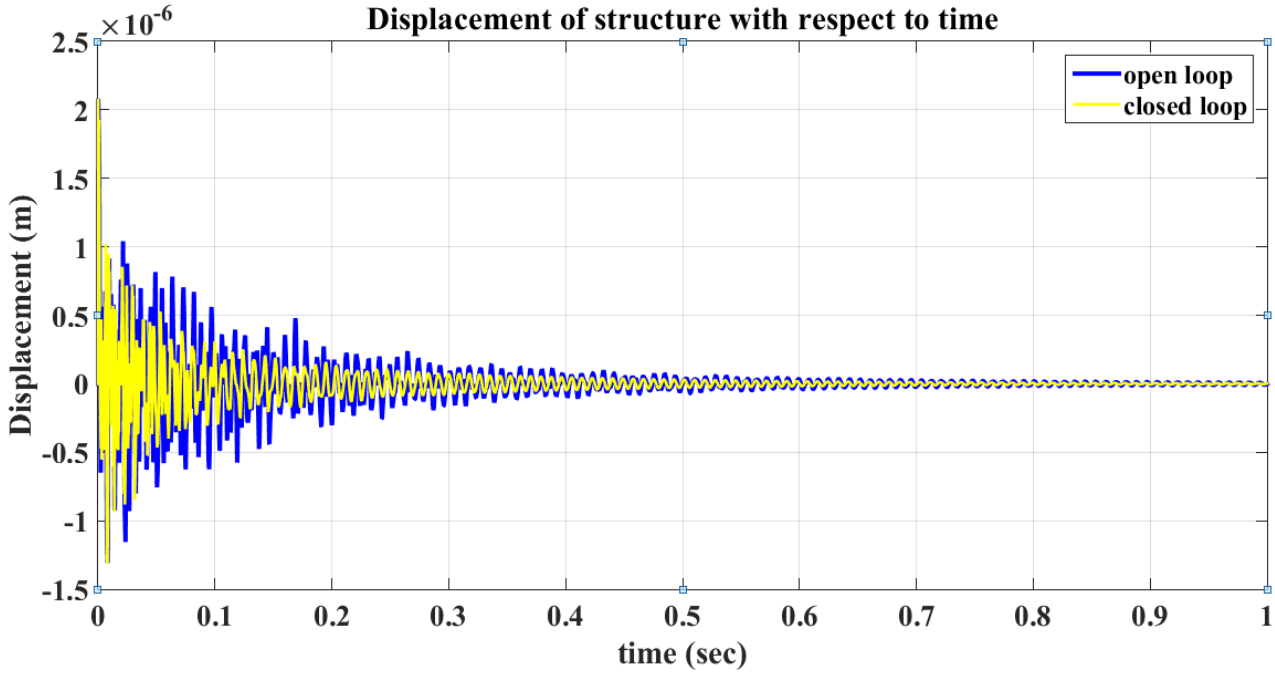

Fig (7.19): Displacement response at node number f=103: r=103

Case 7: Then response force is applied at the centre of piezoelectric patchon a plate i.e. node 107. The displacement respone of structure at node 107 was shown in fig (7.20). It was found that control of vibrations which are produced by structure was effective as it was optimal location.

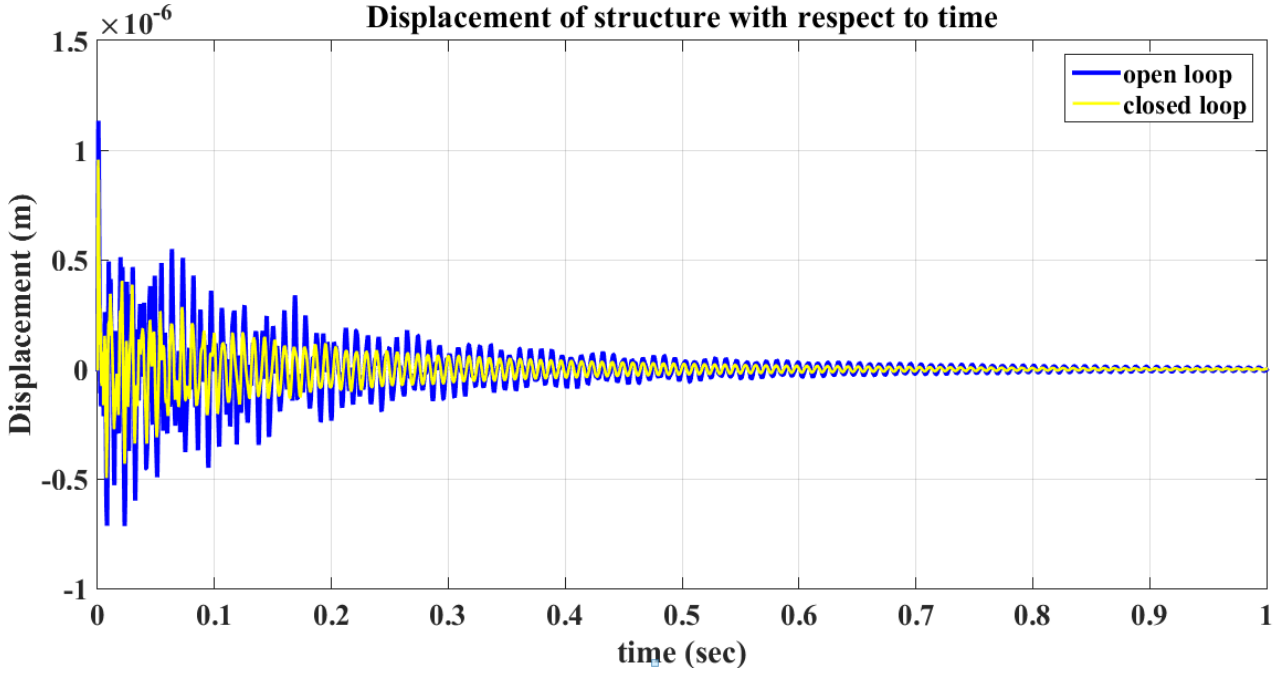

Fig (7.20): Displacement response at node number f=107; r=107

Case 8: Then response force is applied at the centre of plate i.e. node 117. The nodal displacement respone of structure at node 117 was shown in fig (7.21). It was found that control of vibrations which are produced by structure was more effective then compared to the displacement response at centre of piezoelectric patch i.e at node 103.

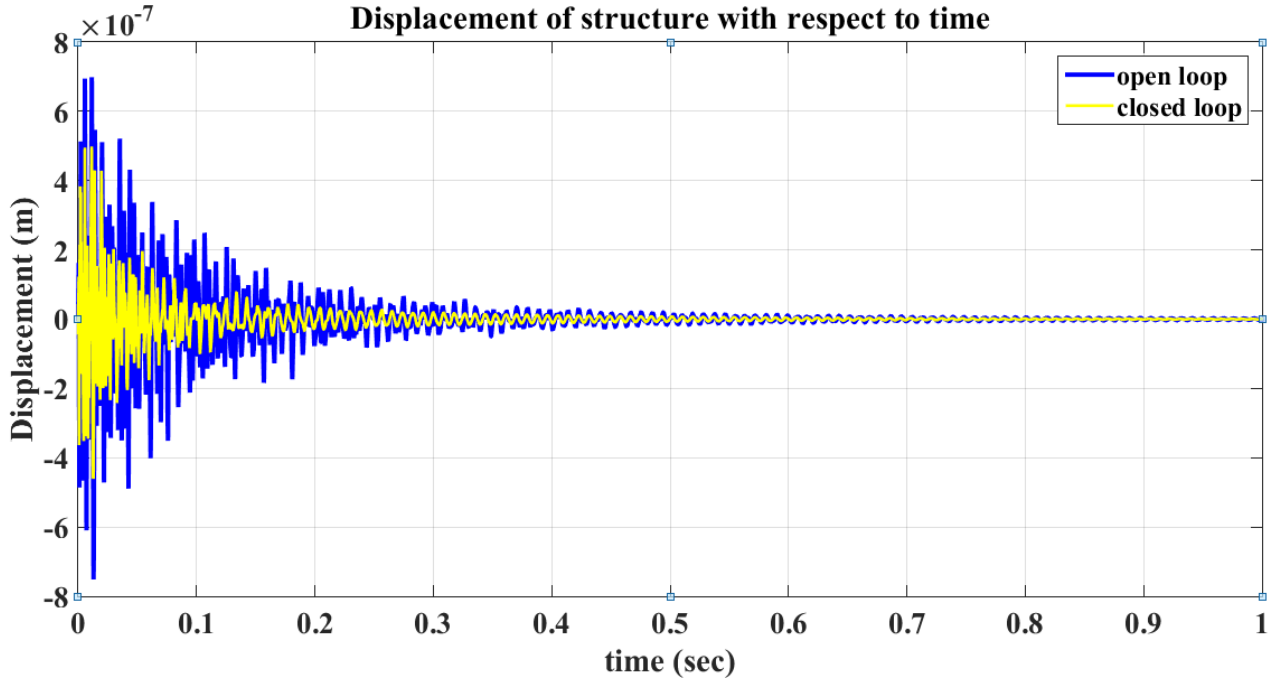

Fig (7.21): Displacement response at node number f=103; r=119

CHAPTER-8

CONCLUSIONS AND FUTURE SCOPE

- In this thesis, the optimal location of piezoelectric patch on bare plate for different boundary conditions like cantilever, free-free, simply supported, clamped at all edges was found.

- A viewing method was proposed for optimal location of piezoelectric patch on plate. In this method, mode shapes are viewed by conducting modal analysis in Abaqus software.

- By viewing the mode shape, it was found out that if piezoelectric patch was placed on the plate where nodal lines are passing it will result in the poor control of vibrations.

- By placing the piezo at different locations with clamped at all edges boundary condition on plate, it was found out that at location L (37, 38, 48, 49) was taken as best optimum location of piezoelectric patch as it is satisfying all the mode shapes where no nodal lines are passing through the piezo.

- For cantilever boundary condition, the location L (28, 29, 39, and 40) was found out as best optimum location of piezoelectric patch on plate as it is satisfying all the mode shapes.

- For free-free boundary condition, the location L (123, 124, 134, and 135) was found out as the optimum location of piezoelectric patch on plate.

- For simply supported boundary condition, the location L (37, 38, 48, and 49) was found out as the optimum location of piezoelectric patch on plate. It was concluded that the viewing method was quick and easy for finding the optimum location of piezoelectric patch.

- The optimum location for different boundary conditions which is obtained through viewing method was accurate and most effective as validation was done by conducting frequency response function (FRF) analysis.

- From FRF output, it was observed that the detection of all mode shapes was possible at optimum location.

- A direct output feedback method was proposed for active vibration control strategy. A pole placement technique was found to be more effective as it evaluates the reduction in the displacement of a structure from pole zero maps and nodal displacement response.

- By plotting a closed loop pole zero maps it was found that the optimal velocity gain (G_v) value is at 0.08 and by plotting open loop pole zero map, it was found that there is no control of vibrations.

- When hammer excitation force is applies on a plate at node number 119, it was found that from nodal displacement response the vibrations produced by structure are controlled more efficiently.

- As in this thesis a viewing method was proposed for the optimum location of piezoelectric patch on a plate but there is scope in future a lot of robustic optimization techniques like Linear quadratic regulator, H_∞, Modal reduction techniques etc. may be used for finding the most preferable location and to apply the active vibration control strategy for complete reduction of vibrations.

REFERENCES

[1] K. B. Lim, “Method for Optimal Actuator and Sensor Placement for Large Flexible Structures,” vol. 15, no. 1, 1992.

[2] J. Han and I. Lee, “Optimal placement of piezoelectric sensors and actuators for vibration control of a composite plate using genetic algorithms,” *Smart Mater. Struct.*, vol. 257, 1999.

[3] A. M. Sadri, J. R. Wright, and R. J. Wynne, “Modelling and optimal placement of piezoelectric actuators in isotropic plates using genetic algorithms,” vol. 490, 1999.

[4] M. Strassberger and H. Waller, “Active noise reduction by structural control using piezo-electric actuators,” *Mechatronics*, vol. 10, no. 8, pp. 851–868, 2000.

[5] A. H. S. LI BIN, LI YUGANG, YIN XUEGANG, “Maximal Modal Force Rule for Optimal Placement of Point Piezoelectric Actuators for Plates,” *J. Intell. Mater. Syst. Struct.*, vol. 11, no. July 2000, pp. 512–515, 2000.

[6] H. Zhang, B. Lennox, and P. R. Goulding, “A float-encoded genetic algorithm technique for integrated optimization of piezoelectric actuator and sensor placement and feedback gains,” *Smart Mater. Struct.*, vol. 552, 2000.

[7] H. D. A. G. O. K. HIRAMOTO, “OPTIMAL SENSOR / ACTUATOR PLACEMENT FOR ACTIVE VIBRATION CONTROL USING EXPLICIT SOLUTION OF ALGEBRAIC RICCATI EQUATION,” *J*, vol. 229, pp. 1057–1075, 2000.

[8] O. J. Aldraihem, S. Arabia, T. Singh, and R. C. Wetherhold, “Optimal Size and Location of Piezoelectric Actuator / Sensors : Practical Considerations,” vol. 23, no. 3, 2000.

[9] D. Sun and L. Tong, “Vibration Control of Plates Using Discretely Distributed Piezoelectric Quasi-Modal Actuators / Sensors,” vol. 39, no. 9, 2001.

[10] P. Liu, V. S. Rao, and M. Derriso, “Active Control of Smart Structures with Optimal Actuator and Sensor Locations,” vol. 4693, pp. 1–12, 2002.

[11] Y. J. Y. and L. H. Yam, “Optimal design of number and locations of actuators in active vibration control of a space truss,” *Smart Mater. Struct.*, vol. 496, 2002.

[12] D. Halim and S. O. R. Moheimani, “An optimization approach to optimal placement of collocated piezoelectric actuators and sensors on a thin plate q,” vol. 13, pp. 27–47, 2003.

[13] G. Caruso, S. Galeani, and L. Menini, “Active vibration control of an elastic plate using multiple piezoelectric sensors and actuators,” vol. 11, pp. 403–419, 2003.

[14] P. U. Sik, C. J. Weon, Y. Wan-suk, L. M. Hyung, S. Kwon, L. J. Myung, and L. M. Cheol, “Optimal Placement of Sensors and Actuators Using Measures of Modal Controllability and Observability in a Balanced Coordinate,” vol. 17, 2003.

[15] I. S. Sadek, J. C. Bruch, J. M. Sloss, and S. Adali, “Feedback control of vibrating plates using piezoelectric patch sensors and actuators,” *Compos. Struct.*, vol. 62, no. 3–4, pp. 397–402, 2003.

[16] J. F. Ribeiro and V. Steffen, “Finite Element Modeling of a Plate with Localized Piezoelectric Sensors and Actuators,” *J. Braz. Soc. Mech. Sci. Eng. Copyr.*, vol. XXVI, no. 2, pp. 117–128, 2004.

[17] V. M. Franco and P. G. Martins, “Optimal design in vibration control of adaptive structures using a simulated annealing algorithm,” vol. 75, pp. 79–87, 2006.

[18] W. Seemann, A. Ekhlakov, E. Glushkov, N. Glushkova, and O. Kvasha, “The modeling of piezoelectrically excited waves in beams and layered substructures,” *J. Sound Vib.*, vol. 301, no. 3–5, pp. 1007–1022, 2007.

[19] K. R. Kumar and S. Narayanan, “The optimal location of piezoelectric actuators and sensors for vibration control,” *Smart Mater. Struct.*, vol. 2680, 2007.

[20] W. Gawronski and K. B. Lim, “Balanced actuator and sensor placement for flexible structures,” no. March 2015, pp. 37–41, 2007.

[21] Z. Qiu, X. Zhang, H. Wu, and H. Zhang, “Optimal placement and active vibration control for piezoelectric smart flexible cantilever plate,” vol. 301, pp. 521–543, 2007.

[22] M. Pietrzakowski, “Piezoelectric control of composite plate vibration: Effect of electric potential distribution,” *Comput. Struct.*, vol. 86, no. 9, pp. 948–954, 2008.

[23] G. Zhao, J. Wang, and Y. Gu, “Optimal placement of piezoelectric active bars in vibration control by topological optimization,” pp. 699–708, 2008.

[24] E. E. Murat Guney, “Optimal actuator and sensor placement in flexible structures using closed-loop criteria,” *J. Sound Vib.*, vol. 312, pp. 210–233, 2008.

[25] K. D. Dhuri and P. Ã. Seshu, “Multi-objective optimization of piezo actuator placement and sizing using genetic algorithm,” vol. 323, pp. 495–514, 2009.

[26] Z. cheng Qiu, H. xin Wu, and D. Zhang, “Experimental researches on sliding mode active vibration control of flexible piezoelectric cantilever plate integrated gyroscope,” *Thin-Walled Struct.*, vol. 47, no. 8–9, pp. 836–846, 2009.

[27] M. S. A. N. T. VIVEK GUPTA, “Optimization Criteria for Optimal Placement of Piezoelectric Sensors and Actuators on a Smart Structure :,” vol. 21, no. August, 2010.

[28] I. Bruant, L. Gallimard, and S. Nikoukar, “Optimal piezoelectric actuator and sensor location for active vibration control , using genetic algorithm,” *J. Sound Vib.*, vol. 329, no. 10, pp. 1615–1635, 2010.

[29] L. Malgaca, “Integration of active vibration control methods with finite element models of smart laminated composite structures,” *Compos. Struct.*, vol. 92, no. 7, pp. 1651–1663, 2010.

[30] I. Z. M. D. MR. Sajizadeh, “OPTIMAL LOCATION OF SENSOR FOR ACTIVE VIBRATION CONTROL OF OF FLEXIBLE SQUARE PLATE,” no. Isspa, pp. 393–396, 2010.

[31] D. Starek and P. Solek, “Suppression of vibration with optimal actuators and sensors placement,” vol. 20, no. 1, pp. 99–120, 2010.

[32] B. Behjat, M. Salehi, A. Armin, M. Sadighi, and M. Abbasi, “Static and dynamic analysis of functionally graded piezoelectric plates under mechanical and electrical loading,” *Sci. Iran.*, vol. 18, no. 4 B, pp. 986–994, 2011.

[33] R. Dutta, R. Ganguli, and V. Mani, “Swarm intelligence algorithms for integrated optimization of piezoelectric actuator and sensor placement and,” vol. 105018, 2011.

[34] A. H. D. and J. M. Hale, “Active vibration reduction of a flexible structure bonded with optimised piezoelectric pairs using half and quarter chromosomes in genetic algorithms,” vol. 12039, 2012.

[35] F. Bachmann, A. E. Bergamini, and P. Ermanni, “Optimum piezoelectric patch positioning : A strain energy – based finite element approach,” vol. 23, no. 14, pp. 1575–1591, 2012.

[36] J. M. H. and A. H. Daraji, “Optimal placement of sensors and actuators for active vibration reduction of a flexible structure using a genetic algorithm based on modified H _ infinity,” *Mod. Pract. Stress Vib. Anal.*, 2012.

[37] S. K. Parashar, U. von Wagner, and P. Hagedorn, “Finite element modeling of nonlinear vibration behavior of piezo-integrated structures,” *Comput. Struct.*, vol. 119, pp. 37–47, 2013.

[38] A. Zolfagharian, A. Noshadi, M. R. Khosravani, and M. Z. M. Zain, “Unwanted noise and vibration control using finite element analysis and artificial intelligence,” *Appl. Math. Model.*, vol. 38, no. 9–10, pp. 2435–2453, 2014.

[39] M. Ansari, A. Khajepour, and E. Esmailzadeh, “Application of level set method to optimal vibration control of plate structures,” *J. Sound Vib.*, vol. 332, no. 4, pp. 687–700, 2013.

[40] M. Trajkov and T. Nestorovic, “Optimal actuator and sensor placement based on balanced reduced models,” vol. 36, pp. 271–289, 2013.

[41] K. A. M. Nor, A. G. A. Muthalif, and A. N. Wahid, “Ant colony Optimization for Controller and Sensor-Actuator Location in Active Vibration Control,” vol. 32, no. 4, pp. 293–308, 2013.

[42] N. Darivandi, K. Morris, and A. Khajepour, “An algorithm for LQ optimal actuator location,” vol. 35001, 2013.

[43] Z. Qiu and D. Ling, “Finite element modeling and robust vibration control of two-hinged plate using bonded piezoelectric sensors and actuators,” *Acta Mech. Solida Sin.*, vol. 27, no. 2, pp. 146–161, 2014.

[44] M. Rahmoune, “Optimal Position of Piezoelectric Material on a Smart Structure,” vol. 5, no. 1, pp. 1–9, 2014.

[45] A. K. and S. V. Modak and Abstract, “Virtual Sensing of Acoustic Potential Energy Through a Kalman Filter for Active Control of Interior Sound,” *Proc. 32nd Int. Modal Anal. Conf. (IMAC-XXXII), A Conf. Expo. Struct. Dyn. Florida, USA,(3 -6 February)*, pp. 221–241, 2014.

[46] M. H. and H. C. Xiufeng Huang, “The optimal location of Piezoelectric Sensor/Actuator Based on Adaptive Genetic Algorithm,” *Appl. Mech. Mater.*, vol. 637, pp. 799–804, 2014.

[47] Z. Qiu and B. Ma, “Adaptive Resonant Vibration Control of a Piezoelectric Flexible Plate Implementing Filtered-X LMS Algorithm,” vol. 19, no. 4, 2014.

[48] S. K. Vashist and D. Chhabra, “Optimal Placement of Piezoelectric Actuators on Plate Structures for Active Vibration Control Using Genetic Algorithm,” vol. 9057, pp. 1–13, 2014.

[49] S. Thenozhi and W. Yu, “Stability analysis of active vibration control of building structures using PD/PID control,” *Eng. Struct.*, vol. 81, pp. 208–218, 2014.

[50] S. Zhang, R. Schmidt, and X. Qin, “Active vibration control of piezoelectric bonded smart structures using PID algorithm,” *Chinese J. Aeronaut.*, vol. 28, no. 1, pp. 305–313, 2015.

[51] M. Kerboua, A. Megnounif, M. Benguediab, K. H. Benrahou, and F. Kaoulala, “Vibration control beam using piezoelectric-based smart materials,” *Compos. Struct.*, vol. 123, pp. 430–442, 2015.

[52] N. Sehgal, M. Malik, and D. Chhabra, “Meta-heuristics Approaches for the Placement of Piezoelectric Actuators / Sensors on a Flexible Cantilever Plate : A Review,” vol. 3, no. 6, pp. 7–16, 2014.

[53] K. Khorshidi, E. Rezaei, A. A. Ghadimi, and M. Pagoli, “Active vibration control of circular plates coupled with piezoelectric layers excited by plane sound wave,” *Appl. Math. Model.*, vol. 39, no. 3–4, pp. 1217–1228, 2015.

[54] M. K. Kwak and D.-H. Yang, “Dynamic modelling and active vibration control of a submerged rectangular plate equipped with piezoelectric sensors and actuators,” *J. Fluids Struct.*, vol. 54, no. 0, pp. 848–867, 2015.

[55] P. M. J. Jweeg and T. J. Ntayeesh, “Active Vibration Control Analysis of Cantilever Pipe Conveying Fluid Using Smart Material,” vol. 6, no. 12, 2015.

[56] W. Larbi, J. F. Deü, and R. Ohayon, “Finite element reduced order model for noise and vibration reduction of double sandwich panels using shunted piezoelectric patches,” *Appl. Acoust.*, vol. 108, pp. 40–49, 2016.

[57] V. Jawali, P. Parasivamurthy, and P. Prakash, “The Optimal Placement of Sensors by Minimizing the Maximum Probability of Non-Detection using Genetic Algorithm,” vol. 879, pp. 826–831, 2017.

[58] A. Koszewnik and Z. Gosiewski, “Quasi-optimal locations of piezo-elements on a rectangular plate,” 2016.

[59] K. Kuliński and J. Przybylski, “Piezoelectric effect on transversal vibrations and buckling of a beam with varying cross section,” *Mech. Res. Commun.*, 2016.

[60] Ashok K. Bagha and S.V.Modak, “ACTIVE STRUCTURAL-ACOUSTIC CONTROL OF INTERIOR NOISE USING DIRECT OUTPUT FEEDBACK,” *Proc. 17th ISME Conf. ISME17*, pp. 3–8, 2015.

Appendix

```
Finite element formulation of structure/piezoelectric patch coupled
%             Structure/piezo/cavity system (Properties)
%_____________________________________________________________________________
%Geometry and material properties of the structure:                          |
%For 2D plate: Material ____ steel                                           |
%           Density_______ 7800 Kg/m3                                        |
%           Young's Modulus ___ 200e09 N/m2                                  |
%           Length in x direction ___ 0.261 m                                |
%           Length in y direction ____ 0.3 m                                 |
%           Thickness in z direction ___ 0.001 m                             |
%           Poission's ratio _____________0.30 (no units)                    |
%           Modal damping factor__________0.005                              |
%           Boundary Conditions __________Clamped-Clamped                    |
%           Mesh size____________________5*6                                 |
%_____________________________________________________________________|_________
%Properties of Dura Act P-876 A12 Transducer are:                            |

%           Length in x direction_____0.0522 m                               |
%           Length in y direction_____0.05 m                                 |
%           Thickness in zee direction___0.0005 m                            |
%           Density_____________________7800 Kg/m3                           |
%           Poission's ratio____________0.3400                               |
%Properties (Electrical)                                                     |
%           Piezoelectric stress coefficient:                                |
%                              e31=e32=-8.9678 C/m2                          |
%           Dielectric constant:                                             |
%                                emm_33=6.6075e-9 F/m                        |
%_____________________________________________________________________|_________
%_____________________________________________________________________________
%                   TERMS AND ABBRIVATIONS
%                   _____________________
%                   _____________________
%
%w: mechanical displacement variable in z direction
%v: electrical displacement variable i.e., electric potential difference
%va:electric pot. difference for actuator
%vs:electric pot. difference for sensor
%p: acoustic variable (pressure inside the cavity)
%ML: Mass of the Laminate(Msensor+Mstructure+Mactuator)
%Mass_c: Mass of the acoustic domain
%KL: stiffness of the Laminate(Ksensor+Kstructure+Kactuator)
%stiffness_c: stiffness of the acoustic domain
%S: coupling matrix connecting the mechanical variable(w)and acoustic
var(p)
%Kwva:coupling matrix for actuator which connecting w with v
%Kwvs: coupling matrix for sensor which connecting w with vs
%Kvva:electrical capacitance for actuator
%Kvvs:electrical capacitance for sensor
%Kel: electrical added stiffness matrix
%F: vector of external mechanical loads apply to the structure
%Qa: actuator electric charges brought to the electrode

%_____________________________________________________________________________
clear all % clears all the variables in the MATLAB workspace
clc   %clears the command window
format long
%_____________________________________________________________________________
```

```
fr1=fopen('input_str.m','r+');% input file name is input_str (input file
data related to structural data only)
temp=fscanf(fr1,'%f %f %f %f %f %f %f %f %f %f',10);
Length_x=temp(1,1); % length of plate in X axis direction in meters
Lx=Length_x;        % Lx representation for width in x direction
Length_y=temp(2,1); % length of plate in Y axis direction in meters
Ly=Length_y;        % Ly representation for height in y direction
thickness=temp(3,1);% thickness of plate in Z axis in meters
t=thickness;        % t represents the thickness very small as compared
with width and height of structure
Young_modulus=temp(4,1); % Young's modulus of elasticity of plate in N/m2
E=Young_modulus;    % E represents the mechanical property of isotropic
plate
rho=temp(5,1);      % density of the plate material
neu=temp(6,1);      % Poissions ratio for aluminium taken from Google
source
nele_xs=temp(7,1);  % number of elements in x direction
nele_ys=temp(8,1); % number of elements in y direction
cd=temp(9,1);       %total nodes/coordinates for the structure
nod=temp(10,1);      %total number of elements for structure
DUMMY = fgets(fr1);
DUMMY = fgets(fr1);
temp=fscanf(fr1,'%f%f',[2 cd]);
coordinates=temp';
x=coordinates(:,1);
y=coordinates(:,2);
DUMMY = fgets(fr1);
DUMMY = fgets(fr1);
for ii=1:nod
    nodes(ii,:)=str2num(fgets(fr1));
end
fclose(fr1);

a=Length_x/(nele_xs*2); %a represents the element size from its center in x
direction
b=Length_y/(nele_ys*2); %b represents the element size from its center in y
direction

%~~~~~~~~~~~~~~~~~~~~~~~~~~~~~~~~~~~~~~~~~~~~~~~~~~~~~~~~~~~~~~~~~~~~~~~~~~~
%plotMesh5(coordinates,nodes)    % Mesh, number of elements, node numbers
for the structure
%~~~~~~~~~~~~~~~~~~~~~~~~~~~~~~~~~~~~~~~~~~~~~~~~~~~~~~~~~~~~~~~~~~~~~~~~~~~

nel=length(nodes);              % Total number of elements in the system for
structure
nnel=4;                         % number of nodes per element usually 4
ndof=3;                         % number of dof per node usually 3
nnode=length(coordinates);      % total number of nodes/coordinates in the
system for structure
sdof=nnode*ndof;                % total system dof for the structure
edof=nnel*ndof;                 % dof per element___for structure its value
is 4*3=12
h2=t^3/12;                      % Inertia propoertiy for structure
represented by h2

%~~~~~~~~~~~~~~~~~~~~~~~~~~~~~~~~~~~~~~~~~~~~~~~~~~~~~~~~~~~~~~~~~~~~~~~~~~~
% Initialization of matrices and vectors
%~~~~~~~~~~~~~~~~~~~~~~~~~~~~~~~~~~~~~~~~~~~~~~~~~~~~~~~~~~~~~~~~~~~~~~~~~~~
stiffness=zeros(sdof,sdof);     % Global system stiffness matrix for
structure
```

```
Mass=zeros(sdof,sdof);          % Global system mass matrix for structure
index=zeros(edof,1);            % index vector for an element of structure
%_____________________________________________________________________
% STRUCTURE : STIFFNESS

for iel=1:nel                   % loop for the total number of elements for
structure

for i=1:nnel
node(i)=nodes(iel,i);           % extract connected node for (iel)-th
element of structure
xx(i)=coordinates(node(i),1);   % extract x value of the node
yy(i)=coordinates(node(i),2);   % extract y value of the node
end
%-------------------------------------------------------------------------
% ---------------------Element stiffness matrix for structure -----------
%-------------------------------------------------------------------------
[X] = Xmatrix( a,b );
[A] = Jaccobi( a,b );
E1=E/(1-neu^2);
G=E/(2*(1+neu));
D=[E1 E1*neu 0;E1*neu E1 0;0 0 G];  %Bending property of plate
material.....
h2=t^3/12;
temp1=0;
for i=1:4
    x=A(i,1);
    y=A(i,2);
    Lk=[0 0 0 2 0 0 6.*x 2.*y 0 0 6.*x.*y 0;
        0 0 0 0 0 2 0 0 2.*x 6.*y 0 6.*x.*y;
        0 0 0 0 2 0 0 4.*x 4.*y 0 6.*x.^2 6.*y.^2];
    LKT=Lk';
    KK=LKT*D*Lk+temp1;
    temp1=KK;
end
K1=a*b*h2*(inv(X))'*KK*inv(X);
ke = K1;                        % element stiffness matrix of size 12 * 12
%-------------------------------------------------------------------------
%--------calculation for global stiffness matrix for structure ------------
%-------------------------------------------------------------------------

index=elementdof(node,nnel,ndof);
                                % extract system dofs associated with element

[stiffness]=assemble(stiffness,ke,index);
                                % "assemble function" for assembly for
stiffness
                                % assemble Global stiffness  matrices

 %-------------------------------------------------------------------------
 %-----------------Element mass matrix for structure ----------------------
 %-------------------------------------------------------------------------

 % STRUCTURE: MASS

 H=[t 0 0;0 h2 0;0 0 h2];
 temp2=0;
 for i=1:4
     x=A(i,1);
     y=A(i,2);
```

```
    Lm=[1 x y x.^2 x.*y y.^2 x.^3 x.^2.*y x.*y.^2 y.^3 x.^3.*y x.*y.^3;
        0 1 0 2.*x y 0 3.*x.^2 2.*x.*y y.^2 0 3.*x.^2.*y y.^3;
        0 0 1 0 x 2.*y 0 x.^2 2.*x.*y 3.*y.^2 x.^3 3.*x.^2.*y];
    LM=Lm'*H*Lm+temp2;
    temp2=LM;
 end
 M1=a*b*rho*(inv(X))'*LM*inv(X);

 me=M1;                          % element mass matrix of size 12 * 12
 %-------------------------------------------------------------------------
 %-----------------  Global Mass matrix for structure --------------------
 %-----------------------------------------a
index=elementdof(node,nnel,ndof);
                                 % extract system dofs associated with element

[Mass]=assemblemass(Mass,me,index);
                                 % "assemblemass function" is used for
assembly
                                 % assemble Global mass matrices
end

%-------------------------------------------------------------------------
% Mass and stiffness of the structure:

Kstr=stiffness;    % Global stiffness of the structure
Mstr=Mass;         % Global mass of the structure

%-------------------------------------------------------------------------


% MODELING OF ACTUATOR/SENSOR ON STRUCTURE

% PZT-5H ACTUATOR

frp=fopen('input_actuator.m','r+');% input file name is input_piezo (input
file data related to actuator data only)
temp=fscanf(frp,'%f %f %f %f %f %f %f %f %f %f %f %f %f %f %f %f %f
%f',18);
Length_x_a=temp(1,1);      % length of actuator in X axis in m
Lx_a=Length_x_a;
Length_y_a=temp(2,1);      % length of actuator in Y axis in m
Ly_a=Length_y_a;
thickness_a=temp(3,1);     % thickness of Actuator in Z axis in m
ha=thickness_a;            %ha is the thickness of the actuator
Young_modulus=temp(4,1);   % modulus of elasticity of PZT5 Material in N/m2
E_a=Young_modulus;
rho_a=temp(5,1);           % density of the PZT material Kg/m3
neu_a=temp(6,1);           % Poissions ratio of PZT
act_em=temp(7,1);          % actuator elements and connectivity
nele_xpzo_a=temp(8,1);     % division of number of elements of piezoelectric
actuator in x direction
nele_ypzo_a=temp(9,1);     % division of number of elements of piezoelectric
actuator in y direction
C11=temp(10,1);            %Coefficient of elastic stiffness matrix
C33=temp(11,1);            %Coefficient of elastic stiffness matrix
C13=temp(12,1);            %Coefficient of elastic stiffness matrix
C12=temp(13,1);            %Coefficient of elastic stiffness matrix
C44=temp(14,1);            %Coefficient of elastic stiffness matrix
C66=temp(15,1);            %Coefficient of elastic stiffness matrix
```

```
e31=temp(16,1);           %Piezoelectric stress coefficient
e32=temp(17,1);           %Piezoelectric stress coefficient
emm_33=temp(18,1);        %emmisivity in 33 direction
DUMMY = fgets(frp);
DUMMY = fgets(frp);
for ii=1:act_em
   act_em_c_c(ii,:)=str2num(fgets(frp));% number of actuator elements
end
fclose(frp);
apzo_a=Length_x_a/(nele_xpzo_a*2); %apzo_a represents the element size from
its center in x direction for PZT actuator (xpzo=xi*apzo_a)
bpzo_a=Length_y_a/(nele_ypzo_a*2); %bpzo_a represents the element size from
its center in y direction for PZT actuator (ypzo=eta*pzo_a)

%~~~~~~~~~~~~~~~~~~~~~~~~~~~~~~~~~~~~~~~~~~~~~~~~~~~~~~~~~~~~~~~~~~~~~~~~~~~~
% Initialization of matrices and vectors for actuator
%~~~~~~~~~~~~~~~~~~~~~~~~~~~~~~~~~~~~~~~~~~~~~~~~~~~~~~~~~~~~~~~~~~~~~~~~~~~~
index_actuator=zeros(edof,1);        % index vector for laminate part
Mass_Able_actuator=zeros(sdof,sdof); % Mass matrix for laminate elements
Global
stiffness_Able_actuator=zeros(sdof,sdof); % stiffness matrix for laminate
elements Global
%_____________________________________________________________________________

%EXTRACT ACTUATOR ELEMENTS

for i=act_em_c_c
    act_em_c=nodes(i,:);% connectivity between actuator elements
end
%_____________________________________________________________________________

%GEOMETRY OF STRUCTURE COUPLED WITH PZT-5H(MESH, NO. OF ELEMENTS, NODE
NO'S)

PlotMesh_str_piezo(coordinates,nodes,act_em_c)
%_____________________________________________________________________________

h1=ha*(t/2 + ha/2)^2+ ha^3/12;
Ha=[ha 0 0;0 h1 0;0 0 h1];

% MASS OF THE ACTUATOR

[Apzo_a] = Amatrix(apzo_a,bpzo_a);

A_a=[-1/sqrt(3).*apzo_a -1/sqrt(3).*bpzo_a;
    1/sqrt(3).*apzo_a -1/sqrt(3).*bpzo_a;
    1/sqrt(3).*apzo_a 1/sqrt(3).*bpzo_a;
    -1/sqrt(3).*apzo_a 1/sqrt(3).*bpzo_a];

for iiel=1:act_em
    for ii=1:nnel
        node_actuator(ii)=act_em_c(iiel,ii);
    end
    temp3=0;
    for i=1:4
        x_a=A_a(i,1);
        y_a=A_a(i,2);
        Lm_a=[1 x_a y_a x_a.^2 x_a.*y_a y_a.^2 x_a.^3 x_a.^2.*y_a
x_a.*y_a.^2 y_a.^3 x_a.^3.*y_a x_a.*y_a.^3;
```

```
            0 1 0 2.*x_a y_a 0 3.*x_a.^2 2.*x_a.*y_a y_a.^2 0
3.*x_a.^2.*y_a y_a.^3;
            0 0 1 0 x_a 2.*y_a 0 x_a.^2 2.*x_a.*y_a 3.*y_a.^2 x_a.^3
3.*x_a.^2.*y_a];
        LM_a=Lm_a'*Ha*Lm_a+temp3;
        temp3=LM_a;
    end

    Ma=apzo_a*bpzo_a*rho_a*(inv(Apzo_a))'*LM_a*inv(Apzo_a);% element mass
matrix for actuator (Ma)

    index_actuator=elementdof_actuator(node_actuator,nnel,ndof);

[Mass_Able_actuator]=assemblemass_actuator(Mass_Able_actuator,Ma,index_actu
ator);% Total assemble mass of the Actuator
end

%STIFFNESS OF THE ACTUATOR

[ce_bar_pz,e_bar_pz,epsilon_pz,thick_pz,rho_pz,poir_pz] =
fpiezo_P876_A12_mat_pic255();

Da=ce_bar_pz;

for iiel=1:act_em
    for ii=1:nnel
        node_actuator(ii)=act_em_c(iiel,ii);
    end
    temp4=0;
    for i=1:4
        x_a=A_a(i,1);
        y_a=A_a(i,2);
        Lk_a=[0 0 0 2 0 0 6*x_a 2*y_a 0 0 6*x_a.*y_a 0;
            0 0 0 0 0 2 0 0 2*x_a 6*y_a 0 6*x_a.*y_a;
            0 0 0 0 2 0 0 4*x_a 4*y_a 0 6*x_a.^2 6*y_a.^2];
        LKT_a=Lk_a';
        K_Q_act=LKT_a*Da*Lk_a+temp4;
        temp4=K_Q_act;
    end
    ka=apzo_a*bpzo_a*h1*(inv(Apzo_a))'*K_Q_act*inv(Apzo_a);% element
stiffness matrix for actuator of size 12*12
    index_actuator=elementdof_actuator(node_actuator,nnel,ndof);

[stiffness_Able_actuator]=assemblestiffness_actuator(stiffness_Able_actuato
r,ka,index_actuator);% Total assemble stiffness of the Actuator
end

%-------------------------------------------------------------------------
Mact=Mass_Able_actuator;     % Global mass of the actuator
Kact=stiffness_Able_actuator;% Global stiffness of the actuator
%-------------------------------------------------------------------------

% ELECTROMECHANICAL COUPLING MATRIX Kwva

ea=e_bar_pz';

%ea=[ e31 e32 0];  %PZT stiffness matrix
```

```
Bz= 1/ha;          % Strain-displacement matrix which relates electric field
with electric potential (v)for a single layer
Kwva=zeros(sdof,1);%Electromechanical coupling vector
index_wv=zeros(edof,1);
for iiel=1:act_em
    for ii=1:nnel
        node_actuator(ii)=act_em_c(iiel,ii);
    end
    temp5=0; %pre-assumed value
    for i=1:4
        x_a=A_a(i,1);
        y_a=A_a(i,2);
        Lk_wv=[0 0 0 2 0 0 6*x_a 2*y_a 0 0 6*x_a.*y_a 0;
            0 0 0 0 0 2 0 0 2*x_a 6*y_a 0 6*x_a.*y_a;
            0 0 0 0 2 0 0 4*x_a 4*y_a 0 6*x_a.^2 6*y_a.^2];
        LKT_wv=Lk_wv';
        Kwv_e=LKT_wv*ea'+temp5;
        temp5= Kwv_e;
    end
    Cwv_e=-apzo_a*bpzo_a*(inv(Apzo_a))'*0.5*(ha^2 +ha*t)*Kwv_e*Bz; % Cwv_e
element coupling electromechanical vector (12*1)
    index_wv=index_a(node_actuator,nnel,ndof);
    Kwva=assemble_wv(Kwva,Cwv_e,index_wv);% Global electromechanical
coupling matrix
end

%-------------------------------------------------------------------------
% ELECTRICAL CAPACITANCE Kvv (actuator)

emm_33=epsilon_pz;

Kvva=-act_em*1/(ha) *4*apzo_a*bpzo_a*emm_33;
%-------------------------------------------------------------------------


%PZT SENSOR

frs=fopen('input_sensor.m','r+');% input file name is input_piezo (input
file data related to actuator data only)
temp=fscanf(frs,'%f %f %f %f %f %f %f %f %f %f %f %f %f %f %f %f
%f',18);
Length_x_s=temp(1,1);      % length of sensor in X axis in m
Lx_s=Length_x_s;
Length_y_s=temp(2,1);      % length of sensor in Y axis in m
Ly_s=Length_y_s;
thickness_s=temp(3,1);     % thickness of sensor in Z axis in m
hs=thickness_s;            %hs is the thickness of the sensor
Young_modulus=temp(4,1);   % modulus of elasticity of PZT5 Material in N/m2
E_s=Young_modulus;
rho_s=temp(5,1);           % density of the PZT material Kg/m3
neu_s=temp(6,1);           % Poissions ratio of PZT
sen_em=temp(7,1);          % sensor elements and connectivity
nele_xpzo_s=temp(8,1);     % division of number of elements of piezoelectric
sensor in x direction
nele_ypzo_s=temp(9,1);     % division of number of elements of piezoelectric
sensor in y direction
C11=temp(10,1);            %Coefficient of elastic stiffness matrix
C33=temp(11,1);            %Coefficient of elastic stiffness matrix
C13=temp(12,1);            %Coefficient of elastic stiffness matrix
C12=temp(13,1);            %Coefficient of elastic stiffness matrix
```

```
C44=temp(14,1);           %Coefficient of elastic stiffness matrix
C66=temp(15,1);           %Coefficient of elastic stiffness matrix
es31=temp(16,1);          %Piezoelectric stress coefficient
es32=temp(17,1);          %Piezoelectric stress coefficient
emm_s33=temp(18,1);       %emmisivity in 33 direction
DUMMY = fgets(frs);
DUMMY = fgets(frs);
for ii=1:sen_em
   sen_em_c_c(ii,:)=str2num(fgets(frs));% number of actuator elements
end
fclose(frs);
apzo_s=Length_x_s/(nele_xpzo_s*2); %apzo_s represents the element size from
its center in x direction for PZT sensor (xpzo=xi*apzo_s)
bpzo_s=Length_y_s/(nele_ypzo_s*2); %bpzo_s represents the element size from
its center in y direction for PZT sensor (ypzo=eta*pzo_s)

%~~~~~~~~~~~~~~~~~~~~~~~~~~~~~~~~~~~~~~~~~~~~~~~~~~~~~~~~~~~~~~~~~~~~~~~~~~~~
% Initialization of matrices and vectors for sensor
%~~~~~~~~~~~~~~~~~~~~~~~~~~~~~~~~~~~~~~~~~~~~~~~~~~~~~~~~~~~~~~~~~~~~~~~~~~~~
index_sensor=zeros(edof,1);            % index vector for sensor
Mass_Able_sensor=zeros(sdof,sdof);     % Mass matrix for laminate elements
Global
stiffness_Able_sensor=zeros(sdof,sdof);% stiffness matrix for laminate
elements Global
%_____________________________________________________________________________

%EXTRACT SENSOR ELEMENTS

for i=sen_em_c_c
    sen_em_c=nodes(i,:);% connectivity between actuator elements
end
%_____________________________________________________________________________

%GEOMETRY OF STRUCTURE COUPLED WITH PZT-5H(MESH, NO. OF ELEMENTS, NODE
NO'S)

PlotMesh_str_piezo_sensor(coordinates,nodes,sen_em_c)
%_____________________________________________________________________________

h3=hs*(t/2 + hs/2)^2 + hs^3/12;
Hs=[hs 0 0;0 h3 0;0 0 h3];

% MASS OF THE SENSOR

[Apzo_s] = Amatrix_s(apzo_s,bpzo_s);

A_s=[-1/sqrt(3).*apzo_s -1/sqrt(3).*bpzo_s;

    1/sqrt(3).*apzo_s -1/sqrt(3).*bpzo_s;
    1/sqrt(3).*apzo_s 1/sqrt(3).*bpzo_s;
    -1/sqrt(3).*apzo_s 1/sqrt(3).*bpzo_s];

for iiel=1:sen_em
    for ii=1:nnel
        node_sensor(ii)=sen_em_c(iiel,ii);
    end
    temp6=0;
    for i=1:4
        x_s=A_s(i,1);
```

```
        y_s=A_s(i,2);
        Lm_s=[1 x_s y_s x_s.^2 x_s.*y_s y_s.^2 x_s.^3 x_s.^2.*y_s
x_s.*y_s.^2 y_s.^3 x_s.^3.*y_s x_s.*y_s.^3;
            0 1 0 2.*x_s y_s 0 3.*x_s.^2 2.*x_s.*y_s y_s.^2 0
3.*x_s.^2.*y_s y_s.^3;
            0 0 1 0 x_s 2.*y_s 0 x_s.^2 2.*x_s.*y_s 3.*y_s.^2 x_s.^3
3.*x_s.^2.*y_s];
        LM_s=Lm_s'*Hs*Lm_s+temp6;
        temp6=LM_s;
    end

    Ms=apzo_s*bpzo_s*rho_s*(inv(Apzo_s))'*LM_s*inv(Apzo_s);% element mass
matrix for sensor (Ms)

    index_sensor=elementdof_sensor(node_sensor,nnel,ndof);

[Mass_Able_sensor]=assemblemass_sensor(Mass_Able_sensor,Ms,index_sensor);%
Total assemble mass of the sensor
end

%STIFFNESS OF THE SENSOR

Ds=ce_bar_pz;

for iiel=1:sen_em
    for ii=1:nnel
        nodesensor(ii)=sen_em_c(iiel,ii);
    end
    temp7=0;
    for i=1:4
        x_s=A_s(i,1);
        y_s=A_s(i,2);
        Lk_s=[0 0 0 2 0 0 6*x_s 2*y_s 0 0 6*x_s.*y_s 0;
            0 0 0 0 0 2 0 0 2*x_s 6*y_s 0 6*x_s.*y_s;
            0 0 0 0 2 0 0 4*x_s 4*y_s 0 6*x_s.^2 6*y_s.^2];
        LKT_s=Lk_s';
        K_Q_sen=LKT_s*Ds*Lk_s+temp7;
        temp7=K_Q_sen;
    end
    ks=apzo_s*bpzo_s*h3*(inv(Apzo_s))'*K_Q_sen*inv(Apzo_s);% element
stiffness matrix for sensor of size 12*12
    index_sensor=elementdof_sensor(nodesensor,nnel,ndof);

[stiffness_Able_sensor]=assemblestiffness_sensor(stiffness_Able_sensor,ks,i
ndex_sensor);% Total assemble stiffness of the Actuator
end

%--------------------------------------------------------------------------
Msen=Mass_Able_sensor;     % Global mass of the sensor
Ksen=stiffness_Able_sensor;% Global stiffness of the sensor
%--------------------------------------------------------------------------

% ELECTROMECHANICAL COUPLING MATRIX Kwvs (Sensor)

es=e_bar_pz';

%es=[ es31 es32 0];  %PZT stiffness matrix
```

```
Bzs= 1/hs;          % Strain-displacement matrix which relates electric
field with electric potential (v)for a single layer
Kwvs=zeros(sdof,1); %Electromechanical coupling vector
index_wvs=zeros(edof,1);% index vector for sensor
for iiel=1:sen_em
    for ii=1:nnel
        nodesensor(ii)=sen_em_c(iiel,ii);
    end
    temp8=0; %pre-assumed value
    for i=1:4
        x_s=A_s(i,1);
        y_s=A_s(i,2);
        Lk_wvs=[0 0 0 2 0 0 6*x_s 2*y_s 0 0 6*x_s.*y_s 0;
            0 0 0 0 0 2 0 0 2*x_s 6*y_s 0 6*x_s.*y_s;
            0 0 0 0 2 0 0 4*x_s 4*y_s 0 6*x_s.^2 6*y_s.^2];
        LKT_wvs=Lk_wvs';
        Kwv_es=LKT_wvs*es'+temp8;
        temp8= Kwv_es;
    end
    Cwv_es=apzo_s*bpzo_s*(inv(Apzo_s))'*0.5*(hs^2 +hs*t)*Kwv_es*Bzs; %
Cwv_e element coupling electromechanical vector (12*1)
    index_wvs=index_s(nodesensor,nnel,ndof);
    Kwvs=assemble_wvs(Kwvs,Cwv_es,index_wvs);% Global electromechanical
coupling matrix
end

%-------------------------------------------------------------------------
% ELECTRICAL CAPACITANCE Kvvs

emm_s33=epsilon_pz;

Kvvs=-sen_em*1/(hs) *4*apzo_s*bpzo_s*emm_s33;
%-------------------------------------------------------------------------

%_________________________________________________________________________
PlotMesh_str_piezo_sensor_actuator(coordinates,nodes,sen_em_c,act_em_c)
%_________________________________________________________________________


%-------------------------------------------------------------------------
%MASS OF THE LAMINATE

ML=Msen+Mstr+Mact;

%-------------------------------------------------------------------------
%STIFFNESS OF THE LAMINATE

KL=Ksen+Kstr+Kact;

%-------------------------------------------------------------------------
%DAMPING MATRIX FOR LAMINATED STRUCTURE

% alpha_M=0.000001;
%  beta_K=0.000001;
%
% CL=alpha_M*ML+beta_K*KL;


%-------------------------------------------------------------------------
```

```
% Boundary conditions
%-------------------------------------------------------------------------
% BC = Clamped-Clamped case

L1 = find(coordinates(:,2)==min(coordinates(:,2))) ; % at y = 0 (along X-
axes)
n = length(L1) ;
dofL1 = zeros(1,3*n) ;
for i=1:n
    i1 = 3*(i-1)+1 ;
    i2 = i1+1 ;
    i3 = i2+1;
    dofL1(i1) = 3*L1(i)-2;
    dofL1(i2) = 3*L1(i)-1 ;
    dofL1(i3) = 3*L1(i);
end

L3 = find(coordinates(:,2)==max(coordinates(:,2))) ; % at y = b (along X-
axes)
n = length(L3) ;
dofL3 = zeros(1,3*n) ;
for i=1:n
    i1 = 3*(i-1)+1 ;
    i2 = i1+1 ;
    i3 = i2+1;
    dofL3(i1) = 3*L3(i)-2;
    dofL3(i2) = 3*L3(i)-1 ;
    dofL3(i3) = 3*L3(i);
end

L2 = find(coordinates(:,1)==max(coordinates(:,1))) ; % at x = a (along Y-
axes)
n = length(L2) ;
dofL2 = zeros(1,3*n) ;
for i = 1:n
    i1 = 3*(i-1)+1 ;
    i2 = i1+1 ;
    i3 = i2+1;
    dofL2(i1) = 3*L2(i)-2;
    dofL2(i2) = 3*L2(i)-1 ;
    dofL2(i3) = 3*L2(i);
end

L4 = find(coordinates(:,1)==min(coordinates(:,1))) ; % at x = 0 (along Y-
axes)
n = length(L4) ;
dofL4 = zeros(1,3*n) ;
for i = 1:n
    i1 = 3*(i-1)+1 ;
    i2 = i1+1 ;
    i3 = i2+1;
    dofL4(i1) = 3*L4(i)-2;
    dofL4(i2) = 3*L4(i)-1 ;
    dofL4(i3) = 3*L4(i);
end

L1UL3 = union(dofL1,dofL3) ;
L2UL4 = union(dofL2,dofL4) ;
bcdof = union(L1UL3,L2UL4)' ;
```

```
%MODAL ANALYSIS:

%------------EigenValues/EigenVectors-----------------------------------

[Eig_vec,Eig_val]=eig(KL,ML);
[seigvl,seigvt]=seigdat(Eig_val,Eig_vec);
natural=sqrt(seigvl);
fre=natural/(2*pi); % natural frequency in rad/sec
disp('Frequency ''fn_str_piezo''of coupled structure in (Hz)')
frequency=diag(fre);
diag(frequency);
fn_str_piezo=diag(frequency);
format short
fn_str_piezo(1:1:10)

_____________________________________________________________________

% Calculation of Damping Matric Cs assumed modal damping factor is 0.005
% for 500 Hz and after that it is zero.

modal_damping_constant=0.005;

interested_modes=5;

rem=size(KL,1)-interested_modes;

modal_dam_vector=modal_damping_constant*[ones(1,interested_modes)
1*ones(1,rem)];

%CL=(inv(seigvt))'*2*diag(seigvl)*diag(modal_dam_vector)*inv(seigvt);


%seigvt'*CL*seigvt % there is need of mass normalized mode shape matrix
%rather simple mode shape matrix

% Mass normalized modal matrix U

for i=1:size(seigvt,1)
    Us(:,i)=seigvt(:,i)/sqrt(seigvt(:,i)'*ML*seigvt(:,i));
end

Mass_normalized_matrix=Us;

% Mr=Mass_normalized_matrix'*ML*Mass_normalized_matrix; %Modal mass matrix
%
% Kr=Mass_normalized_matrix'*KL*Mass_normalized_matrix; % Modal stiffness
matrix
%
% Cr=Mass_normalized_matrix'*CL*Mass_normalized_matrix; % Modal damping
matrix

CL=(inv(Mass_normalized_matrix))'*2*diag(sqrt(seigvl))*diag(modal_dam_vecto
r)*inv(Mass_normalized_matrix);

%-----------------------------------------------------------------------
% Hammer Excitation node number
%-----------------------------------------------------------------------
```

```
force_number=103; % It is the node number where hammer/shaker excitation is
applied

Force=zeros(sdof,1);           % Global system force matrix for structure
Force(force_number*ndof-2)=10;
for I=bcdof
    Force(I,:)=[];
end
f=find(Force>0); % dof where we want the response of the structure

%-------------------------------------------------------------------------
% Response dof
%-------------------------------------------------------------------------

res_node=103;% accelerometer node number

Response=zeros(sdof,1);

Response(res_node*ndof-2)=1;

for I=bcdof
    Response(I,:)=[];
end

r=find(Response>0); % dof of selected node for response


%-------------------------------------------------------------------------
% Voltage applied by actuator because it is an open loop system

 Va=0;
%-------------------------------------------------------------------------

%-------------------------------------------------------------------------
%System 1 : Steel plate and PZT's (Open Loop)
%-------------------------------------------------------------------------
A1=[zeros(size(ML)) eye(size(ML));-inv(ML)*KL -inv(ML)*CL];% State Matrix

B1=[zeros(size(ML)) zeros(length(ML),1);inv(ML) -inv(ML)*Kwva]; % Input
Matrix

C1=[Response'  zeros(size(Response'))]; % Output Matrix for displacement

D1=0; % Direct Transmission Matrix

%% OPEN LOOP SYSTEM

sys1=ss(A1,B1,C1,D1); % construct a system model
%-------------------------------------------------------------------------
% System 2: Closed Loop---Direct Velocity feedback controller (DVFB)
%-------------------------------------------------------------------------

G1=0.000; % displacement feedback gain
G2=0.0800; % Velocity feedback gain

%-------------------------------------------------------------------------
% Charge amplifier sensitivity
```

```
% Range : 0.01 mV/pC to 10 V/pC

mV=0.01e-3;% 1mV=1e-3 V

pC=1e-12; % 1 pC = 1e-12 C

Sca=mV/pC; % Sensitivity of charge amplifier (0.01 mV/pC)

%--------------------------------------------------------------------------
Kctrl=G1*Kwva*Kwvs'*Sca; % Active stiffness matrix

Cctrl=G2*Kwva*Kwvs'*Sca;% Active damping matrix
%--------------------------------------------------------------------------

A2=[zeros(size(ML)) eye(size(ML));-inv(ML)*(KL-Kctrl) -inv(ML)*(CL-Cctrl)];
% State Matrix

B2=[zeros(size(ML));inv(ML)]; % Input Matrix

C2=[Response'  zeros(size(Response'))];% Output Matrix for displacement

D2=0;% Direct Transmission Matrix


%% CLOSED LOOP SYSTEM

sys2=ss(A2,B2,C2,D2); % construct a system model

%%
%--------------------------------------------------------------------------
% lsim command for open/closed loop
%--------------------------------------------------------------------------

% Step 1:

fc=max(fn_str_piezo);% highest frequency in the signal

% fs>=2*fc

fs=2.56*fc; % sampling frequency (according to Nyquist theorm)

final_time=1; % time in sec

sampling_period=1/fs;

% Step 2:

t=0:sampling_period:final_time; % simulation time = 1 seconds

% Step 3:

u_o=[Force;Va]*zeros(size(t));  % input vector..... function of time u_o(t)

u_o(f,1)=10;  % u_o = 1, a transient input

% Step 4:
```

```
[w]=lsim(sys1,u_o,t); % simulate
% Step 5:
plot(t,w,'-b','Linewidth',3.0); % plot the output vs. time
hold on
% lsim command for closed loop
% Step 6:
u_c=Force*zeros(size(t)); % input vector ..... function of time u_c(t)
u_c(f,1)=10;  % u_c = 1, a transient input
% Step 7:
[w_c]=lsim(sys2,u_c,t); % simulate
% Step 8:
plot(t,w_c,'-y','Linewidth',2.0); % plot the output vs. time
grid on
xlabel('time (sec)')
ylabel('Displacement (m)')
legend('open loop','closed loop')
title('displacement of structure with respect to time')
%% DESIGN FOR OPTIMAL GAIN G1 AND G2
figure()
pzmap(sys1,'b')
hold on
pzmap(sys2,'r')
legend('Open loop','Closed loop')
```

List of publications:

"Choice of optimal location of collocated piezoelectric sensors on steel plate using mode shapes" Accepted in journal of **"International Journal of Control Theory and Applications "**

SERIALS PUBLICATIONS

PUBLISHERS & DISTRIBUTORS (JOURNALS • BOOKS)

4830/24, Ansari Road, Darya Ganj, New Delhi-110002 (India)
Phone: 91-11-23245225, **Fax:** 91-11-2327 2135
E-mail: *serialspublications.india@gmail.com, serials@sify.com*
Website: www.serialspublications.com

SP\SKJ\2017
2nd March, 2017
ID: IJCTA-2017-8047

Title: " Choice of optimal location of collocated piezoelectric sensors on steel plate using mode shapes "

AUTHOR: Tharun Kumar and Ashok K Bagha

LETTER OF ARTICLE ACCEPTANCE

Dear Author,

Thank you very much for the submission of your article in "**International Journal of Control Theory and Applications ISSN : 0974-5572"**

We are happy to inform you that your paper mentioned above has been accepted for publication in our **SCOPUS INDEX JOURNAL** titled "**International Journal of Control Theory and Applications Vol.10 May (2017)**

Hope to work for you in the near future & Congratulations again for the creative and wonderful job.

Thanking you

Yours sincerely,

For Serials Publications,
S. K. Jha
Director

==========

SERIALS PUBLICATIONS
4830\24, Ansari Road
Darya Ganj
New Delhi – 110 002
e-mail: serialsjournals@gmail.com